

Dissertation

*zur Erlangung des Doktorgrades der Fakultät für Biologie
der Ludwig-Maximilians-Universität München*

Functional Analysis of the Role of Chloroplasts in Senescence

Vorgelegt von
Jing Wang



Erstgutachter: Prof. Dr. Dario Leister

Zweitgutachter: PD. Dr. Cordelia Bolle

Tag der Einreichung: 16.08.2013

Tag der mündlichen Prüfung: 09 August 2013

Table of Contents

Summary.....	1
Zusammenfassung	2
Abbreviations	3
Units	5
1. Introduction	6
1.1. Biogenesis and development of chloroplasts.....	6
1.1.1. Structure and function of chloroplasts.....	6
1.1.2. Origin of chloroplasts	7
1.1.3. Development of chloroplasts	7
1.2 Senescence of chloroplasts	8
1.3 Senescence of plants	11
1.4 Roles of chloroplasts in plant development.....	12
1.4.1 Embryogenesis	13
1.4.2 Leaf development	13
1.4.3 Fertilization.....	14
1.4.4 Light tolerance and dark acclimation	14
1.5 Aim of this work	15
2. Material and Methods.....	16
2.1. Plant materials.....	16
2.2. Gateway cloning and generation of overexpression lines.....	17
2.3. Growth conditions.....	18
2.3.1. Growth for seed production.....	18
2.3.2. Growth conditions for senescence experiments	18
2.3.3. Sterile growth conditions.....	18
2.4. Physiological experiments	20
2.4.1. Measurement of leaf area	20
2.4.2. Flowering time and leaf number at bolting	20
2.4.3. Chlorophyll quantification.....	20
2.4.4. Chlorophyll fluorescence.....	20
2.4.5. H ₂ O ₂ detection	21
2.4.6. Trypan blue staining	21
2.5. Molecular biology methods	21
2.5.1. Polymerase Chain Reaction (PCR)	21
2.5.2. Cloning strategies	22
2.5.3. Isolation of DNA plasmids	22

2.5.4.	Preparation of genomic DNA from <i>Arabidopsis thaliana</i>	22
2.5.5.	Determination of DNA and RNA concentrations.....	22
2.5.6.	DNA sequencing	22
2.5.7.	RNA extraction and expression analysis	23
2.6.	Cell biology and biochemical methods.....	23
2.6.1.	Determination of metabolic levels.....	23
2.6.2.	Isolation of total protein	24
2.6.3.	Isolation of chloroplasts	25
2.6.4.	TCA protein precipitation.....	25
2.6.5.	Immunoblot assays	25
2.6.6.	Isolation of <i>Arabidopsis</i> protoplasts and transient expression	26
2.6.7.	Transient assay for localization using onion epidermal cells	26
3.	Results	28
3.1.	Senescence of mutants with defects in photosynthesis.....	28
3.1.1.	Interplay between senescence and photosynthesis	28
3.1.2.	Establishment of a non-invasive method to measure chlorophyll.....	29
3.1.3.	Characterization of the dynamics of the leaf and plant senescence in the <i>Arabidopsis thaliana</i> accession Col-0	29
3.1.2.	Flowering time of mutants.....	31
3.1.3.	Changes in the Chlorophyll content during age-dependent senescence.....	32
3.1.4.	Real-time PCR with <i>SAG12</i>	35
3.1.5.	Activity of PSII during age-dependent senescence	36
3.1.6.	Analysis of dark-induced senescence	40
3.1.7.	Changes in the chlorophyll content of mutants during dark-induced senescence	41
3.2.	Isolation of plants with defects in senescence	44
3.2.1.	Screening of <i>stn8</i> EMS lines	44
3.2.2.	Isolation of mutants with early senescence phenotype.....	46
3.3.	The Reticulate-related (RER) protein family.....	46
3.3.1.	Characterization of the RER protein family	46
3.3.2.	Intracellular localization of RER protein family members	48
3.3.3.	Co-expression analysis of RER5 and RER6	50
3.3.4.	Phenotypic characterization of loss-of-function lines of RER5 and RER6...	51
3.3.5.	Metabolic analysis of <i>rer5-3/rer6-1</i>	54
3.3.6.	Overexpression lines for RER5 and RER6.....	57
4.	Discussion.....	60
4.1.	Photosystem and Senescence.....	60
4.1.1.	Age-dependent senescence	60

4.1.2. Dark-induced senescence	62
4.2. RER protein on senescence.....	65
4.2.1. Characterisation of RER proteins	65
4.2.2. Physiological characteristics of premature senescence mutants in RER.....	66
References	70
Acknowledgements	88

Summary

Senescence is governed by the developmental age, but is influenced by both internal and environmental signals. There are many evidences that chloroplasts are important in plant development. Therefore, senescence as a process of plant development is also integrated with chloroplast function. The chloroplast is the organelle where photosynthesis and biosynthesis of many important metabolites takes place. *Arabidopsis thaliana* is a suitable model plant to study senescence as it shows a monocarpic development, which means that after flowering (and setting seeds) the whole plant will die.

The thylakoid membranes inside a chloroplast are a system of interconnected membranes harboring four protein complexes, which carry out the light reactions of photosynthesis. Several mutant lines with defects in Photosystem I (PSI), the electron transport to PSI and state-transition were characterized in their age-dependent senescence as well as dark-induced senescence. The results suggest that several different factors could be responsible for the observed early senescence phenotype. In *psal-2*, although retaining a high chlorophyll content even after flowering, a steeper decline of chlorophyll than in Col-0 was observed at the later stage of senescence. The early degradation of chlorophyll in *psan-2* can be best explained by its early flowering, and therefore an early initiation of the senescence program. The result from the *psbs* mutant confirmed previous reports that high non-photochemical quenching (NPQ) can prevent premature cell death, as the absence of the PsbS protein caused a dramatic decline of NPQ and induced ROS production, which could cause senescence. When plants were put into dark conditions, a defect to acclimate to changing light intensities led to an induction of senescence. That was the case for the state transitions mutants *stn7*, *stn8* and *stn7stn8*. Also a lack of plastocyanin and PsaN makes the plants more susceptible to the dark stress and leads to the induction of senescence. The early senescence of *stn8-1* after 10 days darkness was used to perform a suppressor screen, and until now one *stn8-EMS* line could already be identified, which display a WT-like senescence

Mutants with defects in RER proteins were analyzed, as the *rer5* and *rer6* mutants showed early senescence. RER5 and RER6 were localized in the inner chloroplast envelope. The double mutant *rer5-3/rer6-1* was generated and showed a stronger phenotype compared to the parental lines as it was very small and pale. Ultrastructure revealed a smaller cell size, high frequency of stomatal clusters and chloroplasts with less starch granules. The double mutant contained less myo-inositol than Col-0 and it can be rescued by feeding with myo-inositol. Overexpression lines for RER5 and RER6 showed necrosis on their leaves. This suggests that these proteins act as transporters of metabolites and a wrong or missing compartmentalization leads to drastic effects on plant development.

Zusammenfassung

Seneszenz wird durch das Entwicklungsalter beeinflusst, aber auch durch verschiedene interne und externe Signale. Es gibt viele Indizien, dass Chloroplasten wichtig für die Entwicklung von Pflanzen sind, wird auch der Prozess des Altern mit der Chloroplastfunktionen koordiniert. Der Chloroplast ist die Organelle in der die Photosynthese und Biosynthese von vielen wichtigen Metaboliten erfolgt. *Arabidopsis thaliana* ist eine geeignete Modellpflanze für die Seneszenz, da sie monocarpisch ist, was bedeutet, dass nach der Blüte (und Abreifen der Samen) die ganze Pflanze abstirbt.

Die Thylakoidmembranen innerhalb eines Chloroplasten enthält vier Protein-Komplexe, die für die Lichtreaktion der Photosynthese wichtig sind. In mehrere Mutantenlinien mit Defekten im Photosystem I (PSI), im Elektronentransports zum PSI und der „state-transition“ wurden die altersabhängigen Seneszenz sowie die durch Dunkelheit induzierte Seneszenz charakterisiert. Die Ergebnisse zeigten, dass verschiedene Faktoren für den beobachteten Phänotyp der frühen Seneszenz verantwortlich sein können. Der steilere Rückgang von Chlorophyll in der späteren Phase der Seneszenz in *psal-2* war gekoppelt mit einem höherer Chlorophyll-Gehalt während der Blüte. Der frühe Abbau von Chlorophyll in *psan-2* lässt sich am besten durch die frühe Blühzeit und somit mit einer frühzeitigen Einleitung des Seneszenz-Programms erklären. Die Ergebnisse von der *psbs* Mutante bestätigen Berichte, dass ein hohes „high non-photochemical quenching“ (NPQ) den vorzeitigen Zelltod verhindern kann, da das Fehlen des PsbS Proteins zu einen dramatisch Rückgang des NPQ führte und die ROS-Produktion, die Seneszenz induzieren kann, steigerte. Ein Defekt in der „state transition“ wie bei *stn7-1*, *stn8-1* und *stn7stn8* könnte verhindern, dass sich die Pflanze an veränderte Lichtintensitäten akklimatisieren kann, weshalb die Inkubation im Dunklen zu der stärkeren Induktion der Seneszenz führt. Auch das Fehlen von Plastocyanin und PsaN macht die Pflanzen mehr anfällig für Dunkelstress und führt zur Induktion von Seneszenz. Die frühzeitige Seneszenz von *stn8-1* nach 10 Tagen Dunkelheit wurde ausgenützt, um eine Suppressor-Mutante in einer EMS Population von *stn8-1* zu identifizieren und zu charakterisieren.

Mutanten mit Defekten in den RER Proteinen wurden analysiert, da die *rer5* und *rer6* Mutante eine frühe Seneszenz zeigten. RER5 und RER6 konnten in Chloroplasten als innere Hüllproteine identifiziert werden. Die Doppelmutante *rer5-3/rer6-1* wurde hergestellt und zeigte einen stärkeren Phänotyp im Vergleich zu den elterlichen Linien, da sie sehr klein und blass war. Die Ultrastrukturanalyse zeigte, dass die Doppelmutante kleinere Zellen besaß, eine höhere Frequenz von Stomata und Chloroplasten mit weniger Stärkeörnern. Die Doppelmutante enthielt auch weniger myo-Inositol als Col-0, und das Wachstum konnte durch das Zuführen von externem myo-Inositol deutlich verbessert werden. Überexpressionslinien für RER5 und RER6 zeigten Nekrosen an ihren Blättern. Dies deutet darauf hin, dass diese Proteine als Transporter von Metaboliten fungieren und dass eine falsche oder fehlende Kompartimentalisierung zu drastischen Auswirkungen auf die Entwicklung der Pflanzen führt.

Abbreviations

Col-0	Columbia
ABA	abscisic acid
atp	ATP synthase
ATP	Adenosine triphosphate
BASTA	glufosinate ammonium
Chl	Chlorophyll
CO ₂	Carbon dioxide
cpDNA	chloroplast DNA
cTP	Chloroplast transit peptide
<i>cue1</i>	<i>chlorophyll a/b binding protein underexpressed 1</i>
Cytb6f	cytochrome b6f
DAB	3,3'-diaminobenzidine
dag	days after germination
DNA	Deoxyribonucleic acid
<i>dov1</i>	<i>differential developmental of vascular associated cells 1</i>
DTT	Dithiothreitol
EDTA	Ethylene diamine tetraacetic acid
EMS	Ethyl methane sulfonate mutagenesis
FW	fresh weight
GC-MS	Gas chromatography–mass spectrometry
GFP	Green fluorescent protein
HEPES	4-(2-hydroxyethyl)-1-piperazineethanesulfonic acid
Lhcb	chlorophyll a/b binding protein
IRE1	Inositol-requiring enzyme 1
JA	jasmonic acid
<i>lcd1</i>	<i>lower cell density 1</i>
LHC	Light harvesting complex
miRNA	microRNA
mRNA	Messenger RNA
MS	Murashige and Skoog
NADPH	Nicotinamide adenine dinucleotide phosphate
NASC	Nottingham Arabidopsis Stock Centre
NDH	NAD(P)H dehydrogenase complex
ndhb	NAD(P)H dehydrogenase
NPQ	Non-photochemical quenching
OEP7	outer envelope membrane protein 7
Tic40	translocon 40 at inner envelope membrane of chloroplast

PAGE	Polyacrylamide gel electrophoresis
pet	photosynthetic electron transport
PC	Plastocyanin
PCR	polymerase Chain Reaction
PCD	programmed cell death
ppGpp	guanosine 5'-diphosphate 3'-diphosphate
PPT	phosphoenolpyruvate/phosphate translocator
PQ	Plastoquinone
psbA	D1 core reaction center protein of photosystem II
PSI	Photosystem I
PSII	Photosystem II
PVDF	Polyvinylidene difluoride
rbcL	large subunit of Rubisco
<i>re</i>	<i>reticulata</i>
RER	RETICULATA-RELATED
RNA	Ribonucleic acid
RNAP	RNA polymerases
RNase	Ribonuclease
ROS	Reactive oxygen species
rpoC1	chloroplast RNA polymerase
rRNA	Ribosomal RNA
RT-PCR	real-time PCR
Rubisco	Ribulose-1,5-bisphosphate carboxylase oxygenase
SA	salicylic acid
SAGs	senescence associated genes
SAVs	senescence associated vacuoles
SDS	Sodium dodecyl sulfate
SE	standard error
TBS	Tris Buffered Saline
TBST	TBS-Tween solution
TCA	tricarboxylic acid
T-DNA	transferred DNA
Tris	Tris (hydroxymethyl)-aminomethane
tRNA	Transfer RNA
UV-B	ultraviolet radiation-B
WRKY	pronounced 'worky' proteins
WT	Wild type
YFP	yellow fluorescent protein
YLS3	yellow-leaf-specific gene

Units

°C	degree Celsius
g	gram
h	hour
m ²	square meter
mg	milligram
min	minute
ml	millilitre
M/L	Mole(s) per litre
mM	millimolar
mol	molar
nM	nanomolar
s	second
v	volume
w	weight
µg	microgram
µl	microlitre
µm	micrometer
µM	micromolar per liter
µmol	micromolar

1. Introduction

1.1. Biogenesis and development of chloroplasts

1.1.1. Structure and function of chloroplasts

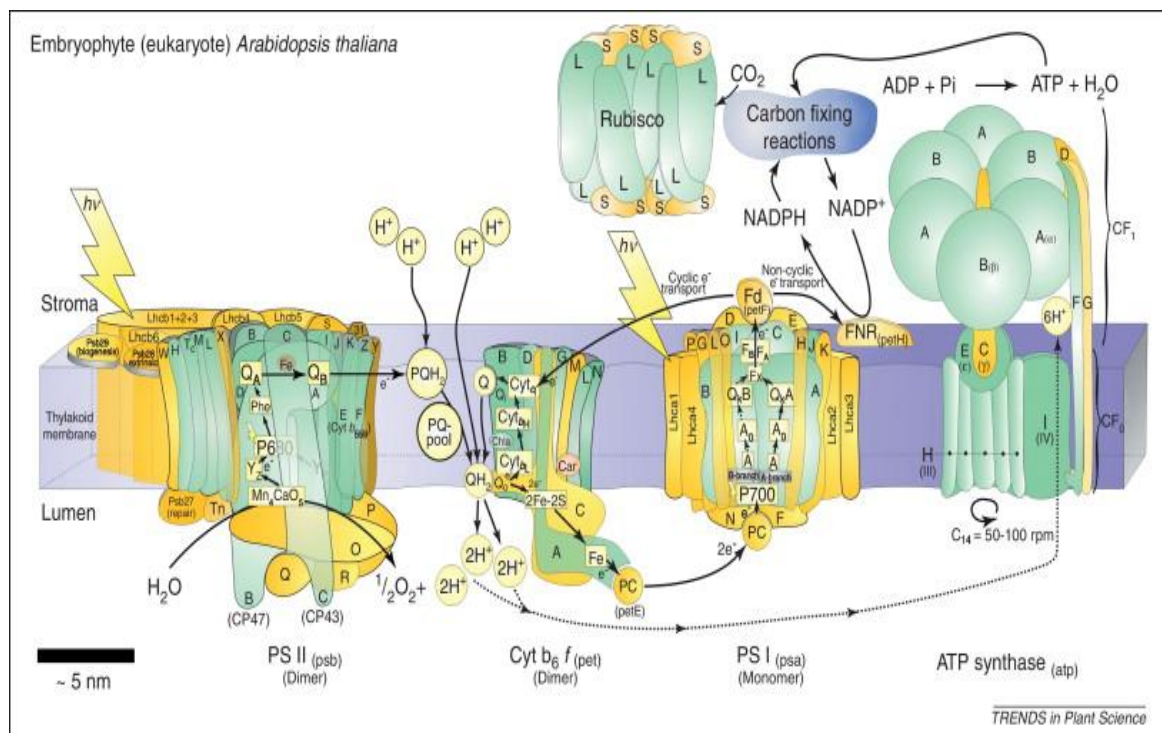


Figure 1 Components of the chloroplast photosynthetic apparatus of *Arabidopsis thaliana*. Photosystem II (PSII); cytochrome b₆f (Cyt b₆f); photosystem I (PSI); ATP synthase and Rubisco. Subunits are given single-letter names, psa for photosystem I; Psb for photosystem II; pet (photosynthetic electron transport) for the cytochrome b₆f complex and secondary electron carriers; atp for the ATP synthase; and rbc for Rubisco. Chloroplast gene products are green, those of nuclear gene products, imported as precursors from the cytoplasm, are yellow. Reprinted from Allen et al., 2013 with permission from Elsevier.

Photosynthesis is the light-dependent process involving uptake of molecular carbon dioxide and water to synthesize glucose, thereby releasing molecular oxygen. Within the plant cell this process takes place in the chloroplast, a specialized form of plastid. Chloroplasts are organelles which can only be found in plant, algae and cyanobacteria. They are surrounded by a double membrane (envelope) and contain internal membranes, so called thylakoid membranes that are either organized as grana lamella or stroma lamella. These membranes are important for photosynthesis as they harbor the two photosystems, the cytochrome b₆f complex and the ATP Synthase, which are essential for the light-reaction (Fig. 1). These four protein complexes are encoded by chloroplast and nuclear gene products (Fig. 1). During photosynthesis, chloroplasts capture the sun's light and store it in ATP and NADPH + H⁺ while freeing oxygen from water. They then use the ATP and

NADPH + H⁺ to generate organic molecules from carbon dioxide via the Calvin cycle. Additionally, almost all fatty acids synthesis takes place in chloroplast. They produce several amino acids and components of the secondary metabolism such as isoprenoids, carotenoids and tetrapyroles.

1.1.2. Origin of chloroplasts

Chloroplasts are similar to mitochondria in that they both originate from an endosymbiotic event. The endosymbiosis theory postulates that the chloroplasts of red algae, green algae, and plants evolved from endosymbiotic cyanobacteria. When a eukaryotic cell engulfed a photosynthesizing cyanobacterium, it remained and became a permanent resident in the cell. This was first suggested by Mereschkowsky in 1910 after an observation by Schimper in 1883 that chloroplasts closely resemble cyanobacteria. There are some other evidences such as that chloroplasts can only originate from existing chloroplasts in a cell and that DNA molecules coding for chloroplast genes can be found in the stroma. The genome of the chloroplast in *Arabidopsis thaliana* has been determined as a circular DNA containing 154,478 base pairs. Its genome structure in comparison with cyanobacterium provides evidence that ancestral photosynthetic prokaryotes of cyanobacteria are the origin of plant chloroplasts (Sato et al., 1999). During evolution many genes formerly encoded by the cyanobacterium were transferred to the nuclear genome (Leister and Kleine, 2011). Because now nuclear genes encode only some of the proteins needed within the chloroplasts, these genes are transcribed in the nucleus and then translated in the cytosol and imported into the chloroplast. Chloroplasts have their own protein-synthesizing machinery, and it resembles that of bacteria not that of the nuclear genome. Therefore many chloroplastidic protein complexes, as indicated in Figure 1, consist of nuclear and chloroplast subunits.

1.1.3. Development of chloroplasts

The successive stages in chloroplast development are proplastid or eoplast (early), pregranal plastid, etioplast, mature and senescing chloroplast or gerontoplast (Wise, 2006). The etioplast is considered a transition state between eoplast and chloroplast in tissues that develop in darkness (Table 1).

In addition to the basic developmental pathway, several optional diversions from it have been recognized, and these lead to the formation of alternative plastid forms which are frequently nongreen, such as amyloplasts, leucoplasts or chromoplasts. Variants may also be formed following dedifferentiation of plastids and sometimes after redifferentiation.

Table 1 Description of consequential developmental stages of chloroplast

developmental stage	phenotype
Proplastid, eoplast	Earliest stage, can develop into all other plastid types, usually small with a dense stroma. The internal membrane system is poorly developed. Found in meristematic and embryonic cells.
etioplast	Transitional stage that develops in dark-grown tissue and can convert to a chloroplast in light, contains the prolamellar body, contain protochlorophyllide.
Pregranal plastid	Green or non-green, variant of the etioplast
mature chloroplasts	Most active photosynthetically
senescent chloroplast or gerontoplast	Mostly catabolic activity, controls the recycling of the photosynthetic apparatus during senescence

During cell differentiation, proplastids differentiate into certain plastid types according to the type of cell in which they are located. Until now, the biogenesis of chloroplasts is the best studied of plastid development pathways during the differentiation process of leaf mesophyll cell. In addition the molecular biology and biochemistry of this differentiation process has been unraveled (Voelker and Barkan, 1995; Pyke, 1999; Bisanz et al., 2003; Inaba and Ito-Inaba, 2010).

All plastids are surrounded by two membranes, the outer and inner envelope. Together, these membranes provide a flexible boundary between the plastid and the surrounding cytosol. Stromules, as extensions and protrusions of the plastid envelope, are generally accepted features of chloroplasts and nongreen plastids (Kohler et al., 1997). Stromules exist more frequently in nongreen plastids than on chloroplasts (Kohler and Hanson, 2000; Pyke and Howells, 2002; Waters et al., 2004; Natesan et al., 2005; Schattat et al., 2012).

Gerontoplasts, the aging chloroplasts, are sometimes similar to chromoplasts as they accumulate carotenoids that are responsible for the yellow/red colouring of leaves in autumn.

1.2 Senescence of chloroplasts

Senescence is the final developmental stage of plant organs and it happens in a highly regulated process (Buchanan-Wollaston et al., 2003). The earliest changes occur in the chloroplast. However, the nucleus and mitochondria that are mainly important for gene expression and energy production, respectively, remain intact until the last stages of senescence (Lim et al., 2007). By changing the main function of the chloroplast from

metabolic processes to catabolic processes in the gerontoplast, plants can recycle most of the nutrients and building blocks (components) and redirect them to other organs (Hurkman et al., 1979). Conserving the nitrogen from proteins (especially the very abundant protein Rubisco) and chlorophylls is probably the most important process.

The chloroplast numbers are only slightly decreased during senescence and chloroplasts are not transported into the vacuole for degradation, as suggested previously (Wittenbach et al., 1982; Minamikawa et al., 2001; Evans et al., 2010). However, inside chloroplasts the degradation takes place. Analysis of the ultrastructure demonstrated that thylakoids follow a sequential dismantling. First the stroma thylakoid membranes disappear and the grana stacks are loosened and finally there is a massive increase in plastoglobuli (Lichtenthaler, 1969). The plastoglobuli are thought to contain the lipid-soluble degradation products from the thylakoid membranes (Matile et al., 1988; Matile, 1992). This indicates that stroma thylakoids are degraded before the grana thylakoids, which implies that PSI is degraded before PSII. However, reports on the sequence of degradation of the two photosystems during senescence are rather contradictory (Humbeck and Krupinska, 2003). While in most studies indeed an early loss of PSI is observed (Yamazaki et al., 2000; Tang et al., 2005), others report on a higher stability of PSI (Hilditch et al., 1986). Prakash JS (2003) suggest that the migration of LHCII to the stroma lamellae region and its possible association with PSI might cause the destacking and flattening of grana structure during senescence. Among the thylakoid complexes involved in photosynthetic electron transport and ATP synthesis, the loss of cytochrome b_6/f may precede the degradation of the photosystems and of ATP synthase. Therefore, electron transport between PSII and PSI could become the limiting step in NADP^+ reduction (Holloway et al., 1983; Guiamet et al., 2002).

These ultrastructural changes parallel the loss of chloroplast proteins, pigments, nucleic acids and lipids (Krupinska and Humbeck, 2004). The degradation of chloroplastic proteins is an early event during senescence, resulting in decrease of the photosynthetic capacity of the cells because of the progressive loss of proteins in the chloroplast, such as ribulose biphosphate carboxylase (Rubisco) and chlorophyll a/b binding protein (Lhcb) (Hortensteiner and Feller, 2002; Chrost et al., 2007). At least the first steps in the degradation of plastidic proteins occur inside the organelle. Later, degradation of these proteins proceeds by the action of vacuolar proteases either through a physical association between chloroplasts and the central vacuole or the mobilization of chloroplast components to the vacuole within senescence-specific vesicles (Hortensteiner and Feller, 2002; Martinez-Gutierrez et al., 2008; Martinez et al., 2008). Despite the massive amounts

of protein involved, the mechanism responsible for chloroplast protein degradation in senescing leaves remains relatively unclear (Feller et al., 2008; Martinez et al., 2008).

Chloroplastic proteases are likely involved in the breakdown of the D1 and LHCII proteins of photosystem II. Various proteases have been implicated in the degradation of Ribulose-1, 5-bisphosphate carboxylase/oxygenase (Rubisco) (Gregersen et al., 2008; Martinez et al., 2008; Izumi et al., 2010). Proteases involved in the degradation of chlorophyll-binding proteins are largely unknown, except the chloroplast-localized DegP and FtsH are reported to involve in the degradation of the D1 protein of the photosystem II (PSII) reaction centre (Adamchuk et al., 2002). Small senescence-associated vacuoles (SAVs) with high-proteolytic activity develop in senescing leaf cells, and there is evidence that SAVs might participate in the degradation of some chloroplast proteins. Hydrolysis of proteins to free amino acids depends on the actions of several endo- and exopeptidases. Plastidic and extra-plastidic pathways might cooperate in the degradation of chloroplast proteins, or they might represent alternative, redundant pathways for photosynthetic protein degradation (Martinez et al., 2008).

Chloroplasts are the main targets of ROS-linked damage during various environmental stresses and natural senescence as ROS detoxification systems decline with age (Khanna-Chopra, 2012). Thylakoids photoreduce oxygen to O_2^- due to the presence of a high concentration of oxygen originated from an electron transport chain (Navari-Izzo et al., 1999). Therefore chloroplasts have strong photooxidative potential. It has been shown that degradation of Rubisco along with several stromal proteins may be initiated by ROS (Roulin and Feller 1998). Reactive oxygen species may directly cleave the large subunit or modify it to become more susceptible to proteolysis (Feller et al., 2008). Oxidative damage to proteins may be a prerequisite to protein loss, a characteristic feature of stress and senescence is known to have an increased level of ROS.

An important catabolic process of leaf senescence is chlorophyll breakdown. Degradation of chlorophyll to colourless tetrapyrroles during senescence occurs partially within the vacuoles and is catalyzed by the acidic vacuolar pH (Oberhuber et al., 2003). In order to detoxify the potentially phototoxic pigment chlorophyll and some of its breakdown products, its degradation needs to be controlled and coordinated to prevent cell damage (Hortensteiner and Krautler, 2011). For example, mutants impaired in the breakdown of the tetrapyrrole ring of chlorophyll accumulate photodynamic catabolites (red chlorophyll catabolite) during senescence and this may lead to uncontrolled formation of reactive oxygen species and cell death (Matile et al., 1999). Chloroplast breakdown may

be viewed as a balancing act, in which degradation must be achieved without extensive cell damage in order to maintain export capacity and redistribute the released nutrients to other parts of the plant.

A massive decrease in nucleic acids can be observed during leaf senescence (Taylor et al., 1993). Beth A. Rowan (2004) reported the surprising observation that cpDNA levels decline during plastid development in *Arabidopsis thaliana* until most of the leaves contain little or no DNA long before the onset of senescence.

In another study it was shown that although chloroplast DNA did decrease, the chloroplast nuclear gene copy ratio was still 31:1 in yellow leaves. Interestingly, mRNA levels for the four loci differed: *psbA* and *ndhB* mRNAs remained abundant late into senescence, while *rpoC1* and *rbcL* mRNAs decreased in the same way as chloroplast DNA (Evans et al., 2010).

1.3 Senescence of plants

Plants can be divided into two groups according to their life span: annual plants and perennial plants. For annual plants, leaf senescence along with the organismal-level senescence is taking place until they reach the end of their life, usually with the ripening of the seeds. For perennial plants, leaf senescence is independent from the death of the whole plant and can be observed in autumn mainly by the color changes and subsequent loss of leaves.

Leaf senescence is basically governed by the developmental age. It can be interpreted as a response of leaf cells to age information and other internal and environmental signals. The environmental signals include abiotic and biotic factors. The abiotic factors are such as extreme temperature, drought, nutrient limitation, shading, oxidative stress by UV-B irradiation and ozone. The biotic factors are usually pathogen infections. Leaf senescence can happen earlier under stressful conditions (Lim et al., 2003). Detached leaves in darkness and ethylene have the strongest induced senescence and visible yellowing (Weaver et al., 1998). Also the nutritional status of a plant could play an important role in senescence as a high concentration of sugars lowers photosynthetic activity and induces leaf senescence (Jang et al., 1997; Dai et al., 1999; Quirino et al., 2000; Moore et al., 2003). Additionally, hormones as endogenous developmental signals are essential for senescence response of plants to their environment. Many studies on senescence response to the phytohormones such as abscisic acid (ABA), jasmonic acid (JA), ethylene, and salicylic acid (SA) have been performed (Yang et al., 2011; Arrom and Munne-Bosch, 2012). Furthermore, phytohormone responses are extensively involved in response to

various abiotic and biotic stresses, which in turn affect leaf senescence (Fukao et al., 2012; Oka et al., 2012; Kim et al., 2013).

Arabidopsis thaliana as a monocarpic plant has a short life cycle. So it is easier to study genetics of leaf senescence by using *Arabidopsis* plants. On the cellular level, programmed cell death (PCD) occurs in leaf senescence. This process starts from mesophyll cells and then proceeds to other cell types. Cell death spreads highly controlled and finally encompass the entire leaf. On the molecular level, recent technological advances such as microarray analysis are used in investigation of senescence-associated genes (SAGs) during leaf senescence at the genome-wide scale in *Arabidopsis* and other plants (Lim and Nam, 2007). About 800 SAGs have been identified, which demonstrates the dramatic alteration in cellular physiology that occurs during senescence (Buchanan-Wollaston et al., 2005; Van der Graaff et al., 2006). SAG12, encoding a cysteine protease, is specially used as a molecular marker for the study of developmental senescence (Noh and Amasino, 1999). Transcripts of YLS3 (yellow-leaf-specific gene) accumulated at the highest level at an early senescence stage (Yoshida et al., 2001), therefore YLS3 can be used as a early senescence marker.

Several other regulatory genes of leaf senescence have been identified, Such as WRKY54 and WRKY70 (Besseau et al., 2012), WRKY53 (Zentgraf et al., 2009) and ubiquitin. Regulation of leaf senescence involves ubiquitin-dependent proteolysis (Woo et al., 2001) and proteolysis by the N-end rule pathway (Yoshida et al., 2002). Furthermore, it has also been reported that miRNAs are important for regulation of leaf senescence (Sarwat et al., 2013).

Not only proteins are degraded during senescence but also the overall cellular content of polysomes and ribosomes decreases fairly early, reflecting a decrease in protein synthesis. This occurs concomitantly with reduced synthesis of rRNAs and tRNAs. Total RNA levels are rapidly reduced along with progression of senescence. The initial decrease in the RNA levels is distinctively observed for the chloroplast rRNAs and cytoplasmic rRNAs. The amount of various rRNA species is likely regulated coordinately, although this aspect has not been analyzed. The decrease of the amount of rRNAs is followed by that of the cytoplasmic mRNA and tRNA and an increased activity of several RNases (Taylor et al., 1993).

1.4 Roles of chloroplasts in plant development

Plastids involve in many essential metabolic pathways, and alteration of plastid function affects numerous aspects of plant growth and development.

1.4.1 Embryogenesis

Embryogenesis is the first step of plant development. Mutations in many plastidic proteins lead to embryo-lethal phenotype (Bryant et al., 2011), as shown in Table 2. According to a recent estimate, >30% of genes required for proper embryo formation encode plastid-targeted proteins (Hsu et al., 2010). This indicates that plastids play an essential role in embryogenesis. The reason for this is that plastids produce amino acid, vitamin, and fatty acids or compounds for nucleotide biosynthesis. Chloroplast translation is also required for embryo development. Compromised photosynthesis, either by defects within the photosynthetic apparatus or due to reduced levels of chlorophyll or carotenoids, is also often lethal, if not at the embryo stage then at the early seedling stage.

Table 2 Examples of plant growth and development affected by plastid proteins

	Genes identified	Reference
Embryogenesis	PPR8522	Sosso et al., 2012
	RPL21C	Yin et al., 2012
	SPP	Trosch and Jarvis, 2011
	AtPPR2	Lu et al., 2011
	AtcpRRF	Wang et al., 2010
Leaf development	VAR1, VAR2,	Chen et al., 2000; Takechi et al., 2000; Sakamoto et al., 2002; Sakamoto et al., 2009
	IM	Carol et al., 1999; Wu et al., 1999
Fertilization ^c	CRSH	Masuda et al., 2008
	Z11	Zhang et al., 1992
Light tolerance and dark acclimation	STN7 and STN8	Bonardi et al., 2005; Pesaresi et al., 2009; Pesaresi et al., 2011; Rochaix et al., 2012
	PsbS	Roach and Krieger-Liszkay, 2012

1.4.2 Leaf development

Plastid biogenesis, particularly chloroplast biogenesis, affects leaf development because the chloroplasts serve as the photosynthetic apparatus in leaf tissues. Mutants defective in chloroplast protein often exhibit albino or pale yellow phenotypes. Seedling phenotypes with different colors and aerial shapes can be classified into six phenotypic categories: albino, pale-green, pale-green cotyledons, weakly pale-green, variegated leaves and morphologically abnormal. Albino or pale yellow phenotypes are typically caused by improper development of chloroplasts (Myouga et al., 2010). Often pale mutants also

exhibit small or narrow leaves, a dwarf phenotype or a combination of these traits. This shows that normal chloroplasts are important in leaf growth and development.

Surprisingly, in variegated mutants, green sectors contain normal chloroplasts and white sectors contain improper chloroplasts (Sakamoto, 2003). This phenotype also showed in the immutans (*im*) and yellow variegated (*var*) mutants. The *var* mutants lack the plastid-localized FtsH protease, and exhibit a chloroplast photobleaching phenotype (Chen et al., 2000; Takechi et al., 2000; Sakamoto et al., 2002). FtsH protease is known to be involved in degradation of photodamaged proteins.

Reticulation is a kind of leaf phenotype, as clearly distinguished as a green reticulation on a paler lamina. A marked reduction in the density of mesophyll cells in interveinal regions led to reticulated leaf of *re* mutant (Barth and Conklin, 2003; Gonzalez-Bayon et al., 2006). Mutant *cue1* (chlorophyll *a/b* binding protein underexpressed) also exhibits reticulate leaves (Streatfield et al., 1999). Reticulated EMS-mutant *dov1* is impaired in the first step of purine metabolism (Rosar et al., 2012).

1.4.3 Fertilization

Few studies have focused on the role of plastids in reproductive development. However, some reports have been shown that interaction between mitochondria and the nucleus plays key roles in pollen fertility (Chase, 2007; Kazama et al., 2008). The role of plastids in pollen development is much less known. Nucleotide sequence of a radish chloroplast BafHI-EcoRI fragment (ZL1), derived from B21, is related to cytoplasmic male sterility. It is assumed that chloroplast ribosomal proteins may play a role in cytoplasmic male sterility in higher plants.

In bacterial cells, the stringent response acts as a regulatory system for gene expression mediated by a small nucleotide (ppGpp), that is necessary for cell adaptation to diverse environmental stress such as amino acid starvation. Reports from a knockdown mutant of CRSH indicated that plant reproduction is under the control of chloroplast function through a ppGpp-mediated stringent response (Raskin et al., 2007; Masuda et al., 2008).

1.4.4 Light tolerance and dark acclimation

Plants have the remarkable ability to adapt rapidly to changes in light conditions. When plants are exposed to high light intensities which exceed need to saturate photosynthetic electron transport, light-induced damage of the photosystems happens (Sonoike, 2011; Vass, 2012). Therefore, plants have developed several regulation mechanisms to reduce photoinhibitory damage. Specific mechanisms are running either as energy dissipators (when the light energy absorbed by the light-harvesting system exceeds the capacity of the

photosynthetic system) or as energy collectors (when the absorbed light is limiting). Plants have evolved several mechanisms to help dissipate too high light energy. Some plants can move their leaves lower their exposure to solar radiation. In addition, chloroplasts can migrate within the cell to increase self-shading thereby redistributing damage throughout the leaf to reduce the amount of inhibition received by individual chloroplasts and prevent a decrease in photosynthetic potential overall (Davis and Hangarter, 2012).

Within the chloroplast the xanthophyll cycle (Demmig-Adams et al., 1996), can release absorbed light energy as heat. On the other hand acclimatory processes are mediated to a large extent through thylakoid protein phosphorylation. The Stt7/STN7 kinase and Stt1/STN8 have been identified and characterized to be important for this process (Bonardi et al., 2005; Pesaresi et al., 2009; Pesaresi et al., 2011; Herbstova et al., 2012; Rochaix et al., 2012). The PsbS protein is an important component in dissipating excess light energy through its regulation of non-photochemical quenching in higher plants, thereby playing an important role in the protection of photosystems I and II against high light in *Arabidopsis thaliana* (Roach and Krieger-Liszkay, 2012).

1.5 Aim of this work

Although photosynthesis is down-regulated by senescence it is still not clear if photosynthesis can influence senescence. Mutants with defects in proteins directly involved in photosynthesis were studied on their dynamics of senescence. Senescence parameters observed were chlorophyll content, developmental age and activity of PSII.

On the other hand, senescence also can be induced by stress, for example darkness. Dark-induced senescence can provide a more synchronous and better controlled senescence process between wild type and mutants. To our surprise mutants that showed early aged-dependent senescence did not completely overlap with those that showed early senescence after darkness, suggesting different categories of factors initiating senescence in these lines.

Furthermore, two approaches to study age-dependent senescence by utilizing mutant analysis were followed. In a suppressor screen of an early senescing mutant, *stn8*, a candidate could be isolated, that has an enhanced survival rate after dark stress. On the other hand, this led to the description of the RER protein family and their role in communicating signals between cytoplasm and chloroplast to influence development.

2. Material and Methods

2.1. Plant materials

Arabidopsis thaliana accession Columbia (Col-0) was used in this study as a wild type (WT), but in some cases also the Wassilewskija-4 accession (Ws) was used. These accessions were obtained from NASC (Nottingham Arabidopsis Stock Centre; accession number N1092 and N2223). Previously described mutant lines employed in this study were *psad2-1*, *psal-1*, *psal-2*, *psan-2*, *psbs*, *pete2*, *stn7-1*, *stn8-1*, *stn7stn8*, STN8-overexpression line (*oeSTN8*), *psae2-1* (Ws). Furthermore, the following lines from the GABI-Kat or SALK collection were used: *re-9*, *rer1-1*, *rer5-3* and *rer6-1* (Table 3).

Table 3 List of mutants used in this work

Gene	Protein	Mutant	Reference
<i>At1g03130</i>	subunit of photosystem I, PsaD	<i>psad2-1</i>	Ihnatowicz et al., 2004
<i>At4g12800</i>	subunit of photosystem I, PsaL	<i>psal-1</i>	Pesaresi et al., 2009
<i>At5g64040</i>	subunit of photosystem I, PsaN	<i>psan-2</i>	AG Leister
<i>At1g44575</i>	chlorophyll A-B binding protein	<i>psbs</i>	AG Leister
<i>At1g20340</i>	plastocyanin	<i>pete2</i>	AG Leister
<i>At1g68830</i>	thylakoid protein kinasesSTN7	<i>stn7-1</i>	Bonardi et al., 2005
<i>At5g01920</i>	thylakoid protein kinasesSTN8	<i>stn8-1</i>	Bonardi et al., 2005
	double mutant	<i>stn7stn8</i>	Bonardi et al., 2005
	overexpressor of STN8	<i>oeSTN8</i>	Wunder et al., 2013
<i>At2g20260</i>	subunit of photosystem I, PsaE2	<i>psae2-1</i>	AG Leister
<i>At2g40400</i>	RER protein family-5	<i>rer5-3</i>	<i>GABI-308C04</i>
<i>At3g56140</i>	RER protein family-6	<i>rer6-1</i>	<i>Salk-111366</i>
<i>At5g22790</i>	RER protein family-1	<i>rer1-1</i>	<i>Salk-126363</i>
<i>At2g37860</i>	RER protein family	<i>re-9</i>	<i>GABI-264a04.23</i>

To create a double mutant, pollen from the mutant *rer5-3* was used to fertilize homozygous mutant *rer6-1* plants. The resulting F1-plant was self-fertilized and *rer5-3/rer6-1* double mutants were identified by PCR-based genotyping in segregating F2 populations. The primers used for the two PCR reaction to genotype were the following

(Table 7): *AB56-L/27ah-R* (confirmation amplicon of *AtRER5*, should be negative if the insertion is present on both chromosomes), *AB56-L/8409* (genotyping amplicon to confirm the presence of the insertion, positive result expected); *AD05-L/29ah-R* (confirmation amplicon for *AtRER6*), *AD05-L/R204* (genotyping amplicon).

To generate double mutants between *RER1* and *RE*, pollen from the mutant *rer1-1* was used to fertilize *re-9* plants. Plants homozygous for *RE* and heterozygous for *RER1* were obtained, but no homozygous double mutant could be generated.

2.2. Gateway cloning and generation of overexpression lines

Table 4 List of plasmids used in this work

Gene	Vector	Description	Purpose
<i>At2g40400 (RER5)</i>	pGFP2	C-terminal GFP-tag	Transient expression in onion and plant
	pB7FWG2.0	C-terminal GFP-tag	Overexpression in plant
<i>At3g56140 (RER6)</i>	pGFP2	C-terminal GFP-tag	Transient expression in onion and plant
	pB7FWG2.0	C-terminal GFP-tag	Overexpression in plant
<i>At5g12470 (RER4)</i>	pGFP2	C-terminal GFP-tag	Transient expression in onion and plant
<i>At5g22790 (RER1)</i>	p2GWF7	C-terminal GFP-tag	Transient expression in onion and plant
<i>At2g37860 (RE)</i>	p2GWF7	C-terminal GFP-tag	Transient expression in onion and plant
<i>At5g24690 (RER7)</i>	pGFP2	C-terminal GFP-tag	Transient expression in onion and plant

Transgenic lines generated in this study included the overexpression lines *oeAtRER5* and *oeAtRER6* (Table 7). To generate *oeAtRER5* and *oeAtRER6* full-length *AtRER5* CDS or full-length *AtRER6* CDS without the respective stop codon was amplified by PCR (primer combinations: *RER5-cacc-forward/RER5-reverse*; *RER6-cacc-forward/RER6-reverse*), cloned into the pENTR TOPO vector (Invitrogen), then transferred into the plant expression vector pB7FWG2 (Karimi *et al.* 2002) using the Gateway cloning strategy

(Invitrogen). In this vector the green fluorescent protein (GFP) was fused to the C-terminus of *RER5* or *RER6* and the transgene was expressed with the 35S promoter. After introducing the vector into *Agrobacterium tumefaciens*, the construct was introduced into Col-0 via the floral dip method (Clough and Bent, 1998). To this end, flowers of 30-day-old *Arabidopsis* plants were dipped into an *Agrobacterium tumefaciens* suspension containing 2.5% sucrose and the surfactant Silwet L-77 (0.02%) for 1 min. After dipping, plants were covered with sterile plastic bags for two days to sustain high humidity levels. Afterwards, plants were grown in the greenhouse and seeds were collected after approximately four weeks. Harvested seeds were grown for 12 days on soil and selected for the BASTA (glufosinate ammonium) resistance conferred by the vector, by spraying with a 0.25% BASTA solution. The selected positive lines were confirmed by RT-PCR by checking the expression level of *RER5* and *RER6* in total RNA. *AB56-L* and *27ah R*, *AD05-L* and *29ah-R* were employed in this PCR (Table 7).

2.3. Growth conditions

2.3.1. Growth for seed production

To obtain seeds plants were transferred to soil and grown in the greenhouse under a long day photoperiod (16h light/8h dark) providing about 200 $\mu\text{mol photons m}^{-2}\text{s}^{-1}$ standard light conditions during the light phase and a temperature of 19 °C to 22 °C.

2.3.2. Growth conditions for senescence experiments

If not stated otherwise, plants were grown in a controlled environment (growth chamber) with a long-day photoperiod (16h light/8h dark) providing 100 $\mu\text{mol photons m}^{-2}\text{s}^{-1}$ during the light phase standard light conditions and a relative humidity of 75%, a temperature cycle of 22 °C day/18 °C night and no fertilizer. Plants of different lines were always grown in parallel and in replicas.

Dark-induced senescence was carried out with *Arabidopsis* plants aged 30 days, transferring the whole plant into the dark room for 3, 7 or 10 days. After this darkness treatment, plants were moved back to the growth chamber. There was no fertilizer and water added during the darkness treatment.

2.3.3. Sterile growth conditions

To grow plants in sterile culture 1 x Murashige and Skoog (MS) medium (basal salt mixture, Duchefa[®]), complemented with 0.05% MES buffered at pH 5.8 (KOH), and 0.8% Agar (Duchefa[®]) was used. To this media different additives were added (see Table 5) for feeding experiments. To analyze metabolites in plants, seeds were surface sterilized, spotted on 1 x MS media (basal salt mixture, Duchefa[®]), containing 0.5% sugar.

In feeding experiment, concentrations of vitamin in the media were changed on the basis of vitamin solution for plant cell culture (Table 6). The concentration of pyridoxine hydrochloride was increased to 20 µg/ml, while thiamine hydrochloride was 50 µg/ml.

Table 5 List of media for feeding experiments

1 x MS medium (basal salt mixture, Duchefa [®]), with 2% sugar.	
1 x MS medium (including vitamins, Duchefa [®]), with 2% sugar and 1mM phenylalanine ² , 1mM tryptophan ² , 1mM tyrosine ² .	1 x MS medium (basal salt mixture, Duchefa [®]), with 2% sugar and 1mM phenylalanine ² , 1 mM tryptophan ² , 1mM tyrosine ² .
1 x MS medium (basal salt mixture, Duchefa [®]), with 2% sugar and 100 µg/ml myo-inositol ¹ .	1 x MS medium (basal salt mixture, Duchefa [®]), with 2% sugar and 0.5 µg/ml nicotinic acid
1 x MS medium (basal salt mixture, Duchefa [®]), with 2% sugar and 20 µg/ml pyridoxine hydrochloride	1 x MS medium (basal salt mixture, Duchefa [®]), with 2% sugar and 50 µg/ml thiamine hydrochloride
1 x MS medium (basal salt mixture, Duchefa [®]), with 2% sugar and 0.5 µg/ml nicotinic acid	

¹ my-inositol stock solution is 50 mg/ml¹

² phenylalanine, tryptophan, tyrosine were added to liquid media before autoclaving.

Arabidopsis seeds were surface sterilized with commercial bleach, 50% diluted with water and 0.01% Tween20, spotted on the different solid media and kept in a controlled environment (growth chamber) with a long day photoperiod (16h light (22 °C)/8h dark (18 °C) providing 100 µmol photons m⁻²s⁻¹ during the light phase.

Table 6 Vitamins solution for plant cell culture

Vitamine Solution contains (µg/ml):
2.0 glycine
100.0 myo-inositol
0.50 nicotinic acid
0.50 pyridoxine hydrochloride
0.10 thiamine hydrochloride

2.4. Physiological experiments

2.4.1. Measurement of leaf area

Whole plants were imaged non-invasively from the emergence of leaf No. 6 at 20 days after seed germination (dag) to 35 dag at 3 pm every three days. Pictures were taken with a digital camera. The leaf area was measured using the free software Image J (Staal et al., 2004). Three biological replicates were used for each of the mutants and Col-0 and three independent measurements were performed.

2.4.2. Flowering time and leaf number at bolting

Flowering time (time to bolting) was determined by days after germination to the appearance of an florescence stem of approximately 0.5 cm. Leaf number at bolting time was counted when the stem length was at least 2 cm. Three independent measurements were performed with at least ten biological replicates.

2.4.3. Chlorophyll quantification

If not mentioned, chlorophyll measurement during the period of senescence was started at 30 dag to 70 dag. Plants were measured at 3pm every three days. The mean of four readings from a portable Monitor chlorophyll meter (SPAD-502; Spectrum Technologies, Inc.) was obtained for each leaf from three individual plants. Reading values were measured at the midpoint of the leaf next to the main leaf vein. To verify the linear relationship between SPAD value and chlorophyll content, quantification of chlorophyll was obtained by the measurement of absorbance at 663, 645, and 480 nm in a spectrophotometer after extraction with 80% v/v aqueous acetone. The fresh weight and the chlorophyll concentration were determined according to the equation of (Lichtenthaler et al., 2013). Leaves were harvested from Col-0. At least twenty different leaves of different ages were measured. During the natural senescence, if not otherwise indicated, leaf No. 6 was measured.

Ten independent measurements were performed. At least three biological replicates were used for each mutant and Col-0.

2.4.4. Chlorophyll fluorescence

In vivo chlorophyll a fluorescence of single leaves was measured using the Dual-PAM 100 (Walz) according to (Pesaresi et al., 2009). The fluorescence of dark adapted leaves was measured (F_0), followed by the application of pulses (0.5 s) of red light ($5000 \mu\text{mol m}^{-2} \text{s}^{-1}$) to determine the maximum fluorescence in the dark (F_m) and there with the ratio F_v/F_m , a measure for the functionality of PSII. F_v is the variable fluorescence.

$$(F_m - F_0)/F_m = F_v/F_m.$$

The light dependence of the photosynthetic parameters qP and the effective quantum yield of PSII (Φ_{II}) were determined by applying increasing red light intensities (0-2000 $\mu\text{mol m}^{-2} \text{s}^{-1}$) in 15 min intervals before the steady state fluorescence (F_s) was measured and a red light pulse (5000 $\mu\text{mol m}^{-2} \text{s}^{-1}$) was given to determine F_m' . The values were calculated according to the following equations (Maxwell and Johnson, 2000):

$$\Phi_{II} = (F_m' - F_s) / F_m'$$

The photosynthetic parameters photochemical quenching:

$$qP = [(F_m' - F_s) / (F_m' - F_0)] ;$$

$$\text{Nonphotochemical quenching: NPQ} = [(F_m - F_m') / F_m']$$

and $qN = [(F_m - F_m') / (F_m - F_0)]$ were determined according to these parameters.

In vivo Chlorophyll a fluorescence of whole plants was recorded using an Imaging Chlorophyll Fluorometer (Imaging PAM; Walz, Germany). Dark-adapted plants were exposed to a pulsed, blue measuring beam (1 Hz, intensity 4; F_0) and a saturating light flash (intensity 4) to obtain F_v/F_m . The plants of wild type and double mutant grown on media with myo-inositol or without myo-inositol were photographed by imaging PAM.

For all experiments, three plants of wild type and mutants were analyzed, mean values and standard deviations were calculated. Three independent experiments were performed.

2.4.5. H_2O_2 detection

Leaves were vacuum infiltrated in the dark for 5 min with a 1 mg/ml solution of 3, 3'-diaminobenzidine (DAB) in water brought to pH 3.8 with 0.1% HCl. After 8h in the dark at room temperature in the same solution, the leaves were illuminated for 15min (by which time brown stains marked areas with H_2O_2). They were then washed twice in 80% Ethanol at 80 °C to remove chlorophyll and fixed in 70% glycerol. In this experiment, three plants of wild type and mutants were analyzed. Images were taken by a digital camera.

2.4.6. Trypan blue staining

Arabidopsis leaves were harvested and stained with lactophenol trypan blue solution (10 ml of lactic acid, 10 ml of glycerol, 10 g of phenol, 10 mg of trypan blue, dissolved in 10 ml of distilled water (Koch and Slusarenko, 1990). Leaves were boiled for 1 min in the solution and then decolorized overnight in chloral hydrate solution (75 g of chloral hydrate dissolved in 30 ml of distilled water). Images were taken by a digital camera.

2.5. Molecular biology methods

2.5.1. Polymerase Chain Reaction (PCR)

DNA fragments for genotyping of plant mutant lines were amplified using the Polymerase Chain Reaction (PCR) (Higuchi et al., 1988). The Taq PCR Core Kit

(QIAGEN) was used for PCR-genotyping. DNA fragments for cloning into vectors were amplified by PCR, using Phusion[®] High-Fidelity DNA Polymerase (New Eng Land BioLabs[®], Inc.). The protocol applied was according to the manufacturer's recommendations.

2.5.2. Cloning strategies

General molecular biological methods such as restriction digestion, DNA ligation, determination of DNA concentrations and agarose gel electrophoresis were performed as described in (Boose et al., 1989). For purification of DNA fragments from agarose gels, QIA quick[®] Gel Extraction Kit (QIAGEN) was used. LR-recombination using the GATEWAY system (Invitrogen) was performed according to the manufacturer's recommendations.

2.5.3. Isolation of DNA plasmids

DNA plasmids preparation from transformed *E.coli* cells was performed by using QIA prep[®] Spin mini prep Kit (QIAGEN). For high yield plasmid purification, the Exprep[™] Plasmid SV Midi Kit (GeneAll[®]) was used according to manufacturer's recommendations.

2.5.4. Preparation of genomic DNA from *Arabidopsis thaliana*

For genotyping T-DNA insertion lines the following protocol was used: 1-2 Arabidopsis rosette leaves were placed in 2 ml tubes supplied with 400 µl of extraction buffer (0.2 M Tris-HCl, pH 7.5; 0.25 M NaCl; 25 Mm EDTA; 0.5% SDS; pH 7.7), one steel bead was added and the tissue was disrupted using the Tissue Lyser from Retsch/Qiagen for 3 min. Afterwards the solution was centrifuged at 13,000 rpm for 8 min to remove debris. The DNA present in the clear supernatant was precipitated with 300 µl isopropanol by vortexing and incubating at room temperature for 2 min, followed by 5 min centrifugation at 13,000 rpm. The pellet was washed with 70% ethanol and after drying 100 µl 10 mM Tris-HCl (pH 8) buffer was added to the DNA. For one PCR reaction (25 µl) 1 µl of DNA was used.

2.5.5. Determination of DNA and RNA concentrations

1 or 2 µl of samples were applied to a Nanodrop spectrophotometer. The values were given under different settings for DNA or RNA concentrations.

2.5.6. DNA sequencing

After DNA fragments were cloned into the appropriate vectors, they were sequenced to ensure that the sequence was correct. For this plasmids extracted from colonies were

diluted 1:5, and 1 μ l of the dilution was mixed with 1 μ l sequence primer and 5 μ l sterilized H₂O. Sequencing work was performed by the genomic service from the department of Biology at the LMU University.

2.5.7. RNA extraction and expression analysis

Two leaves from Arabidopsis plants were harvested with forceps and frozen with liquid nitrogen. Harvesting times were at the age of 30 dag, 40 dag, and 53 dag. Total leaf RNA was extracted following the protocol of the Maxwell® 16 Tissue LEV, Total RNA Purification Kit (Promega). 1 μ g of total RNA was used to prepare cDNA by applying the iScript cDNA Synthesis kit (Bio-Rad) according to the manufacturer's instructions. For real-time PCR analysis cDNA was diluted 1:10 with water and 2 μ l of the dilution were employed for 20 μ l reactions with iQ SYBR Green Supermix (Bio-Rad). An initial denaturation step at 95 °C for 3 min preceded the cycling. Furthermore, the PCR program comprised 40 cycles with denaturation at 95 °C for 10 s, annealing at 55 °C for 30s, and elongation 72 °C for 10s. Subsequently, a melting curve was performed. The iQ5 Multi Color Real-Time PCR Detection System (Bio-Rad) was used for monitoring the reactions. For the amplification of *SAG12*, *WRKY53*, *YLS3*, the primers *SAG12 4F* and *SAG12 4R*, *WRKY53 F2* and *WRKY53 R2*, *YLS3 F* and *YLS3 R* were employed (Table 7). *Actin* was amplified as an internal control, using *Actin RT as*, *Actin RT s* as a primer pair. All reactions were performed in triplicate with at least two biological replicates.

For the amplification of *At2g40400*, *At3g56140*, the primers *AB56-L* and *27ah-R*, *AD05-L* and *29ah-R* were employed (Table 7). Ubiquitin was amplified as an internal control, using *Ubiquitin_forward*, *Ubiquitin reverse* as a primer pair. cDNA from leaves of overexpression lines were used as templates, Col-0 as a control. The PCR program comprised 40 cycles with denaturation at 95 °C for 30 s, annealing at 58 °C for 30s, and elongation 72 °C for 30s. Subsequently, a melting curve was performed. All reactions were performed in triplicate with at least two biological replicates.

2.6. Cell biology and biochemical methods

2.6.1. Determination of metabolic levels

The double mutant (*rer5-3/rer6-1*) and Col-0 were grown three times independently on 1 x MS (basal salt mixture, Duchefa®) with 0.5% sugar. Nine pools of three week old seedlings were generated from the three plant lines (WT, *rer5-3/rer6-1*, *oeAtRER6-1*; 3 independent harvests). For each pool 50 \pm 2 mg plant material were ground and extracted with 360 μ L of precooled (-20 °C) methanol (containing 5 μ g/ml norleucine (Sigma) as internal standard), 200 μ l CHCl₃ and 400 μ l H₂O. All solvents used for extraction and the

GC-MS-system were of MS quality (Roth). Essentially the preparation of the polar fraction was performed as described previously (Erban et al., 2007). For methoxyamination 10 μ l of methoxyamine hydrochloride (dissolved at 20 mg/ml in pyridine, Sigma) was added to a dried 20 μ l aliquot of the hydrophilic fraction and agitated for 90 min at 40 $^{\circ}$ C. Subsequently the per-silylation mixture containing 15 μ l BSTFA (Supelco) and 5 μ l retention index standard (n-alkanes C10-0.5 μ g/ml; C12-0.5 μ g/ml; C15-1.0 μ g/ml; C19-1.5 μ g/ml; C22-1.5 μ g/ml; C28-1.2 μ g/ml; C32-4.0 μ g/ml (Sigma)) was included in the derivatization process followed by an additional 45 min agitation interval at the previous temperature.

The instrumental GC-TOFMS profiling analysis was basically performed as reported in the literature (Erban et al., 2007) using a VF-5 ms column (30 x 0.25 (0.25) + 10 m guard column; Agilent Technologies) and a lower final oven temperature (320 $^{\circ}$ C) due to column specifications. The analyzing GC-MS system (Pegasus HT, Leco; 7890A, Agilent Technologies) was equipped with a multi-purpose sampler for automated derivatization and injection (MPS, Gerstel) as well as a cooled GC inlet (starting temperature 68 $^{\circ}$ C, ramp rate 12 $^{\circ}$ C/s, end temperature 275 $^{\circ}$ C; Cis4, Gerstel). A sample volume of 1 μ l was injected in splitless mode.

Data processing and annotation of peak identity was carried out using the vendor software (ChromaTOF, Leco), including the spectra and retention time index collection of the Golm Metabolome Database (Luedemann et al., 2008; Hummel et al., 2010). The baseline correction value was 0.5 and signal intensities were normalized with the internal standard.

2.6.2. Isolation of total protein

Total protein was isolated in a modified procedure based on (Martin-Cabrejas et al., 1999). Four to five leaves from three week-old adult *Arabidopsis* plants were collected with forceps and placed in a mortar containing 500 μ l buffer E (125 mM Tris-HCl, pH 7.5, 10% (w/v) SDS, 10% (v/v) glycerol, 150 mM NaCl). Plant material was ground in a cold room until the mixture was homogeneous, then transferred to 1.5 ml reaction tubes and samples were warmed to room temperature. After adding 200 μ l β -mercaptoethanol, samples were vortexed and centrifuged at 13.000 g for 10 min. The supernatant was kept in -20 $^{\circ}$ C. Prior to electrophoresis, proteins were resuspended in 5 \times SDS-loading buffer (225 mM Tris-HCl pH 6.8, 0.25 M DTT, 5% (w/v) SDS, 50% (w/v) glycerol, 0.05% (w/v) bromophenol blue), and incubated at 95 $^{\circ}$ C for 10 min. The Nanodrop spectrophotometer was also used to measure protein concentration.

2.6.3. Isolation of chloroplasts

Chloroplast was isolated in a modified procedure based on (Bassi et al., 1995). In brief, leaf material of 4-weeks-old *A. thaliana* plants was homogenized with ice cold isolation buffer (0.4 M sorbitol, 0.1 M Tricine-KOH pH 7.8) in a cold room, filtered through 2 layers of Miracloth (Calbiochem) and centrifuged at 5.000 g for 10 min at 4 °C. The membrane pellet was resuspended in ice cold resuspension buffer (25 mM HEPES-KOH pH 7.5, 10 mM EDTA) followed by a centrifugation step at 10.000 g for 10 min at 4 °C. Thylakoids were resuspended in TMK buffer (10 mM Tris-HCl pH 6.8, 10 mM MgCl₂, 20 mM KCl). The chlorophyll concentration was determined in aqueous 80% acetone according to (Porra, 2002). Intact chloroplasts from Col-0, *oeAtRER5* and *oeAtRER6* lines were used in equal amounts corresponding to the chlorophyll concentration.

2.6.4. TCA protein precipitation

To concentrate proteins one volume of TCA stock (500 g TCA dissolved into 350 ml dH₂O) was added to four volumes of protein sample, vortex and incubated on ice for 10 min. The solution was washed with ice-cold acetone, vortexed and incubated on ice 10 min, then centrifuged at 1.3000 rpm at 4 °C for 15 min. The supernatant was removed and the pellet again washed with cold acetone. 5×SDS-loading buffer (225 mM Tris-HCl pH 6.8, 0.25 M DTT, 5% (w/v) SDS, 50% (w/v) glycerol, 0.05% (w/v) bromophenol blue) was added to the pellet and incubated for 10 min at 65 °C. Concentrated proteins from Col-0, the *oeAtRER5* and *oeAtRER6* lines were resolved on a 10% SDS-PAGE gel for immunoblot assays.

2.6.5. Immunoblot assays

Proteins separated by SDS-PAGE were transferred to PVDF membranes (Millipore) by a semi-dry blotting system (Bio-rad) using a current corresponding to 1 mA cm⁻² with transfer buffer (14.4g/l Glycine, 3g/l Tris and 20% (v/v) methanol). Proteins were visualized by staining the SDS-PAGE gel with Coomassie Solution (0.02% Coomassie R 250 in 50% methanol). The PVDF membrane was incubated with specific GFP antibodies for 4 °C overnight, followed by washing with TBST (1xTBS and 0.1% Tween-20) three times (10 min each). The washed membrane was probed with secondary antibodies (ECL Rabbit IgG, HRP-Linked whole antibody from donkey, Amersham) at room temperature for one hour. After washing with TBST three times (10 min each), signals were detected by enhanced chemiluminescence solution (Pierce® ECL western blotting substrate, Thermo Biosciences) and visualized by the ECL reader (Fusion FX7, PeqLab).

2.6.6. Isolation of Arabidopsis protoplasts and transient expression

Mesophyll protoplasts were isolated from leaves of three to four-week old Arabidopsis plants (Col-0) grown on 1 x MS medium. Leaves were cut into small pieces and incubated for 16 h at 24 °C in the dark in a protoplasting solution (10 mM MES, 20 mM CaCl₂, 0.5 M Mannitol, pH 5.8, 0.1g/ml Cellulase (Duchefa), 0.1g/ml macerozyme (Duchefa)) followed by the isolation of protoplast as described in (Dovzhenko et al., 2003). Plasmid DNA (40 µg) was introduced into protoplast by PEG transfection as previously described (Koop et al., 1996).

The Tape-Arabidopsis-Sandwich method was used to isolate protoplasts of overexpression lines (Wu et al., 2009). Microscope analysis with Fluorescence Axio Imager microscope in ApoTome mode (Zeiss) was conducted after 16 h of incubation at 23 °C in the dark. Images were collected under the Zeiss filter sets: DIC, AF488 (autofluorescence) and 38GFP.

2.6.7. Transient assay for localization using onion epidermal cells

Cloning by restriction enzyme digestion and ligation, the coding region of *AtRER5* (generated by the primers *At2g40400F ATG Sal* and *At2g40400R wo TGA Kpn* by PCR), *AtRER6* (generated by the primers *At3g56140F ATG Sal* and *At3g56140R wo TGA Kpn*), *AtRER4* (generated by the primers *At5g12470F Xba* and *At5g12470R Xho*), *AtRER7* (generated by the primers *At5g24690F Sal* and *At5g24690R Kpn*), were inserted into the destination vector pGFP2 (Kost *et al.*1998). Using the Gateway cloning technology (Invitrogen), *AtRER1* (generated by the primers *At5g22790 F2* and *At5g22790 R2*), *AtRE* (generated by the primers *At2g37860 R3* and *At2g37860 F4*), were inserted into the pENTR-TOPO vector (Invitrogen) and then transferred into the destination vector p2GWF7 by LR-clonase (Invitrogen), which can express the inserted gene fused to an eGFP (enhanced green fluorescent protein) tag at the C-terminus (Karimi *et al.*2002). Vectors with *AtOEP7-YFP* and *AtTic40-YFP* fusions were provided by Norbert Mehler and Ute Vothknecht.

Transient expression assays in onion epidermal cells using particle bombardment (Bio-Rad, Richmond, CA) were carried out as described previously (von Arnim and Deng, 1994). Typically 2 to 5 µg of the plasmid were used per assay. Tissue was examined on a Fluorescence Axio Imager microscope (Zeiss).

Table 7 List of primers used in this work

name	Sequence (5'-3')
<i>AB56-L</i>	ATCCATACTTGCCTCTTCAGTTGT
<i>27ah-R</i>	AATTCATTAAACCAGAGTTGGGTG
<i>AD05-L</i>	CCTGTCACCACTAACAGTAGACCA
<i>29ah-R</i>	AACTCGAAATCGTTAGAAACCTGA
<i>8409</i>	ATATTGACCATCATACTCATTGC
<i>R204</i>	GCGTGGACCGCTTGCTGCAAC
<i>RER5-cacc-forward</i>	CACCATGAAGCCCACGACCAATG
<i>RER5-reverse</i>	TTGATTCTTAAGATCATCCATACTTGC
<i>RER6-cacc-forward</i>	CACCATGAAACTCACCACGAATG
<i>At3g56140-reverse</i>	TTGATTATTGAGCTTATCGATACTTTC
<i>SAG12 4F</i>	GTGTCTACGCGGATGTGAAG
<i>SAG12 4R</i>	CAGCAAACCTGATTTACCGCA
<i>WRKY53 f2</i>	CAGGACCTAGAAGTTCACAC
<i>WRKY53 r2</i>	CCTAAGCAGGATACAGTTGG
<i>YLS3 F</i>	GTGTCTTTGTATGATCATCC
<i>YLS3 R</i>	TAGCTGATAGAACACTTGG
<i>Ubiquitin_forward</i>	GGAAAAAGGTCTGACCGACA
<i>Ubiquitin reverse</i>	CTGTTACGGAACCCAATTC
<i>Actin RT s</i>	TTCACCACCACAGCAGAGC
<i>Actin RT as</i>	ACCTCAGGACAACGGAATCG
<i>At2g40400 F ATG Sal</i>	GGGTCGACATGAAGCCCACGACCAAT
<i>At2g40400R wo TGA Kpn</i>	CCGGTACCTTGATTCTTAAGATCATCCATAC
<i>At3g56140 F ATG Sal</i>	GGGTCGACATGAAACTCACCACGAAT
<i>At3g56140R wo TGA Kpn</i>	CCGGTACCTTGATTATTGAGCTTATCGAT
<i>At5g12470 F Xba ATG</i>	CCTCTAGAATGGCAATCGCTTCCTG
<i>At5g12470 R Xho oTGA</i>	GGCTCGAGGTGAGATTTCTGGATA
<i>At5g24690 F Sal</i>	GGGTCGACATGTCACATATGGTGTTC
<i>At5g12470 R Kpn</i>	CCGGTACCAGAGGCAGATGCAG
<i>At2g37860 F4</i>	AAACTGCATTCCGCCGTAGATG
<i>At2g37860 R3</i>	CACCATGGCAGGATGTGCAATG
<i>At5g22790 F2</i>	CTGAACGCCGGACAATTTAGCC
<i>At5g22790 R2</i>	CACCATGTCTATTTCCCTAAAAATTC

3. Results

3.1. Senescence of mutants with defects in photosynthesis

3.1.1. Interplay between senescence and photosynthesis

Many studies established that the structure and function of chloroplasts are altered during leaf senescence (Raval and Biswal, 1988; Behera et al., 2003; Evans et al., 2010; Zhang et al., 2010; Khanna-Chopra, 2012). The alterations include the degradation of photosynthetic pigments and proteins, inactivation of both photosystems (PS) I and II and down regulation of enzyme activities associated with Calvin-Benson cycle (Behera et al., 2003; Raval et al., 2005; Lim et al., 2007; Feller et al., 2008; Khanna-Chopra, 2012).

To test how far the efficiency of photosynthesis can influence senescence, we selected nine mutants with defects in proteins directly involved in photosynthesis. Four mutants had defects in Photosystem I proteins (*psad2-1* in PsaD, *psal-2* in PsaL, *psan-2* in PsaN and *psae2* in PsaE), whereas *pete2* mutant encodes for the electron transporter plastocyanin (PetE) and PsbS has a photoprotective role under high light (Roach and Krieger-Liszkay, 2012). Furthermore, we chose two kinases that are involved in photosynthetic acclimation, STN7 and STN8, for these analyses (Pesaresi et al., 2011; Wunder et al., 2013).

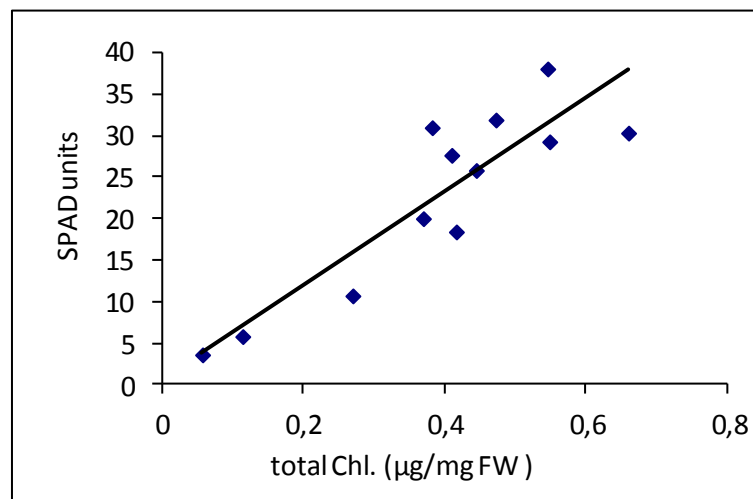


Figure 2 Calibration curves for a SPAD-502 chlorophyll content meter versus total leaf chlorophyll concentration. The data indicate a linear relationship between both measurements. Leaves of different ages were collected from mature plants (Col-0) grown in the green house. FW = fresh weight.

3.1.2 Establishment of a non-invasive method to measure chlorophyll

To determine the levels of chlorophyll extracting chlorophylls from leaves using chemical solvents is time-consuming and destroys the tissue, which is not feasible when following plant development and doing periodic sampling. To assess if a non-invasive method to measure chlorophyll as a marker for senescence could be used, conventional chlorophyll measurements and measurements with a SPAD meter were compared. The SPAD meter reads the optical density difference at 650 nm and 940 nm to calculate chlorophyll content. A linear relation among total leaf chlorophyll concentration and SPAD readings in *Arabidopsis thaliana* accession Col-0 could be demonstrated (Fig. 2). Similar relationships among total leaf chlorophyll concentration and SPAD readings have been established with other plant species (Singh et al., 1986; Marquard and Tipton, 1987; Schaper and Chacko, 1991). The results here indicated the SPAD meter can be used to estimate leaf chlorophyll concentrations accurately.

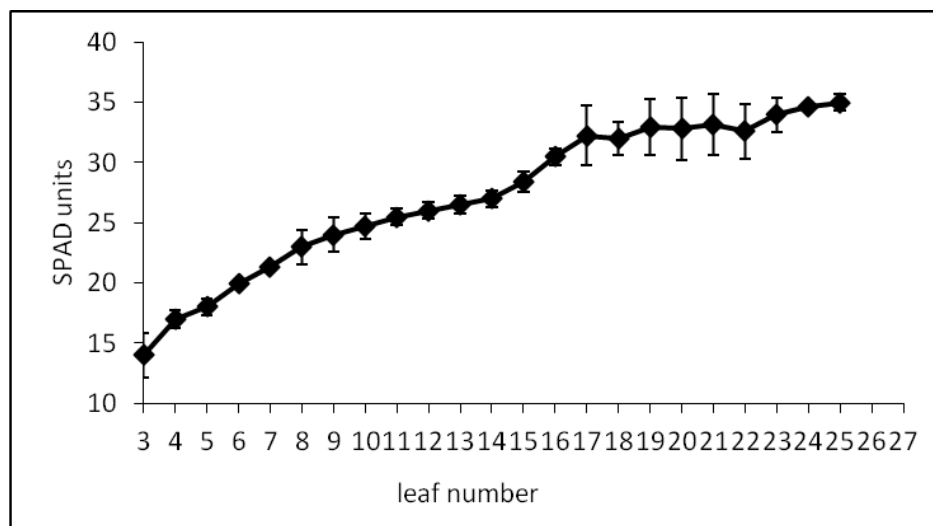


Figure 3 Analysis of chlorophyll content during rosette development in *Arabidopsis Col-0*. Every leaf of several rosettes grown under long-day conditions was measured at 25 days after germination (dag) and analyzed for its chlorophyll content. The youngest leaf measured is leaf No. 20, the oldest leaf is leaf No. 3.

3.1.3 Characterization of the dynamics of the leaf and plant senescence in the *Arabidopsis thaliana* accession Col-0

To estimate the timeline of age-dependent senescence, the chlorophyll content of each leaf of 50-day-old plants was measured (Fig. 3). The data suggested that senescence was starting with leaf No. 15 as here the chlorophyll content started declining. Leaf No. 6 and

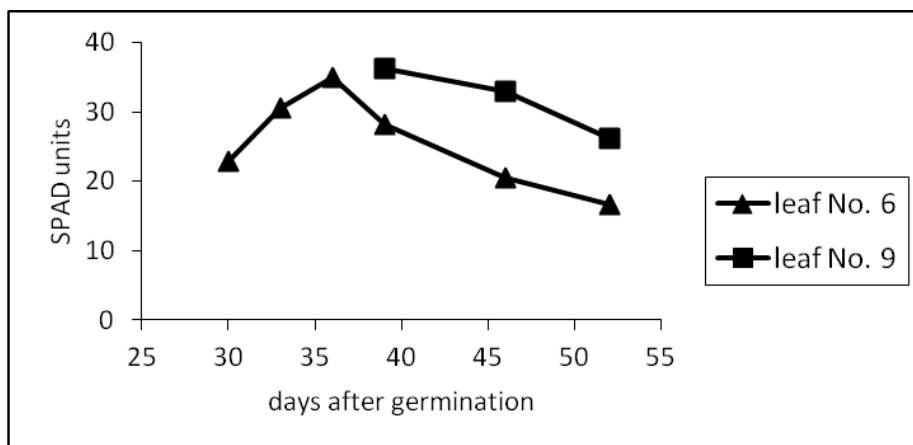


Figure 4 Comparison of the chlorophyll content between leaf No. 6 and leaf No. 9 during the development of Arabidopsis Col-0 under long-day conditions.

No. 9 were used to measure the chlorophyll content during their lifetime (Fig. 4). Due to the size of leaf No. 9, measurement was only possible after day 40. Therefore, we chose leaf No. 6 to represent senescence best. Leaf No. 6 starts senescence at about 35 days after germination (dag) under long-day conditions.

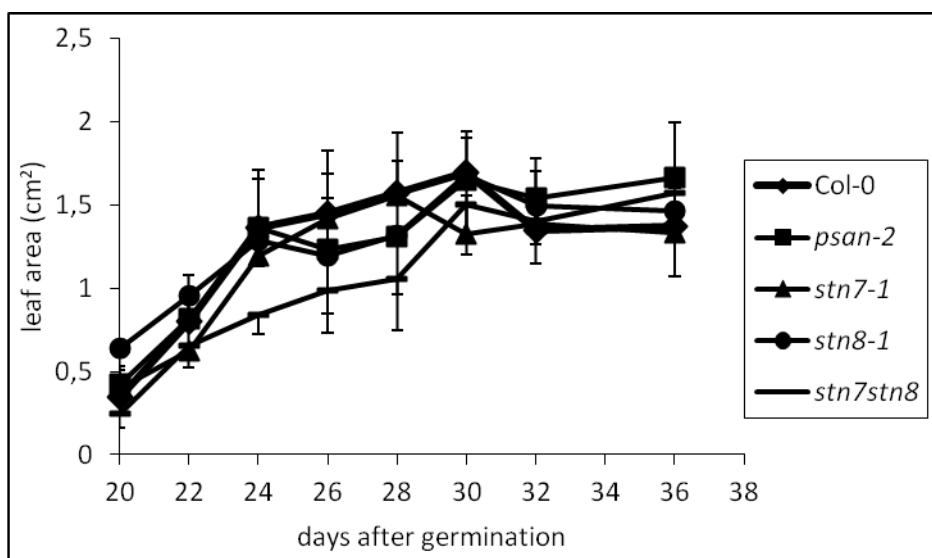


Figure 5 Leaf area of leaf No. 6 in Col-0 and mutants *psan-2*, *stn7-1*, *stn8-1*, and *stn7stn8* during development. Error bars represent the S.E. ($n = 8$ measurements) and in some cases are only indicated in one direction to avoid overlaps.

To compare the stages of leaf development with its chlorophyll accumulation the leaf expansion of leaf No. 6 was measured (Fig. 5). The leaf size stopped to increase at 30 dag, 5 days before maximum chlorophyll accumulation could be observed for Col-0. In comparison to Col-0 the other mutants showed little differences. For example for *stn7stn8* the leaf size was always smaller than Col-0, and *stn7-1* the leaf size reached its maximum about two days earlier (Fig. 5). The slight decrease of the leaf size observed in Figure 5

after 30 dag was due to withering effects of the leaves. These analyses showed that the best time frame to follow senescence by measuring photosynthetic parameters is to start measurements at 30 dag and using leaf No. 6.

Table 8 Days to bolting and leaf number at bolting time in wild type and mutant plants on soil in a growth chamber.

	Days to bolting ^a (dag)	Leaf number at flowering ^b (dag)
Col-0	36.8 ± 1.4	16.8 ± 0.8
<i>psad2-1</i>	37.2 ± 2.7	17.8 ± 1.2
<i>psal-2</i>	34.8 ± 3.2*	15.3 ± 0.8
<i>psan-2</i>	33.5 ± 2.0*	14.6 ± 1.3*
<i>psbs</i>	36.0 ± 0.5	17.9 ± 0.6
<i>pete2</i>	36.0 ± 0.5	15.0 ± 1.0
<i>stn7-1</i>	36.9 ± 1.5	15.8 ± 0.8
<i>stn8-1</i>	32.8 ± 1.8*	15.0 ± 0.7*
<i>oeSTN8</i>	32.3 ± 1.1*	16.5 ± 0.7
<i>stn7stn8</i>	35.0 ± 2.0	15.8 ± 0.7
WS	30.0 ± 0.5	7.5 ± 0.7
<i>psae2-1</i>	30.0 ± 0.5	6.0 ± 0.5

^a Number of days from germination to the development of an inflorescence stem of approximately 0.5 cm length.

^b Leaf number of the rosette was counted when shoot length was about 2 cm. Standard error is given.

* Value is significantly different from the respective wild type (T-test value $p < 0.05$)

3.1.2. Flowering time of mutants

During development, several phase changes can be observed: the transition from the juvenile to the vegetative growth phase, then the change into the reproductive phase and, furthermore, senescence. To judge the developmental speed or age of the different mutants

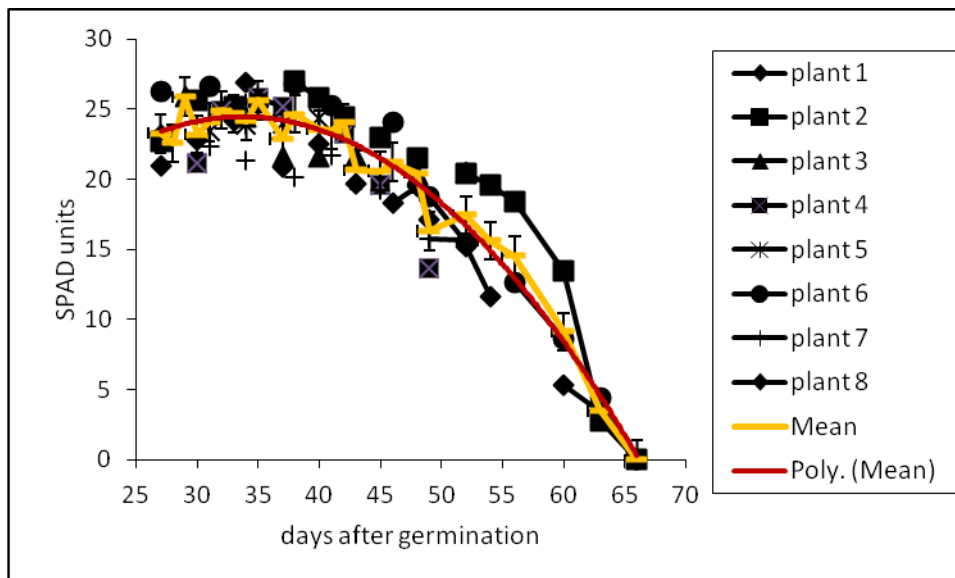


Figure 6 Chlorophyll content of leaf No.6 of Arabidopsis Col-0 during age dependent senescence. Eight different plants in biological and experimental replicates were followed and the mean value was calculated. Error bars represent the S.E. ($n = 8$ measurements).

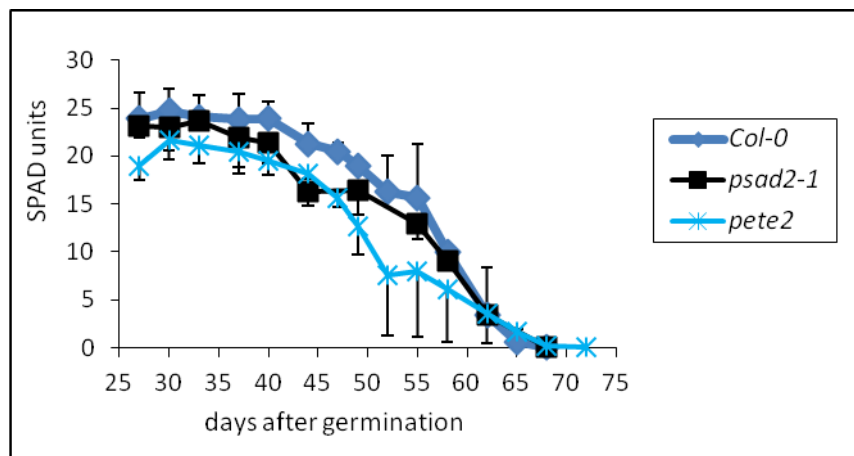
used in this study we compared their flowering time. Two parameters were used to measure flowering time, day of bolting and leaf number at bolting (Table 8).

In comparison to wild-type plants, *psan-2* mutants flowered about three days earlier than wild-type plants. This effect was statistically significant and can also be observed by the decreased number of rosettes leaves at bolting time. Also *stn8-1* and *oeSTN8* were earlier flowering than WT, but *oeSTN8* displayed about same number of rosette leaves as WT at bolting time. However, most mutants did behave similar compared to wild-type plants.

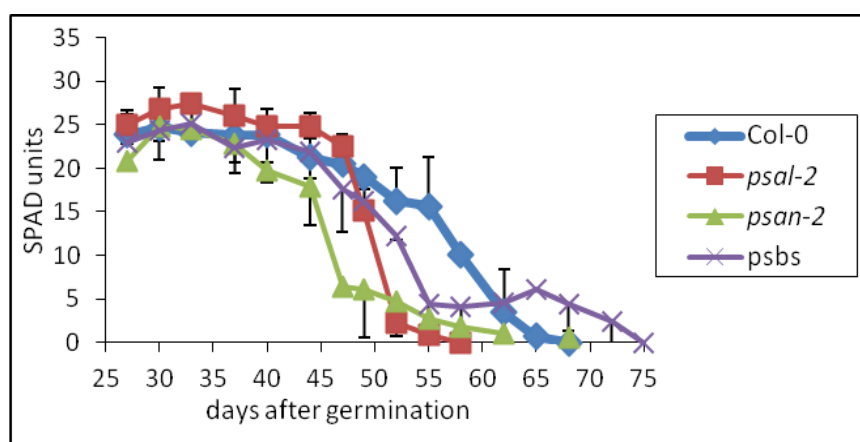
3.1.3. Changes in the Chlorophyll content during age-dependent senescence

During senescence, cell constituents are dismantled in an ordered progression. Chlorophyll degradation is the first visible symptom of senescence, and it occurred before the yellowing can be seen. Fig. 6 depicted the changes in the content of total Chlorophyll during the lifetime of wild-type plants (Col-0). In order to test for reproducibility, we repeated the measurement in eight separate experiments. The trend was similar among the different repeats. Our result confirmed that the chlorophyll content of Col-0 decreased continuously after flowering (36.8 ± 1.4 dag).

(a)



(b)



(c)

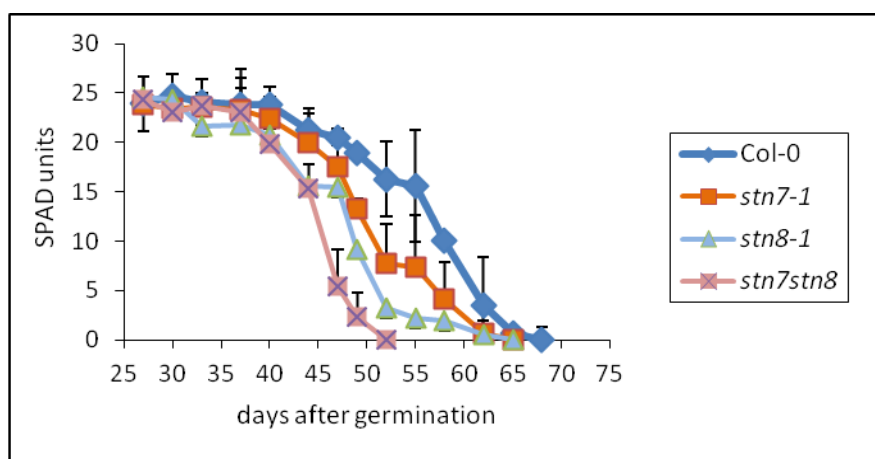


Figure 7 Age-dependent senescence of Col-0 and mutants *psad2-1*, *pete2* (a), *psal-2*, *psan-2*, *psbs* (b), *stn7-1*, *stn8-1* and *stn7stn8* (c). Chlorophyll content of leaf No. 6 was measured. Error bars represent the S.E. ($n = 4-6$ independent experiments with three plants each) and in some cases are only indicated in one direction to avoid overlaps.

We compared different photosynthesis mutants (Table 3) for their behavior during age-dependent senescence. For the mutant *psad2-1* and *pete2* (Fig. 7a) no difference to Col-0 could be observed. *pete2* had a reduced chlorophyll content compared to Col-0, but the overall trend of chlorophyll decline was very similar to Col-0.

In Fig. 7b, all the mutant lines which displayed an earlier decline of chlorophyll content compared to Col-0 are shown. *psan-2* plants showed an earlier onset of senescence (4-5 days), but this decline could be correlated with its earlier flowering time (about 3 days compared to Col-0). *psal-2* and *psbs* showed a faster decline of chlorophyll content after onset of senescence. Although *psal-2* flowers earlier compared to Col-0, senescence started at about the same time as Col-0. Also both mutants involved in phosphorylation of the photosystems, *stn7-1* and *stn8-1* showed earlier senescence (Fig. 7c). *stn8-1* seems to be stronger affected, but the double mutant *stn7stn8* lost the chlorophyll even faster.



Figure 8 Accelerated leaf senescence of the mutants: *psan-2*, *stn7-1*, *stn8-1* and *stn7stn8* during the age-dependent senescence in comparison with WT (Col-0). Plants were grown under long-day conditions in climatic chambers and all rosette leaves from respective plant were photographed at 52 days after germination.

To visualize the progression of senescence in mutants in greater detail, all the rosettes of WT (Col-0) and exemplary mutant plants, grown under normal conditions, were sampled at 52 dag. The loss of chlorophyll was discernible by the different grades of yellow and brown of the leaves. Enhanced yellowing of mutants could be detected except for *psad2-1* (Fig. 8). With regard to Col-0, there were only five fully yellow/brown leaves between twenty-two leaves. However, about half of the leaves were dead for *psan-2*, *stn7-1*, *stn8-1* and *stn7stn8*. This confirms that these lines show early senescence.

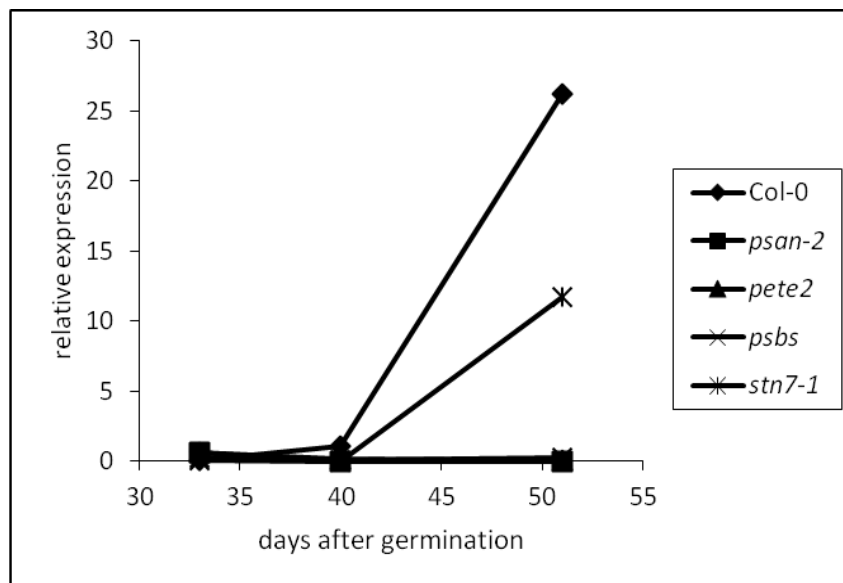


Figure 9 Expression patterns of *SAG12* transcripts in the leaf. No 6 of *Col-0* and mutants *psan-2*, *pete2*, *psbs*, *stn7-1* at sequential stages of senescence (33 dag, 40 dag, 51 dag). Abundances were determined by comparison with an internal Actin control. Data represents $2^{\Delta CT}$ ($\Delta CT = C_T(\text{actin}) - C_T(\text{test})$). Error bars represent the SE ($n = 9$), Where no error bars are present, the SE. was smaller than the size of the symbol.

3.1.4. Real-time PCR with *SAG12*

We monitored expression of three senescence marker genes, *SAG12* (Noh and Amasino, 1999) and *YLS3* (Yoshida et al., 2001), *WRKY53* (Zentgraf et al., 2010), to evaluate progression of senescence. *SAG12*, a marker for later stages of senescence gave the most conclusive results.

Our data revealed that the expression level on *SAG12* of Col-0 was much higher at 51 dag than 33 dag and 40 dag, as shown in Fig. 9. And *stn7-1* exhibited a similar trend as Col-0. The other mutants remained at nearly the same expression level between 33dag and 51dag, but we only harvested leaves from one experiment, so further repeats need to do.

3.1.5. Activity of PSII during age-dependent senescence

To further define the effects of age-dependent senescence on photosynthesis, PSII parameters including Φ_{II} , qP, qN, NPQ and F_v/F_m were determined for WT and mutant plants (Table 9, Fig. 10).

To determine the pre-senescence status plants were first measured at 28 dag. The effective quantum yield of PSII (Φ_{II}) in *pete2* plants had already a significant difference compared to Col-0, and also qP showed great difference compared to Col-0 (Table 9a). Results from Pesaresi et al. (2009) also reveal that *pete2* has lower value of Φ_{II} and qP

(a)

28dag	δII	qP	qN	NPQ	F_v/F_m
Col-0	0.70 \pm 0.02	0.90 \pm 0.02	0.30 \pm 0.06	0.33 \pm 0.09	0.84 \pm 0.01
<i>psad2-1</i>	0.69 \pm 0.04	0.88 \pm 0.02	0.32 \pm 0.09	0.39 \pm 0.15	0.84 \pm 0.01
<i>psal-2</i>	0.69 \pm 0.02	0.88 \pm 0.02	0.30 \pm 0.10	0.36 \pm 0.16	0.84 \pm 0.01
<i>psan-2</i>	0.69 \pm 0.04	0.88 \pm 0.03	0.30 \pm 0.08	0.35 \pm 0.13	0.84 \pm 0.01
<i>psbs</i>	0.71 \pm 0.03	0.87 \pm 0.03	0.21 \pm 0.02*	0.22 \pm 0.02*	0.85 \pm 0.004
<i>pete2</i>	0.59 \pm 0.02*	0.72 \pm 0.02*	0.21 \pm 0.04*	0.22 \pm 0.06*	0.85 \pm 0.01
<i>stn7-1</i>	0.68 \pm 0.02	0.88 \pm 0.01	0.34 \pm 0.07	0.42 \pm 0.13*	0.84 \pm 0.01
<i>stn8-1</i>	0.70 \pm 0.02	0.91 \pm 0.04	0.33 \pm 0.07	0.39 \pm 0.11	0.83 \pm 0.02
<i>stn7stn8</i>	0.67 \pm 0.02	0.85 \pm 0.02	0.32 \pm 0.06	0.38 \pm 0.10	0.84 \pm 0.01
<i>oeSTN8</i>	0.70 \pm 0.01	0.88 \pm 0.01	0.31 \pm 0.02	0.36 \pm 0.04	0.84 \pm 0.01

(b)

40dag	δII	qP	qN	NPQ	F_v/F_m
Col-0	0.57 \pm 0.19	0.73 \pm 0.24	0.30 \pm 0.12	0.36 \pm 0.17	0.84 \pm 0.02
<i>psad2-1</i>	0.60 \pm 0.09	0.78 \pm 0.10	0.35 \pm 0.11	0.45 \pm 0.20	0.84 \pm 0.01
<i>psal-2</i>	0.50 \pm 0.12	0.76 \pm 0.13	0.39 \pm 0.17	0.45 \pm 0.20	0.78 \pm 0.10
<i>psan-2</i>	0.58 \pm 0.07	0.73 \pm 0.08	0.30 \pm 0.08	0.36 \pm 0.14	0.84 \pm 0.02
<i>psbs</i>	0.42 \pm 0.20*	0.56 \pm 0.23*	0.15 \pm 0.07*	0.22 \pm 0.27*	0.69 \pm 0.29*
<i>pete2</i>	0.48 \pm 0.08*	0.61 \pm 0.10*	0.24 \pm 0.04*	0.25 \pm 0.05*	0.83 \pm 0.02
<i>stn7-1</i>	0.57 \pm 0.09	0.75 \pm 0.09	0.35 \pm 0.09	0.41 \pm 0.13	0.83 \pm 0.02
<i>stn8-1</i>	0.55 \pm 0.13	0.70 \pm 0.15	0.29 \pm 0.04	0.32 \pm 0.07	0.83 \pm 0.02
<i>stn7stn8</i>	0.58 \pm 0.12	0.74 \pm 0.13	0.30 \pm 0.08	0.34 \pm 0.12	0.83 \pm 0.04
<i>oeSTN8</i>	0.51 \pm 0.09	0.71 \pm 0.11	0.49 \pm 0.05*	0.69 \pm 0.13*	0.83 \pm 0.004

Table 9 Comparison of changes in the efficiency of PSII (Φ_{II} , qP, qN, NPQ and F_v/F_m) between leaf No.6 of wild type and mutants of *Arabidopsis thaliana* during age-dependent senescence. Significant differences between lines are indicated by asterisk (*, $p < 0.05$). (a) Results represent the mean of four independent experiments measured at 28 dag. (b) Results represent the mean of four independent experiments measured at 40 dag.

compared to Col-0 (Pesaresi et al., 2009). While Φ II is the proportion of absorbed energy used in photochemistry, qP gives an indication of the proportion of PSII reaction centers that are open (Maxwell and Johnson, 2000). qN and NPQ can be used for quantifying non-photochemical quenching. A strong decline in qN and NPQ could be observed in *psbs* and *pete2*. For *pete2* chlorophyll measurements had already shown that the overall chlorophyll content was lower in this mutant (Fig. 7a). After 40 dag WT showed a reduced Φ II, qP and F_v/F_m value, but similar qN and NPQ values compared to 28 dag (Table 9b). The measurement was repeated after 40 dag to be able to document the senescence process. In the *oeSTN8* line, much higher qN and NPQ values could be observed at 40 dag. *psbs* and *pete2* mutant lines after 40 dag were strongly reduced in Φ II and qP, but similar to the 28 dag value in the qN and NPQ value for *pete2*. For F_v/F_m only *psal-2* and *psbs* showed a decline compared to 28 dag, while Col-0 and all the other mutants are similar to the value at 28 dag.

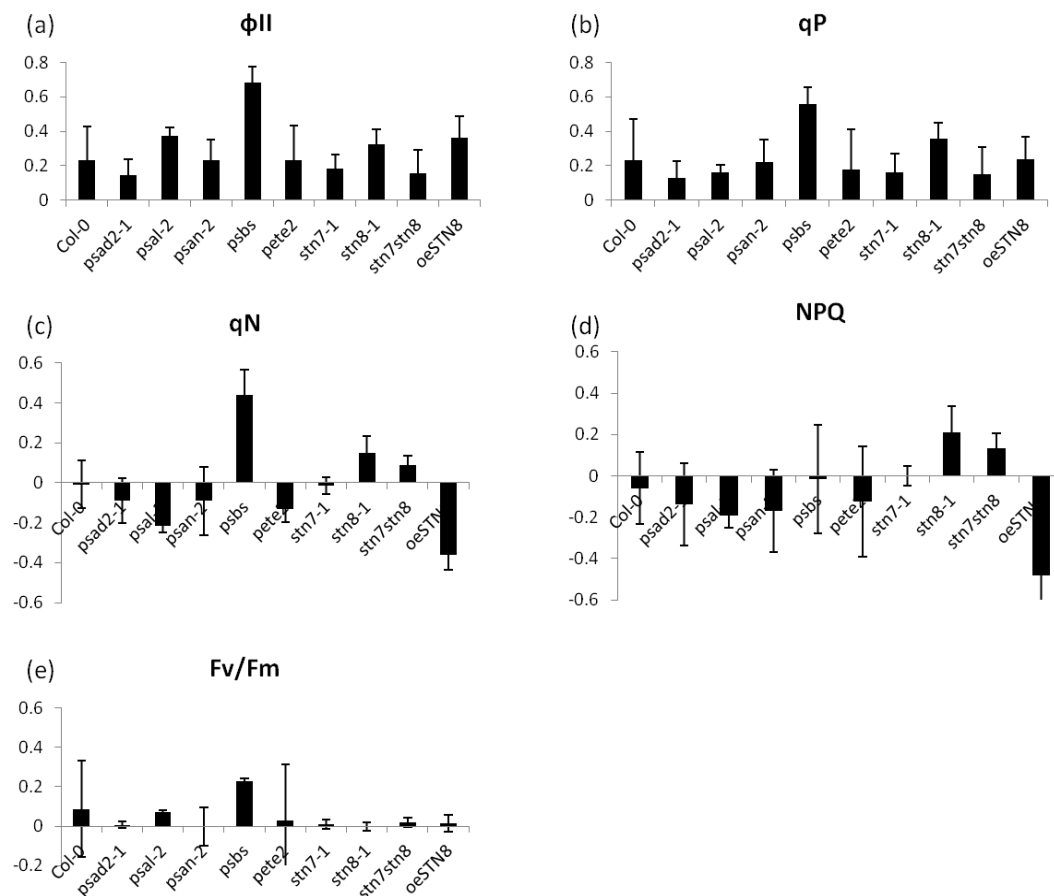


Figure 10 Comparison of changes in efficiency of PSII in leaf No. 6 of WT and mutants of *Arabidopsis thaliana* between 28 dag and 40 dag during age-dependent senescence. Results represent the ratio between 28 dag and 40 dag minus one. The values above (below) zero indicate an increase (decrease) from 28 dag to 40 dag. PSII parameters were Φ II (a), qP (b), qN (c), NPQ (d), F_v/F_m (e).

In Fig. 10 the ratio between the photosynthetic parameters at 40 dag was compared to 28 dag. It can be clearly seen that *psbs* had the most pronounced decrease in Φ_{II} and qP , but also in qN . Interestingly, *pete2* showed same change as Col-0, which suggests that although the PAM values of *pete2* were lower than Col-0, the trend from 28 dag to 40 dag was the same as in Col-0. However, the strong increase in qN and NPQ but not in Yield and qP were seen in *oeSTN8* plants after 40 dag. The other mutants had no significant difference to Col-0. The survival rates of mutants at 40 dag were all 100%.

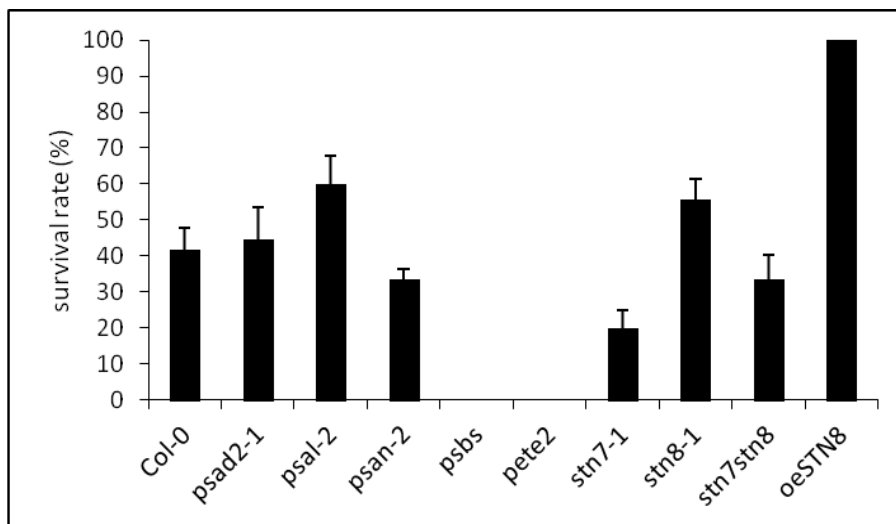


Figure 11 Ratio of plants (wild type and mutants) that were still alive at 52 dag. $n = 12$ measurements from 4 different experiments.

At even later stages of age-dependent senescence, many plants of each line were already dead or the leaf that was being monitored. Therefore we measured the survival rate of mutant lines at 52 dag. The results showed that all the plants of *psal-2*, *psbs* and *pete2* were dead. However, there was no dead plant in the line *oeSTN8* (Fig. 11).

The results of the chlorophyll fluorescence measurement showed that at 40 dag all the mutants behaved as Col-0 (Fig. 12a), except mutant *psbs* (Fig. 12b). The difference between Col-0 and *psbs* was clear as for *psbs* the F_m' value (the maximum fluorescence, obtained after a saturation flash) remained stable for 3 min, without the decline seen in Col-0.

If we relate PSII activity of *psbs* to the chlorophyll decline of the age-dependent senescence (Fig. 7b), it appears that the low PSII activity lead to the early decline on chlorophyll amount of *psbs*. For the *oeSTN8* line its high survival rate at 52 dag was most likely due to the strong increase in qN and NPQ.

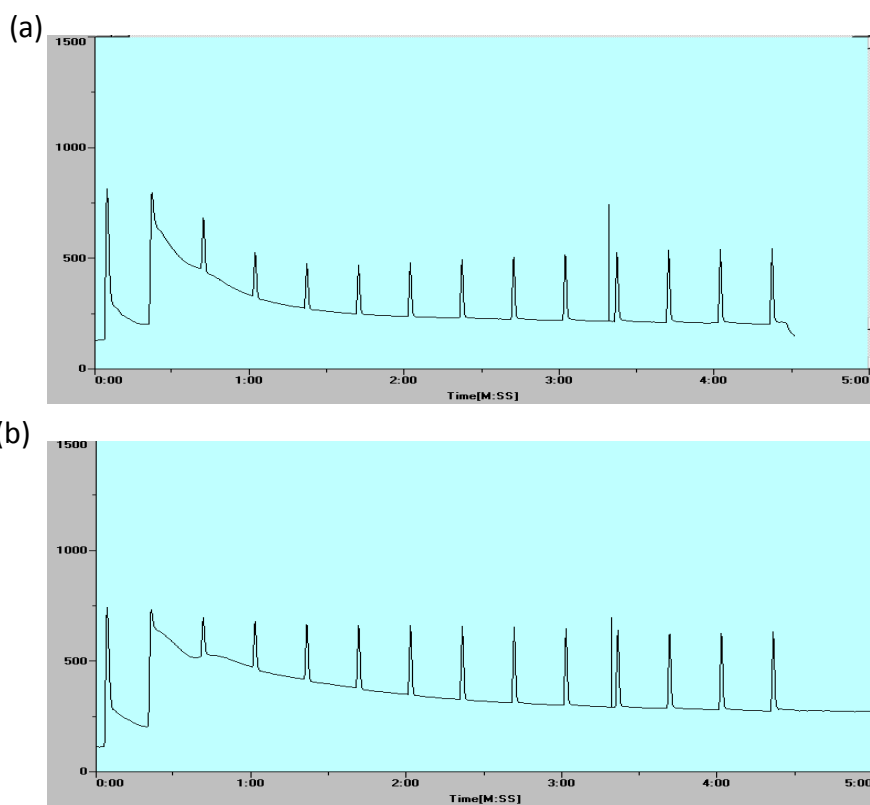


Figure 12 Measurement of chlorophyll fluorescence from an *Arabidopsis thaliana* leaf at 40 dag by a saturation pulse method using a PAM-2000 instrument (Walz). Col-0 (a), *psbs* (b).

To test if ROS level increased during senescence, a DAB staining was done. The detection of hydrogen peroxide (one of several reactive oxygen species) is described in mature *Arabidopsis* rosette leaves by staining with 3, 3'-diaminobenzidine (DAB) (Bindschedler et al., 2006; Daudi et al., 2012). As shown in Fig. 13, brown color reflected the H_2O_2 amount. It is obvious that *psbs* and *psan-2* were stained stronger than Col-0, which means that *psbs* and *psan-2* had more H_2O_2 at 40 dag.



Figure 13 The detection of hydrogen peroxide using DAB staining in leaves of Col-0 and mutants *psbs* and *psan-2* at the age of 40 days.

3.1.6. Analysis of dark-induced senescence

Leaf senescence can be the result of natural aging, but it also can be induced artificially by stresses, such as by shading individual leaves (Weaver and Amasino, 2001; Keech et al., 2007). Utilizing dark-induced senescence can avoid the influence of the differences in development stages of mutant plants which has an effect on age-dependent senescence.

Using this method the progression of leaf senescence was also followed after 30 dag. Covering of the whole plant evoked dark-induced senescence and this treatment was applied for three, seven or ten days.

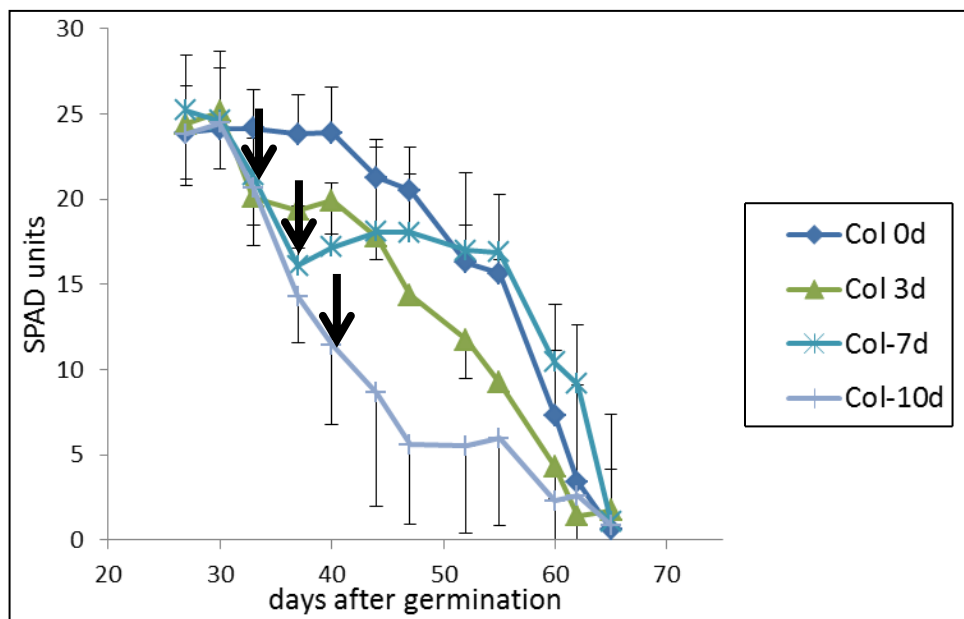


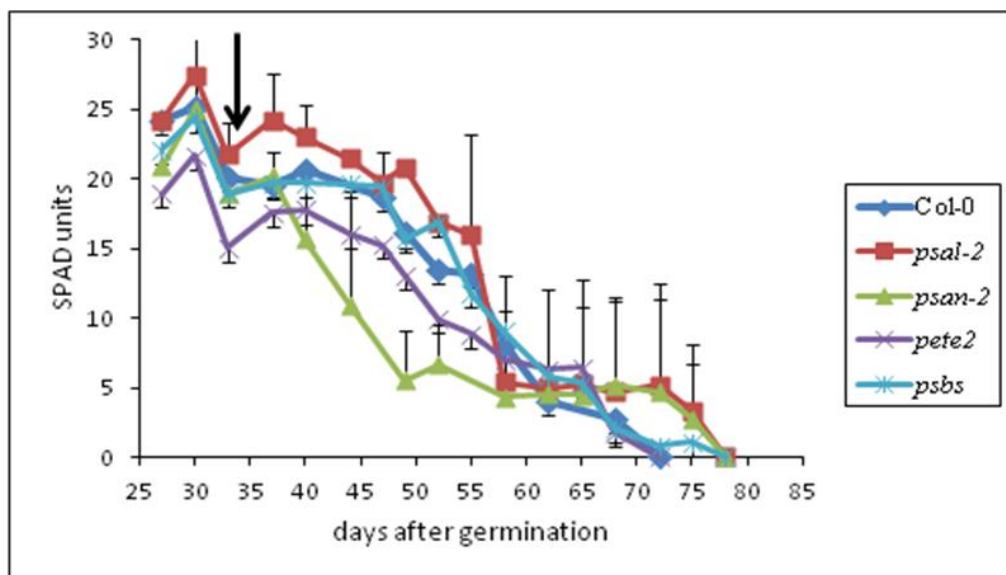
Figure 14 Dark-induced senescence in Col-0 with different periods of darkness treatments (3 days, 7 days and 10 days). Arrows indicate the respective end point of darkness treatment. Error bars represent the S.E. ($n = 12$ measurements from 4 different experiments) and in some cases are only indicated in one direction to avoid overlaps.

Analyzing WT (Col-0) it could be observed that when dark-treated plants returned to normal long-day conditions, the chlorophyll content had declined quickly in the darkness period but could recover in the normal growth conditions (Fig. 14). This could be seen for 3-day- and 7-day-long dark treatments but it was not the case for experiment where ten days of darkness was applied. These plants could no longer recover and early senescence was induced. It suggests that there is a ‘point of no return’ separating the pre-senescence from the irreversible senescence phase. In several plant species dark-induced senescence is fully reversible upon re-illumination and the leaves can re-green, but the re-greening ability depends on the duration of dark incubation (Parlitz et al., 2011).

3.1.7. Changes in the chlorophyll content of mutants during dark-induced senescence

As shown in Fig. 15, after 3 d of dark shading all the mutants showed a similar change in chlorophyll content compared to WT except *psan-2*, which could not recover after this dark-treatment.

(a)



(b)

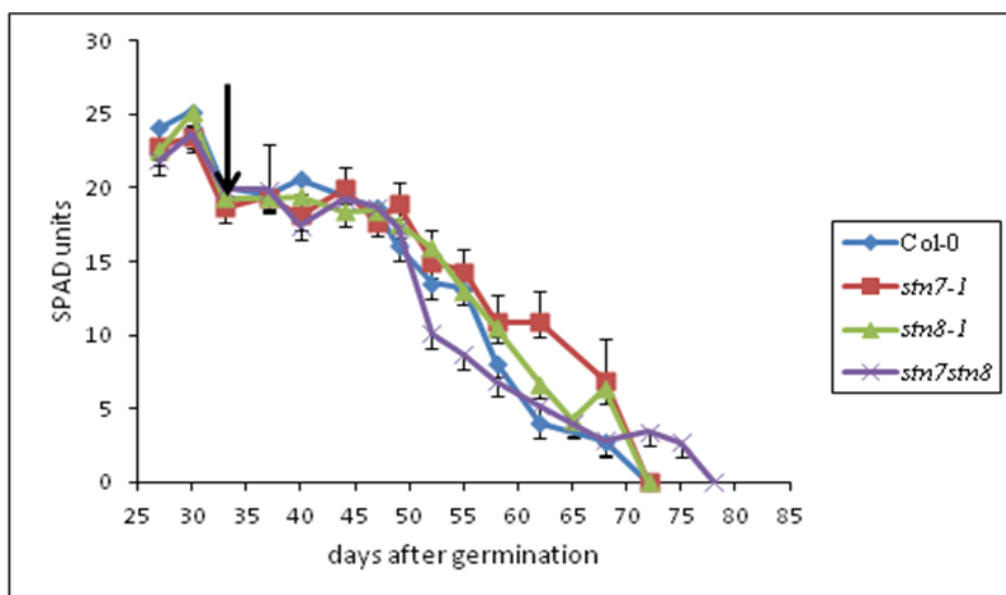
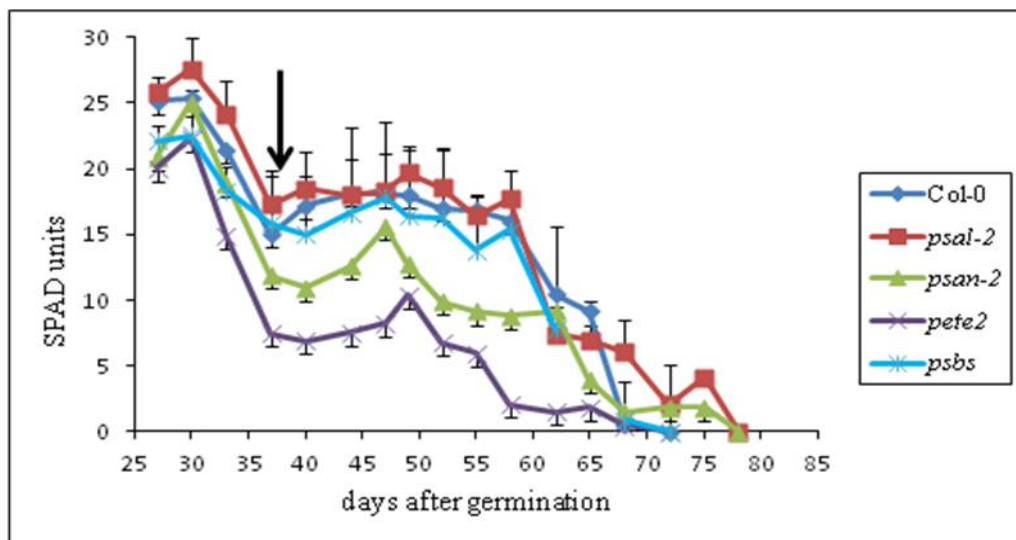


Figure 15 Chlorophyll amount of leaf No. 6 of Col-0 and mutants *psal-2*, *psan-2*, *pete2*, *psbs* (a) *stn7-1*, *stn8-1* and *stn7stn8* (b) after 3 days of darkness. Arrows indicate the respective end point of darkness treatment. Error bars represent the S.E. ($n = 12$ measurements from 4 different experiment) and in some cases are only indicated in one direction to avoid overlaps.

After seven days of dark incubation experiment (37 dag) in the mutants *psan-2*, *pete2*, *stn7-1*, *stn8-1* and *stn7stn8* the chlorophyll level decreased at the end of the dark treatment more than 2.5 fold, whereas Col-0 was only reduced about 1.7 fold (Fig. 16). Nevertheless, all lines could still recover, albeit slower than Col-0 (esp. *pete2*).

(a)



(b)

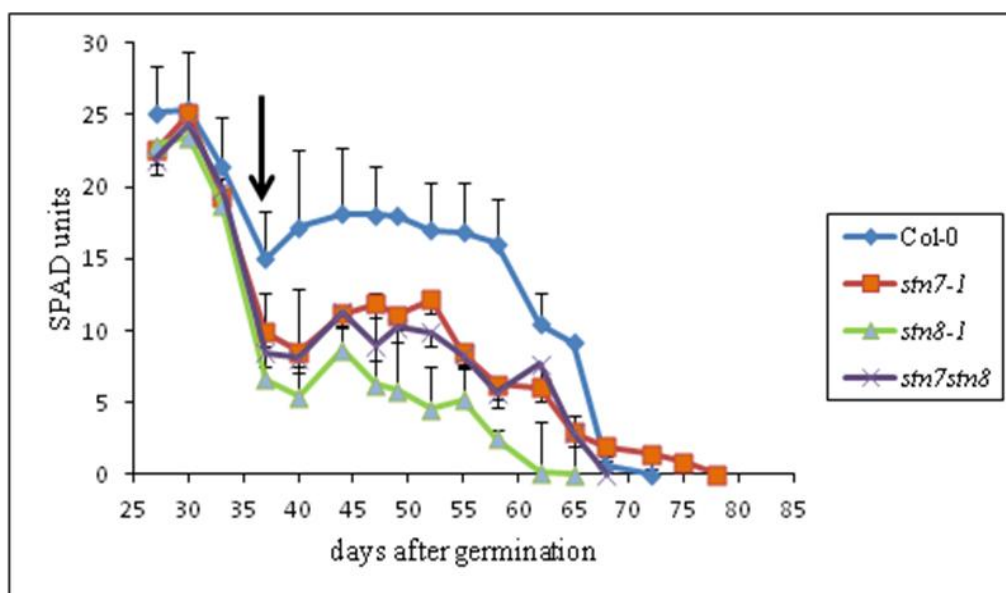
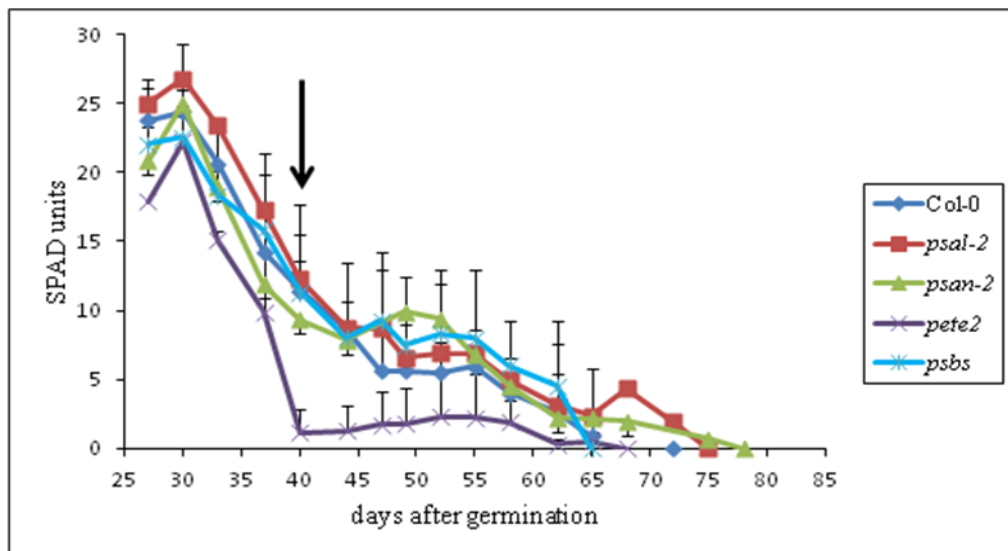


Figure 16 Chlorophyll amount on leaf No.6 of Col-0 and mutants *psal-2*, *psan-2*, *pete2*, *psbs* (a), *stn7-1*, *stn8-1* and *stn7stn8* (b) after 7 days of darkness. Arrows indicate the respective end point of darkness treatment. Error bars represent the S.E. ($n = 12$ measurements from 4 different experiment) and in some cases are only indicated in one direction to avoid overlaps.

Wild-type plants Col-0 lost about 50% of their chlorophyll after 10 d of dark incubation (Fig.14). However, for *pete2*, *stn7-1* and *stn8-1* the chlorophyll content declined more quickly and led to an even earlier plant death (Fig. 17).

(a)



(b)

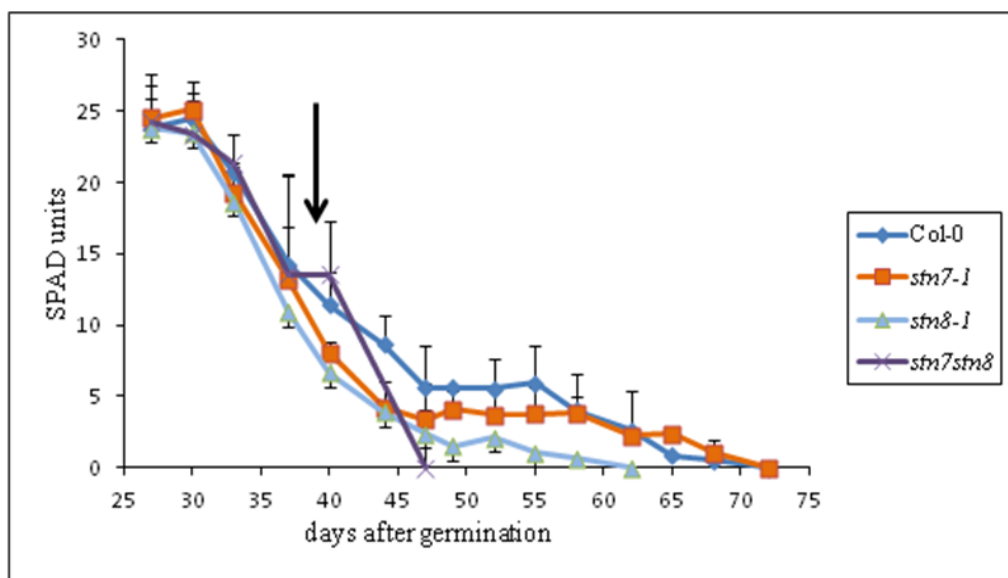


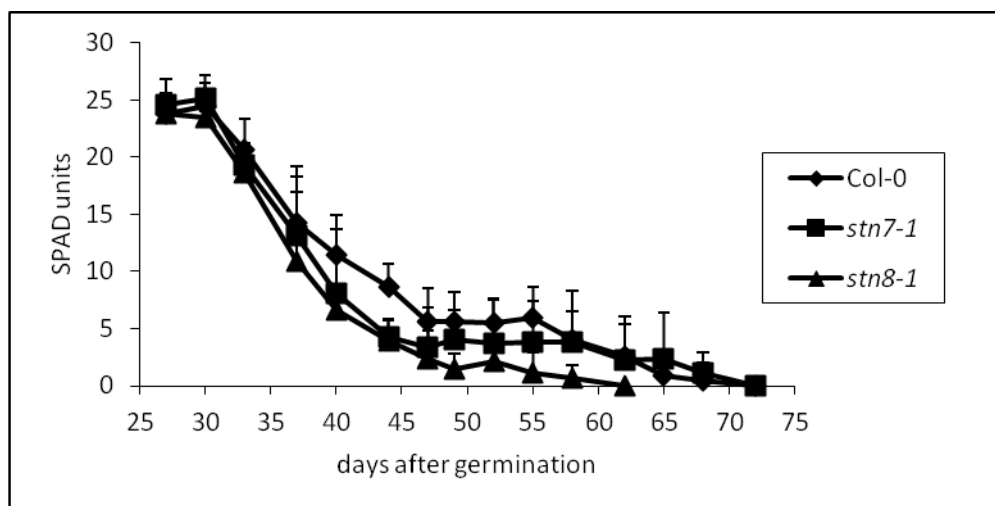
Figure 17 Chlorophyll amount on leaf No. 6 of Col-0 and mutants *psal-2*, *psan-2*, *pete2*, *psbs* (a) and *stn7-1*, *stn8-1* and *stn7stn8* (b) after 10 days of darkness. Arrows indicate the respective end point of darkness treatment. Error bars represent the S.E. ($n = 12$ measurements from 4 different experiment) and in some cases are only indicated in one direction to avoid overlaps.

3.2. Isolation of plants with defects in senescence

3.2.1. Screening of *stn8* EMS lines

The *stn8-1* mutant showed a significantly earlier decrease of chlorophyll content after a 10-day-long dark treatment, which was also reflected in a reduced number of surviving plants on soil. $70 \pm 10\%$ (as shown in Fig. 18a) of Col-0 plants could survive this treatment and recover, whereas for *stn7-1*, $45 \pm 11\%$ plants could recover and nearly all the plants of *stn8-1* were dead ($3 \pm 2\%$ survival rate).

(a)



(b)

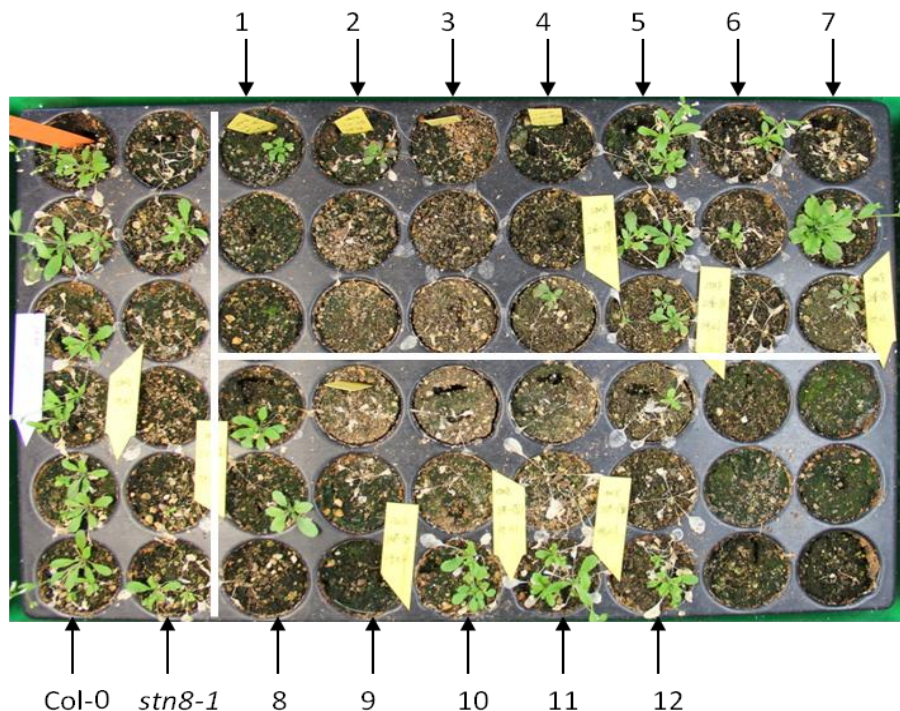


Figure 18 Phenotype of *stn8-1* and *stn8*-EMS lines. (a) Chlorophyll amount of leaf No. 6 of Col-0 and mutants grown in green house after 10 days of darkness. (b) Phenotyping of selected *stn8*-EMS lines after 10 days of darkness. 1-12 indicate the numbers of the reseted mutant lines. For each line 10 seedlings were tested, grown in three pots.

According to this phenotype, we screened a population of *stn8*-EMS lines to isolate lines that are more resistant to the 10 day dark treatment and survive.

Several families of M2 population were screened. In the first round, from each EMS family at least 80 seedlings were grown on soil, and in parallel Col-0 and *stn8-1* as control. Twelve lines were identified to be able to survive after 10 days dark treatment. In order to confirm these lines with positive phenotype, they were retested. For each line 10 seedlings were grown in parallel with Col-0 and *stn8-1* on the same tray. After retesting these 12 lines with three repeats, Fig. 18b shows a typical rescreening experiment where *stn8-1* lines cannot survive well but Col-0 can. Especially line No. 5 showed a high survival rate, but also the lines No. 6-8 and No. 10-11 could survive better compared to lines No.1-4, 9 and 12 and *stn8-1*. Lines No. 5 to 8 lines came from the same EMS family named *stn8-206*, whereas lines No. 10 and 11 were from *stn8-207* and *stn8-209*, respectively. After 10 days of dark treatment, 6 out of 10 plants of the line No.5 can recover. In contrast the survival rate for the other lines was below 20%.

Further physiological analysis of Line No. 5 showed that the size of the plants was not smaller than Col-0. This excludes that the survival of the plants was better due to a slower growth which could have escaped from the induction of the senescence by darkness. Therefore, No.5 (206-no.5) is a good candidate for further experiments.

(a)

lines	days of age with first fertilized flower
Col-0	26.8±0.9
<i>rer5-3</i>	25.0±1.1
<i>rer6-1</i>	26.0±1.0

(b)

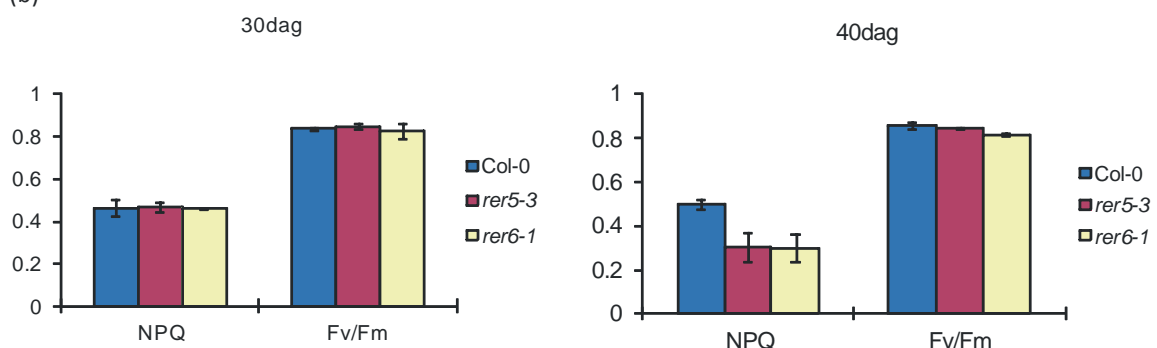


Figure 19 Characteristic of mutants: *rer5-3* and *rer6-1* during senescence. (a) Flowering time of mutants grown in green house. (b) PAM measurement on mutants and WT (Col-0).

3.2.2. Isolation of mutants with early senescence phenotype

In the laboratory a collection of double mutants was generated within the GABI-DUPLO project (Bolle et al., 2013). The parental lines and the generated double mutant lines were phenotypically characterized. One parental line was observed that showed earlier senescence, which was disrupted in *AtRER5* (Perez-Perez et al., 2013). This gene had been selected for the project as it is one homolog of a gene pair generated by segmental duplications, which shares high similarity in sequence and expressing pattern with its partner. To analyze this gene (*At2g40400/RER5*) and its function in more detail we also included the homologous gene (*At3g56140/RER6*) in our analysis.

To confirm the early senescence phenotype the changes in photosynthetic parameters in individual leaves of *rer5-3* and *rer6-1* during process of senescence, chlorophyll fluorescence was measured at two time points during development. According to the flowering time (Fig. 19a), it can be calculated that at the age of 30 dag senescence should start. PAM result indicated that Φ_{II} , qP, NPQ, qN, F_v/F_m were not changed compared to WT at an early senescence stage, but at 40 dag, NPQ declined much more strongly than in WT (Fig. 19b). As NPQ relies on xanthophyll cycle activity and formation of a proton gradient across the thylakoid membrane, it is not surprising that it declines during later stages of senescence (Horton et al., 1994).

3.3. The Reticulate-related (RER) protein family

3.3.1. Characterization of the RER protein family

The homologous proteins RER5 and RER6 belong to a small protein family, which was named after the first mutant isolated, *reticulata* (*re*) (Gonzalez-Bayon et al., 2006). The *Arabidopsis thaliana* mutant was characterized by its reticulate leaves (the leaf vascular network is greener compared to the paler lamina) and has been used for decades as a classical morphological mapping line. The mesophyll cell density was dramatically reduced in *re* mutant alleles of *RE* genes. The *re* mutant turned out to be also allelic to *lower cell density1* (*lcd1*), which shows increased sensitivity to ozone and virulent *Pseudomonas syringae* (Barth and Conklin, 2003).

Seven genes encoding proteins with high sequence similarity to *RE*, including *RER5* and 6, could be were identified in the *Arabidopsis thaliana* genome by BLAST analysis and comparison at the TAIR webpage (<http://www.arabidopsis.org/>). In a recent publication by (Perez-Perez et al., 2013) seven genes have been identified as members of the *RER* family and their nomenclature has been adapted here. Additionally an eighth gene belonging to this protein family could be identified (*RER7*).

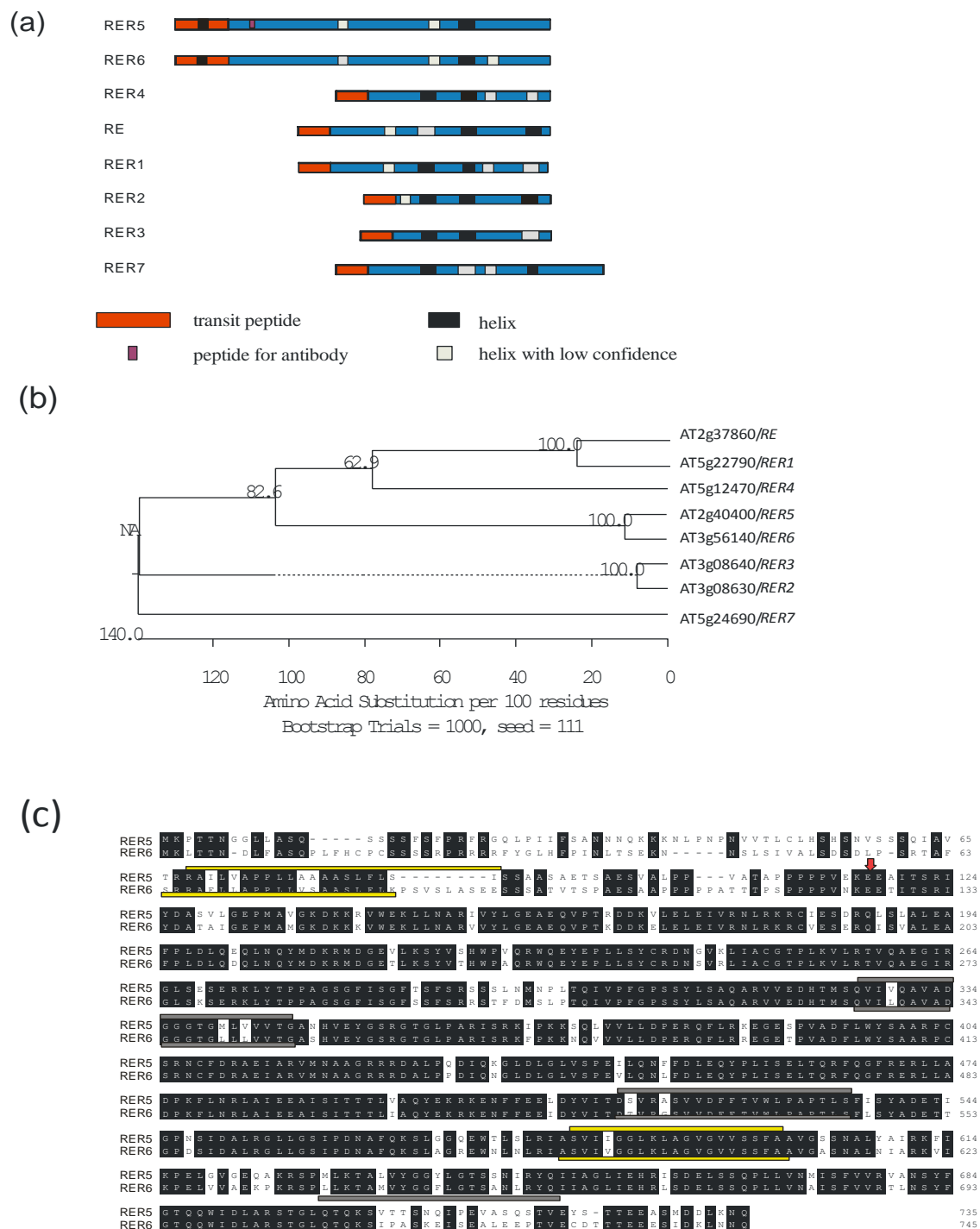


Figure 20 Comparison of the RER protein family.

(a) Schematic diagram of the six proteins of the RER protein family. Structural domains are drawn as rectangles. Red rectangles indicate the position of the transit peptide. Black rectangles (high confidence) and white rectangles (low confidence) mark helix structures. The purple rectangle indicates the peptide used for producing the antibody. (b) Phylogenetic tree showing the relationship between the RER proteins by comparing the amino acid sequences of the eight proteins in *Arabidopsis thaliana*. Evolutionary distances were computed using MegAlign software. The scale shows the number of substitutions per site. Bootstrap analysis was conducted using 1000 replicates. (c) Alignment of amino acid sequences of RER5 (*At2g40400*) and RER6 (*At3g56140*). The red arrow shows the putative cleavage position of the transit peptide, yellow underlined are helices with high confidence whereas underlined with gray indicates helices with low confidence. Prediction of helices is according to the Aramemnon website (<http://aramemnon.botanik.uni-koeln.de/>; Tmconsense).

As shown in Fig. 20a, the phylogenetic tree of the RER family of Arabidopsis was subdivided into four subgroups, with the three pairs, RER5 and RER6, RE and RER1 and RER2 and RER3. The amino acid alignment of RER5 and RER6 revealed that 80.4% of the residues were identical (Fig. 20b). The coding regions of RER5 and RER6 encoded two polypeptides of 735 and 745 amino acids each, with a predicted molecular mass of about 80 kD.

Compared to RER5 and RER6, the other members of the family were much shorter and lacked the N-terminal domain that had been annotated as the DUF399 domain, which contains one putative transmembrane spanning helix. In contrast the C-terminal domain had been defined as the DUF3411 domain and contains several helices that could be membrane spanning. Two to four helices were predicted by the Aramemnon website using Tmconsens (<http://aramemnon.botanik.uni-koeln.de/>; Fig. 20c).

3.3.2. Intracellular localization of RER protein family members

All members of this protein family are predicted to localize in the chloroplast. Indeed for RER5 and 6 we could estimate the size of the transit peptide by comparing the amino acid with homologous proteins in other plant species. For RER5 and RER6 a localization in the thylakoid lumen has been predicted by proteomic approaches (Peltier et al., 2002; Schubert et al., 2002), whereas the other members of the RER protein family have been identified as components of the chloroplast envelope (Ferro et al., 2003; Froehlich et al., 2003; Kleffmann et al., 2004; Dunkley et al., 2006; Zybailov et al., 2008; Ferro et al., 2010).

To verify the localization in plastids we used a transient expression system to localize GFP-fused proteins from the RER protein family in onion epidermis cells. As shown in Fig. 21, a similar subcellular pattern was observed for the six constructs tested, suggesting that RE, RER1, RER4, RER5, RER6 and RER7 were all localized within chloroplasts. The green fluorescence signal appeared additionally as a tail around the plastids, corresponding to so-called stromules. Stromules are extended stroma filled tubules from plastids (Boardman and Wildman, 1962; Schattat et al., 2011). Stromules do not contain thylakoids, suggesting that all RER protein family members, including RER5 and RER6, were localized in the envelope rather than the thylakoid membrane.

In order to accurately determine the sub-cellular distribution of these proteins, known organelle markers for the outer envelope membrane, OEP7 (Lee et al., 2001), and the inner envelope membrane, Tic 40 (Soll and Schleiff, 2004; Kessler and Schnell, 2006), were

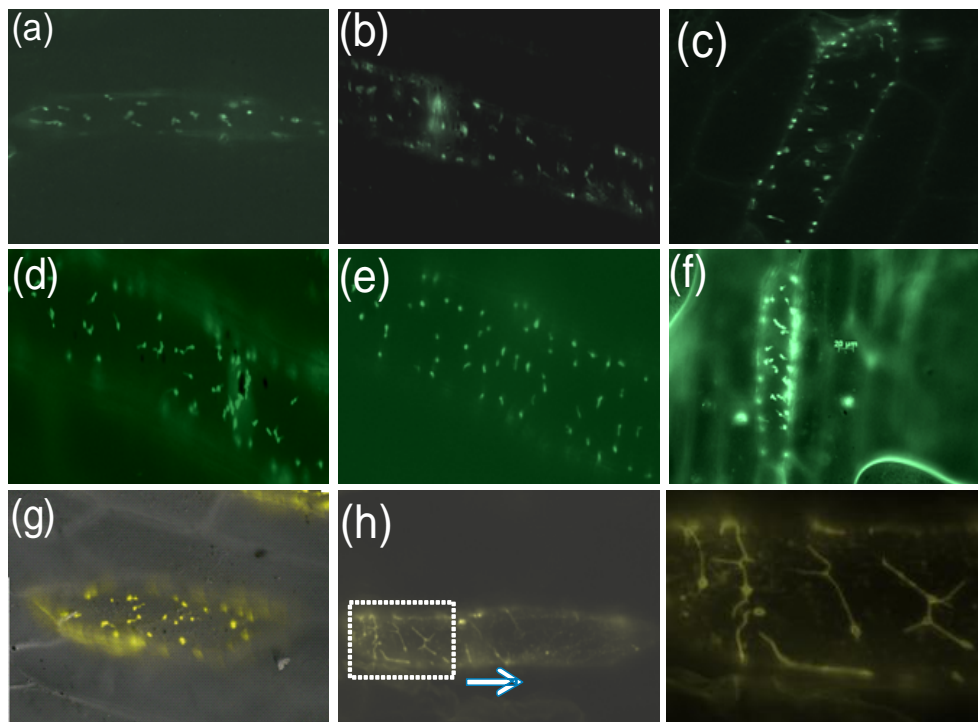


Figure 21 Subcellular localization in onion epidermal cells of *Arabidopsis thaliana* RER proteins. Translational fusion constructs to the reporter GFP were transiently expressed in onion epidermal layers by particle bombardment. Images made by Axio Imager microscope, (a) *AtRER5::GFP*, (b) *AtRER6::GFP*, (c) *AtRER4::GFP*, (d) *AtRER1::GFP*, (e) *AtRE::GFP*, (f) *AtRER7::GFP*, (g) *AtTic40::YFP*, (h) *AtOEP7::YFP*, (i) detail of (h).

tagged with the YFP reporter and expressed in onion epidermis tagged cells (Fig. 21g, 21h). The localization of *AtTic40::YFP* fusion protein showed same pattern as the RER protein family, as the yellow fluorescence signal was observed in stromules, but the stromules were not connected to other plastids. *AtOEP7::YFP* fusion protein displayed as a connecting network within the cell, in accordance with its localization in the outer membrane, described by (Sattarzadeh et al., 2011). These results strongly suggested that the RER protein family is localized in the inner envelope of plastids.

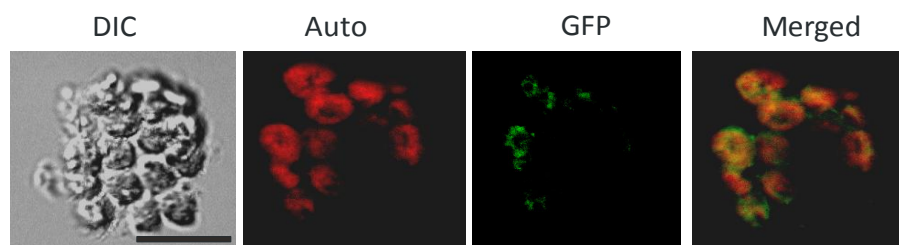


Figure 22 Fluorescence micrographs of *Arabidopsis thaliana* protoplasts extracted from overexpression lines. DIC, differential interference contrast image; Auto, chlorophyll autofluorescence; GFP, fusion protein; Merged, overlay of the two signals. Scale bar, 50 μ m.

To confirm these findings for chloroplasts we used Arabidopsis plants stable transformed with *AtRER5*-GFP and extracted protoplasts. Also here the localization in the envelope of the chloroplasts could be observed (Fig. 22), only when overexpressed RER protein was fused with GFP reporter. GFP fluorescence was found at the periphery of chloroplasts. As stromules are rarely visible in protoplasts, we did not expect to see these under these conditions.

3.3.3. Co-expression analysis of RER5 and RER6

To find some indications to the function of RER5 and RER6 we performed a database search to find genes that are co-regulated either with *AtRER5* and *AtRER6*. The result from this co-expression analysis showed that at least three of the five best correlated genes of *AtRER5* are encoding for proteins that are also localized in the chloroplast (Table 10a): *HEMA1*, which codes for a protein with glutamyl-tRNA reductase (GluTR) activity (Schmied et al., 2011) and which is involved in the early steps of the chlorophyll biosynthesis; *At4g34730*, which encodes for a ribosome-binding factor A family protein (Lit) and *ATOSAI*, which encodes for a chloroplast envelope protein involved in sensitivity toward oxidative stress and high light (Jasinski et al., 2008). *At1g19450* encodes for an integral membrane protein with a predicted carbohydrate transporter activity and *At3g27050* encodes for a protein of unknown function.

(a)RER5

MR	Cor	Locus	Function
3.9	0.64	At1g58290	HEMA1; glutamyl-tRNA reductase
17.8	0.64	At4g34730	ribosome-binding factor A family protein
1.7	0.63	At1g19450	integral membrane protein, putative / sugar transporter family protein
13.1	0.62	At3g27050	unknown protein
20.1	0.62	At5g64940	ATATH13; transporter

(b)RER6

MR	Cor	Locus	Function
4.0	0.68	At5g58870	ftsh9 (FtsH protease 9); ATP-dependent peptidase/ ATPase/ metallopeptidase
10.1	0.64	At5g25630	pentatricopeptide (PPR) repeat-containing protein
13.1	0.67	At4g37200	HCF164; oxidoreductase, acting on sulfur group of donors, disulfide as acceptor
13.9	0.67	At1g49970	CLPR1; serine-type endopeptidase
13.9	0.66	At2g20920	unknown protein

Table 10 Co-expression profile of *AtRER5* and *AtRER6*. Co-expressed genes for Arabidopsis genes were predicted using ATTED-II (<http://atted.jp/>).

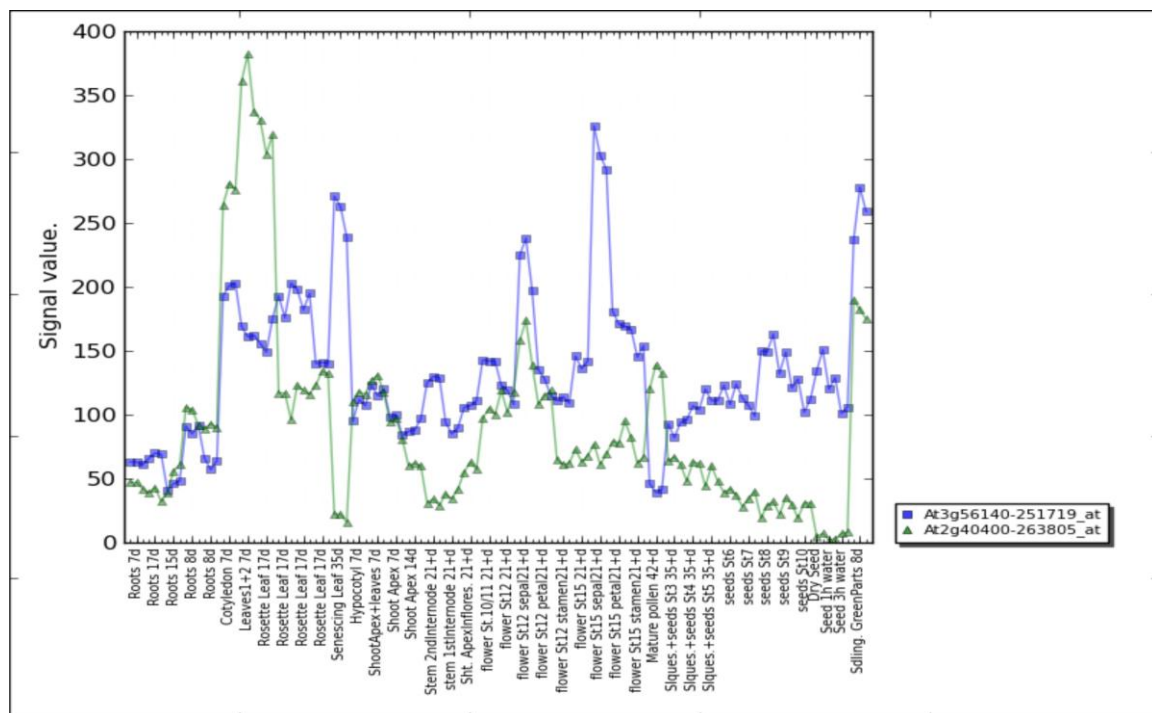


Figure 23 Microarray expression pattern of *AtRER5* and *AtRER6*. The green lines represents *At2g40400* (*AtRER5*), the blue lines indicates *At3g56140* (*AtRER6*). (<http://bar.utoronto.ca/welcome.htm>)

Also *AtRER6* was co-expressed with many genes encoding plastidic proteins: FtsH protease 9, which is important for chloroplast homeostasis (Lindahl et al., 1996; Ostersetzer and Adam, 1997; Bailey et al., 2002); a PPR- repeat containing protein, HCF164, which is a thylakoid membrane anchored thioredoxin-like protein; the endopeptidase ClpR1 which is required for chloroplast development and differentiation (Motohashi and Hisabori, 2006) and *At2g20920* with an unknown function. (Table 10b)

Interestingly, *RER5* and *RER6* were not co-expressed, and utilizing microarray it can be shown that both genes are regulated in opposite ways. The expression of *AtRER5* was high in cotyledon tissue, where *AtRER6* was higher in flower sepal tissue (Fig. 23). This suggests that in younger plants more of *RER5* is present whereas in older plants *RER6* prevails.

3.3.4. Phenotypic characterization of loss-of-function lines of *RER5* and *RER6*

To further examine the function of *RER5* and *RER6* in *Arabidopsis* development, the knock-out mutants *rer5-3* and *rer6-1* were characterized. The mutant termed as *rer5-3* contained a T-DNA within the 7th exon of the *RER5* gene, whereas *rer6-1*, with 2238 bp CDS, harbored a T-DNA insertion at position +927 within 2nd intron. We did PCR tests with DNA templates using primers *AB56-L/27ah-R* (for confirmation amplicon of *AtRER5*), *AB56-L/8409* (genotyping amplicon to confirm presence of insertion); *AD05-*

L/29ah-R (for confirmation amplicon of *AtRER6*), *AD05-L/R204* (genotyping amplicon to confirm presence of insertion). The result showed that both lines were homozygous.

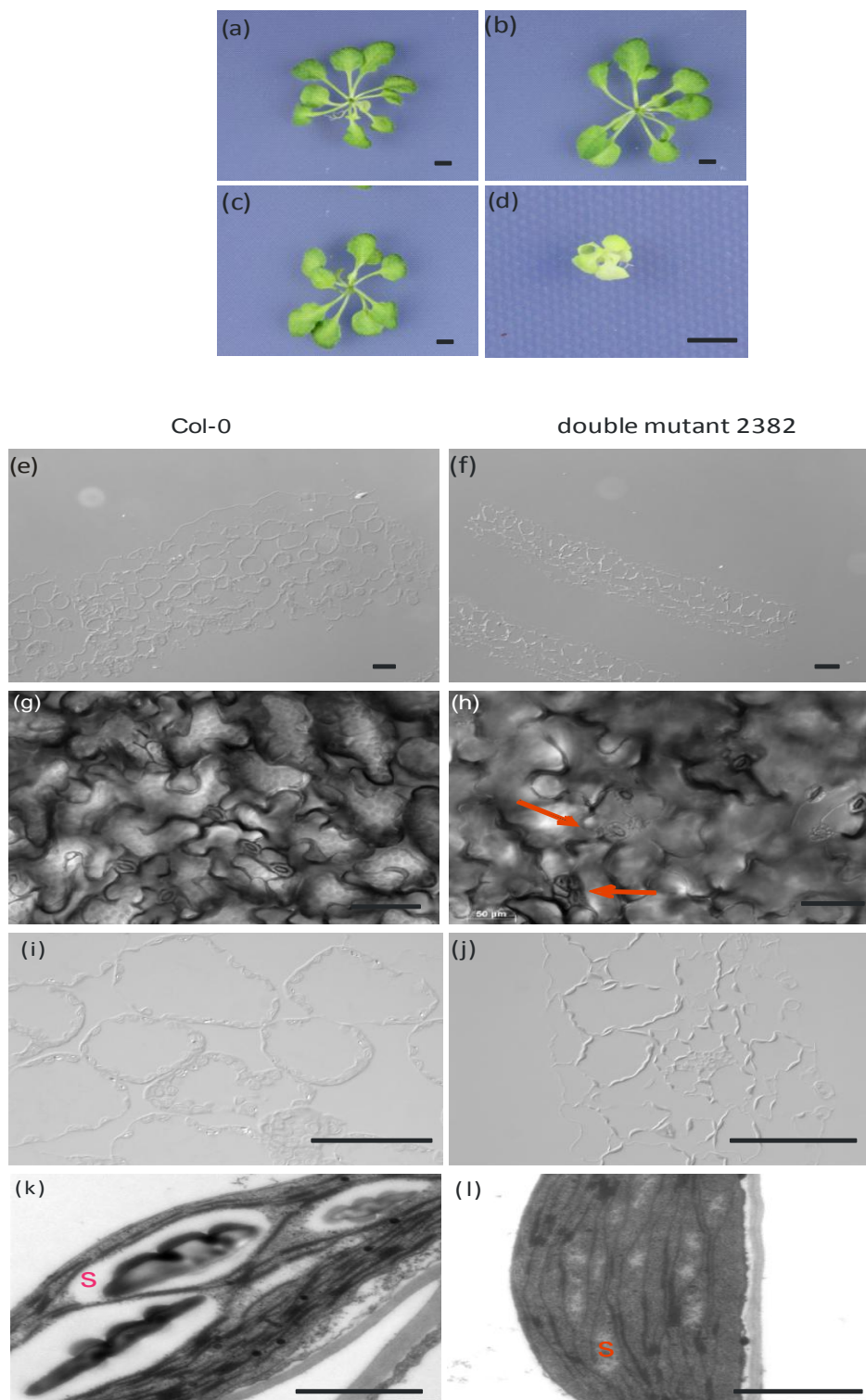


Figure 24 Phenotype characteristic of *Arabidopsis thaliana* RER mutants, compared to wild-type (Col-0), WT. Four-week-old WT (a) and the mutant plants *rer5-3* (b), *rer6-1* mutant (c) and the double mutant *rer5-3/rer6-1* (d), grown on MS plates with 1% sugar. Bars, 5 mm. Structures of cotyledons from WT (e, g, k) and the double mutant *rer5 rer6* (f, h, j, l) (e-f) Transverse sections of the cotyledons. Bars, 10 μ m. (g-h) Leaf epidermis from the abaxial side of the cotyledons. Bars, 10 μ m. Arrows indicate clusters of stomata. (i-j) Details of palisade cells. Bars, 10 μ m. (k-l) Ultrastructures of chloroplast. S, starch granule. Bars, 1 μ m.

As shown in Fig. 24a, no obvious phenotype could be observed in both mutants; especially the reticulated phenotype described for *re* was not visible (Rebeca G et al. 2006). As *AtRER5* and *AtRER6*, which show very high similarity at the protein level functional redundancy between two proteins could be the reason no phenotype was observed. Therefore, a double mutant (*rer5-3/rer6-1*) was generated by crossing *rer5-3* with *rer6-1*. The double mutant was extremely small compared with the parental single mutants, exhibited chlorotic cotyledons and leaves, and was arrested in growth (Fig. 24a). The plants had to be grown on medium with supplied sucrose to survive, were not able to grow on soil and did not enter the reproductive phase.

In the double mutant, the leaf was much smaller than WT (Fig. 24a, 24d). This could be due to a smaller size of the cells, a reduced number of cells or changes in the internal leaf anatomy. In order to compare the double mutant better with WT, we first analyzed the cotyledons of the double mutant and WT that had about the same size and age. Examination of intact cotyledons by electron microscopy is shown in Fig. 24e-l. Transverse sections of the cotyledons from the double mutant *rer5-3/rer6-1* revealed that all the cross sections looked similar to WT, but the thickness was three-folds reduced and whereas in WT six cell layers could be discriminated between the epidermis, in the double mutant four cell layers were visible (Fig. 24e-f, Table. 11). In contrast to *re*, transverse sections revealed areas with a greatly reduced number of both palisade and spongy mesophyll cells (Gonzalez-Bayon et al., 2006). This phenotype could not be observed in the double mutant. Looking at the cell level, as shown in Fig. 24i-j, also the palisade cells were about two-times smaller compared to WT. Additionally it was notable that the chloroplasts were flatter shaped compared to WT.

Table 11 Comparison on cotyledon structure and cell sizes between WT and *rer5-3/rer6-1*.

	Thickness of cotyledons (μm^2)	Size of palisade cells (μm^2)	Total number of stoma (0.6 mm^{-2})
Col-0	288,7 \pm 20,6	3380,4 \pm 461,4	4 \pm 1
<i>rer5-3/rer6-1</i>	99,4 \pm 9,0	1658 \pm 269,3	25 \pm 2

Therefore, we evaluated the ultrastructure of chloroplasts in mesophyll cells of cotyledons from the double mutant and WT. We could observe that the grana stacks

seemed slightly less abundant and the starch grains in chloroplast not really visible for double mutant. The ultrastructural results together with the fact that the double mutant exhibited leaf chlorosis strongly suggested that normal expression of the *AtRER5* and *AtRER6* was not required for chloroplast development, but for proper function.(Fig. 24k-l)

With regard to the abaxial epidermis cells as shown in Fig. 24g-h, stomatal cluster frequency was higher on cotyledons of the double mutant. Additionally, the overall number of stomata was about six-folds more in double mutant compared to WT. Stomatal density reported for the abaxial side of cotyledons was about 25 ± 2 per 0.6 mm^2 field for double mutant (Table 11)

3.3.5. Metabolic analysis of *rer5-3/rer6-1*

As RER5 and RER6 are localized within the inner envelope of chloroplasts and from the morphological analysis we can see a reduced accumulation of starch in the chloroplasts and dwarfish growth we assumed that both proteins could be transporters that shuttle metabolites between the chloroplast and the cytosol. Furthermore, it has been shown that *RE* and *CUE1* act in the same developmental pathway affecting leaf development

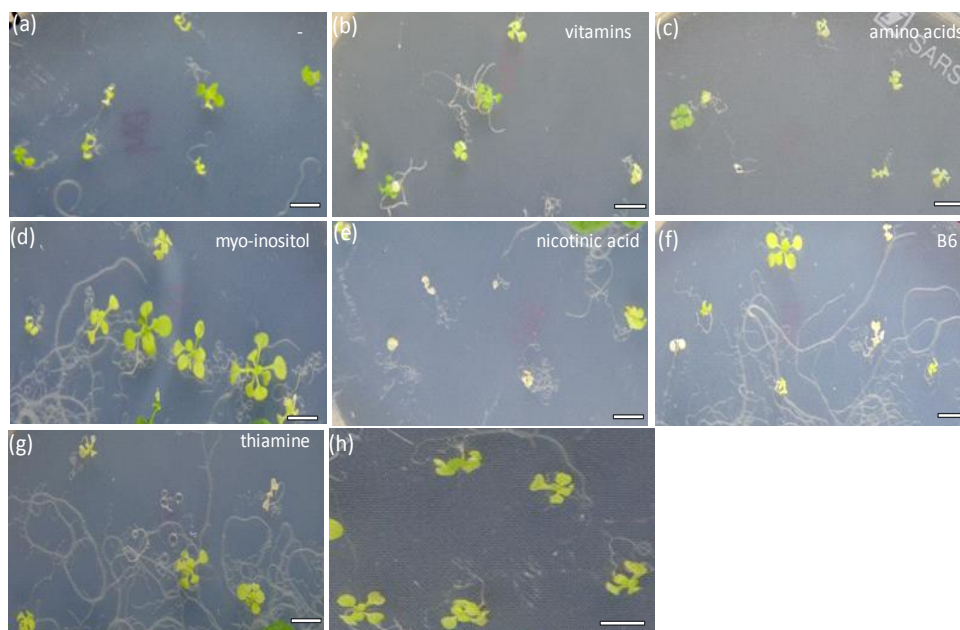


Figure 25 Exogenous application of vitamins and amino acids to two-week-old double mutant (*rer5-3/rer6-1*), photographed after 2 weeks. Bars, 5mm. *rer5-3/rer6-1* was grown on different media. (a) 1x basal MS media with 2% sugar. (b) 1x MS media including vitamins with 2% sugar. (c) 1x basal MS media with 2% sugar, amino acids. (d-g) 1x basal MS media with 2% sugar and either myo-inositol, nicotinic acid, pyridoxine hydrochloride or thiamine hydrochloride. (h) 1x MS media including vitamins with 2% sugar and amino acids.

(Gonzalez-Bayon et al., 2006). CUE has been characterized as a phosphoenolpyruvate (PEP)/phosphate translocator (PPT) of the plastid inner envelope (Voll et al., 2003). As PEP is essential for the shikimate pathway, which leads to the production of aromatic amino acids, the reticulate phenotype of CUE1 mutant can be rescued by feeding aromatic amino acids. Therefore, we did a feeding experiment where the amino acid Tyrosine, Tryptophan and Phenylalanine were supplied to the 1xMS medium (with vitamins). Our results showed that *rer5-1/rer6-1* can grow bigger and greener by this treatment (Fig. 25h), but exhibited variegated leaves (Fig. 26e).

To test whether the *rer5-3/rer6-1* phenotype could be restored by exogenous application of the aromatic amino acids without vitamins, plants were supplemented with these amino acids on basal 1xMS medium, but no improved compared to the control could be observed (Fig. 25c). This indicated that *rer5-3/rer6-1* needed vitamins, not amino acids for better growth. The vitamins solution for plant cell culture contains glycine, myo-inositol, nicotinic acid, pyridoxine hydrochloride and thiamine hydrochloride. Each vitamin was supplemented individually to the double mutant. And the results showed that only myo-inositol could partially rescue the double mutant phenotype (Fig. 25d, 26b).

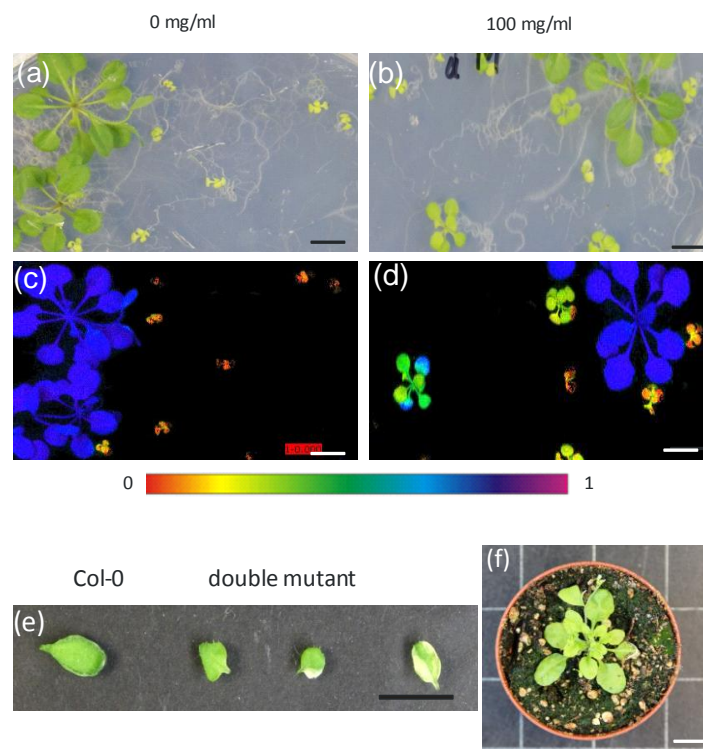


Figure 26 Exogenous application of myo-inositol to two-week-old WT and the double mutant (*rer5-3/rer6-1*). WT and *rer5-3/rer6-1* on MS plates photographed after supplemented without myo-inositol (a) and (b) with 100 µg/ml myo-inositol for two weeks. (c, d) Photosynthetic performance of plants photographed by imaging-PAM displaying the F_v/F_m ratios. (e) Leaf phenotype of double mutant after feeding with vitamins and amino acids. (f) Plant phenotype of double mutant after feeding with 100 µg/ml myo-inositol. Bars, 5mm.

With respect to the phenotype of WT, there was no difference between the treatment with and without myo-inositol (Fig. 26a-b). Furthermore, another chlorotic mutant, *dov1*, could not be rescued by this treatment showing the specificity of myo-inositol for the double mutant. The double mutant, pre-grown on 1x basal MS media with 100 $\mu\text{g}/\text{ml}$ myo-inositol, could be transferred to soil, flower and produce viable seeds (Fig. 26f). Interestingly, Col-0 after feeding with myo-inositol showed a retarded growth phenotype, but the double mutant *rer5-3/rer6-1* displayed an increased size of plant area of five-folds after myo-inositol feeding compared to no feeding, as shown in Fig. 27. In addition the leaves can turn greener, but they are not completely rescued by the feeding experiment. After two weeks feeding, WT and *rer5-1/rer6-1* plants were subjected to Chlorophyll fluorescence measurements to monitor their photosynthetic performance (Fig. 26c-d). According to leaf color from Imaging PAM measurement, in Fig. 26c, the data showed a lower maximum quantum yield of PSII (F_v/F_m) in double mutant compared to WT. In Fig. 26d, the *rer5-3/rer6-1* was able to partly restore F_v/F_m , but not to the WT level.

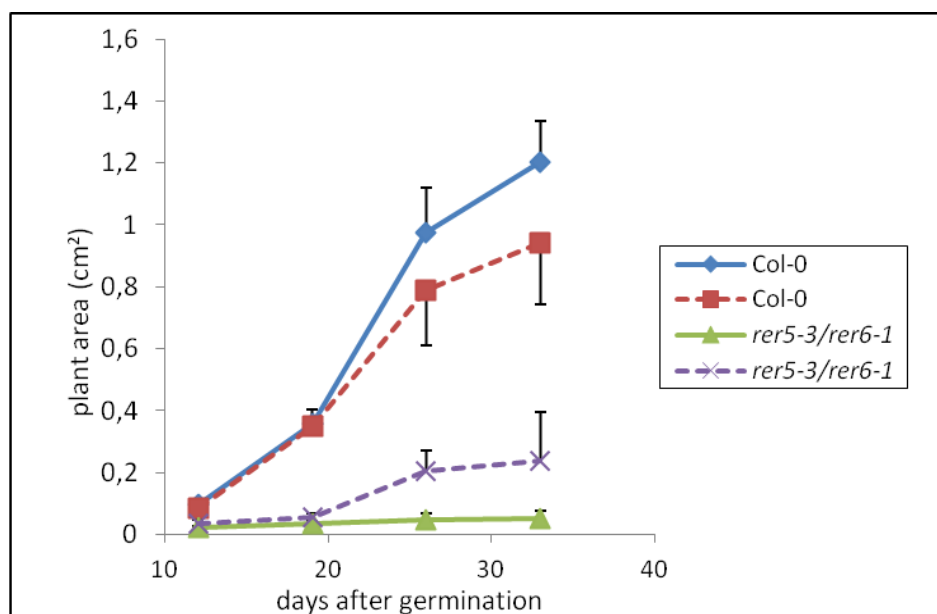


Figure 27 Growth kinetics of Col-0 and double mutant (*rer5-3/rer6-1*). Col-0 and *rer5-3/rer6-1* were grown on 1x basal MS media, dotted lines of Col-0 and *rer5-3/rer6-1* represent plants which were grown on 1x basal MS media with 100 $\mu\text{g}/\text{ml}$ myo-inositol.

To assess whether the double mutant had a defect on the myo-inositol synthesis, we compared 20-day-old plants of Col-0 and using mass spectrometry. As shown in Fig. 28, the level of inositol was significantly decreased (15.7-folds) in the *rer5-3/rer6-1* mutant compared to Col-0.

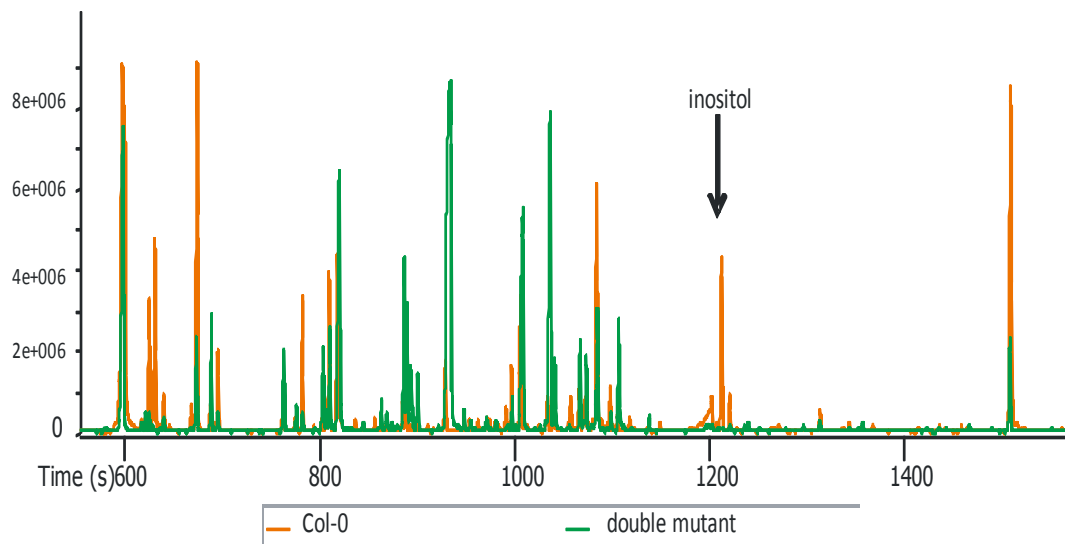


Figure 28 Metabolic analysis of Col-0 and double mutant (*rer5-3/rer6-1*) by mass spectrometry. Orange lines indicates Col-0, green lines shows double mutant. Black arrow points out the fragment of inositol.

3.3.6. Overexpression lines for RER5 and RER6

To further examine the function of RER5 and RER6 in Arabidopsis development, we generated transgenic lines overexpressing RER5 and RER6 under the control of the 35S promoter and fused to the GFP tag (*35S:AtRER5-GFP* and *35S:AtRER6-GFP*). Positive lines were identified and confirmed by RT-PCR (Fig. 29). The semi-quantitative RT-PCR results showed a visible increase in the mRNA in all four lines (Fig. 29e). In order to further confirm that the protein was also overexpressed, we tried western blot with a GFP antibody, but the signal was too weak to detect. A peptide antibody against RER5 which had been generated was also not able to detect any band in the WT and the overexpression lines. We were able to detect a weak GFP signal in isolated protoplast, localized in chloroplasts (Fig. 22).

As shown in Fig. 29b, when grown in the greenhouse, lesion formation on mature leaves of the overexpression lines of both genes could be observed. Lesions typically appeared at the age of four weeks and could spread until they covered the whole leaf, but on most leaves, the main vein and leaf margins remained green (Fig. 29b-c). Mutants also displayed severe growth reduction, and newly formed leaves were crumpled and serrated. When grown on MS agar medium with 1% sugar three weeks after germinating necrosis began to appear on older leaves, whereas WT looked normal.

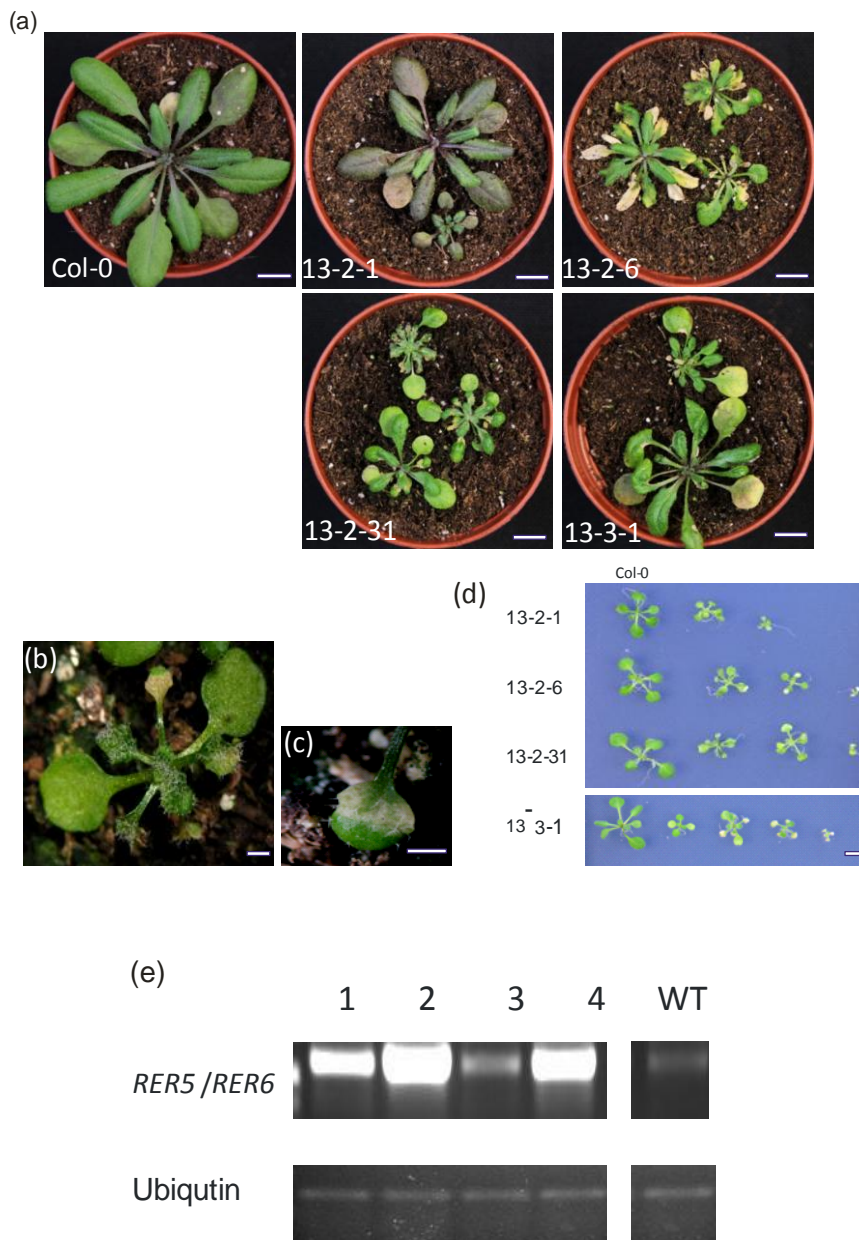


Figure 29 Characterization on F2 generation of four overexpression lines. (a-e) Four-week-old seedlings grown in greenhouse. Col-0, WT; 13-2-1, 13-2-6, 13-2-31, overexpression lines of RER5 fusion with GFP reporter; 13-3-1, overexpression line of RER6 fusion with GFP reporter. Bars, 5 mm. (b-c) Close-up on the leaf phenotype of overexpression line. Bars, 1 mm. (d) Four overexpression lines grown on 1x basal MS agar medium with 1% sugar for three weeks. Bars, 5mm. (e) RT-PCR analysis of four overexpression lines. **1**, 13-2-1; **2**, 13-2-6; **3**, 13-2-31; **4**, 13-3-1.

To determine more precisely where the lesions were positioned, we performed typan blue staining (Fig. 30). Dead cells in the tissues were made visible with a blue color. A comparison between leaves from *rer5-3/rer6-1*, overexpression lines and WT at the same leaf age showed that *rer5-3/rer6-1* displayed more dead cells compared to WT (Fig. 30b). For overexpression lines, as shown in Fig. 30c, the dead cells were accumulated at the basal part of leaf. In Fig. 30d, the crumpled part of the leaf of the overexpression line

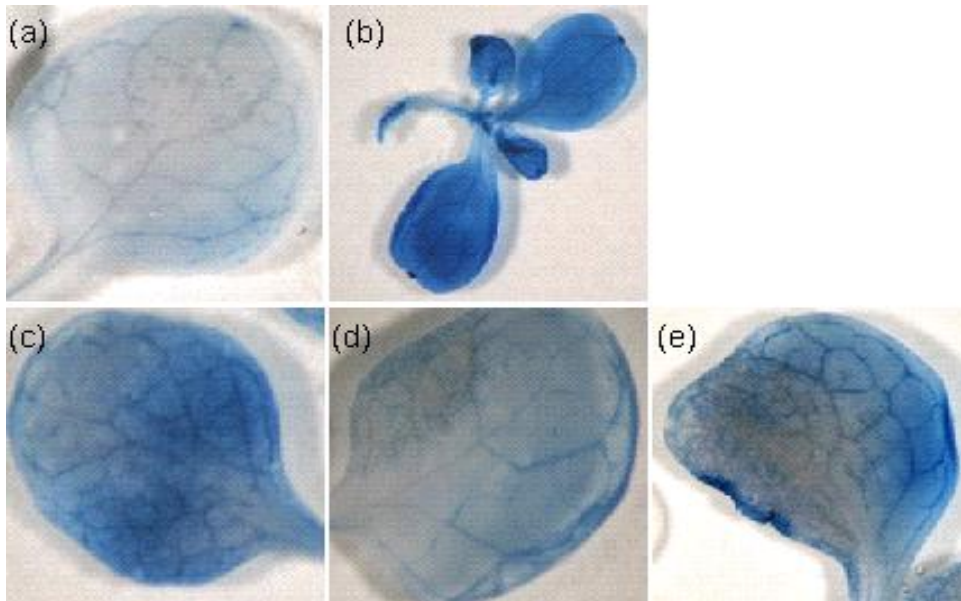


Figure 30 Cell death in leaves caused by mutations in genes of RER family. Typan blue staining in vascular cells from (a) Col-0, WT; (b) double mutant (*rer5-1/rer6-1*); (c)-(e) overexpression lines: 13-2-1, 13-2-6, 13-3-1.

AtRER6 was stained stronger. In Fig. 30e, much more dead cells were visible at the margin area of the leaf from different overexpression lines.

And metabolic analysis on overexpression lines is undergoing, in order to verify if myo-inositol relates to these early cell death phenotype.

4. Discussion

4.1. Photosystem and Senescence

4.1.1. Age-dependent senescence

Leaf senescence is an important phase in every plants life cycle (Nam, 1997; Buchanan-Wollaston et al., 2003; Lim and Nam, 2005), especially in annual plants such as *Arabidopsis thaliana*. Senescence on organ level starts shortly after the initiation of the reproductive phase. It is a regulated degeneration process that helps the recycling of nutrients from old tissue to young tissue or to the reproductive organs. During senescence leaf cells undergo changes in cell structure, metabolism, and gene expression in an orderly fashion. The breakdown of the chloroplast is the earliest and most significant change as chloroplasts contain up to 70% of the leaf protein. On the metabolic level, catabolism of chlorophyll and macromolecules, including proteins, membrane lipids, and RNA replace carbon assimilation via photosynthesis.

Although it has been reported that the total soluble protein content, especially enzymes in Calvin cycle such as Rubisco decreased markedly during senescence (Martinez et al., 2008), it is hard to determine whether the absent of photosynthetic subunits or defects in state transitions contribute to early senescence. Therefore, several mutants with defects in different PS related process were analyzed on their behavior of senescence.

Table 12 Data on senescence parameters of mutants in comparison with wild type (Col-0).

The yellow cell means that the value is the same or similar to Col-0. A much higher (lower/earlier) value is represented by red (green) cells. Blank cell means no data.

mutants	DOS-DF (days) ¹	Ratio of NPQ ²	Ratio of Yield ²	Ratio of Fv/Fm ²	Survival ratio at 52 dag	Decline of Chl. in age dependent senescence	Decline of Chl. in dark induced senescence
<i>psad2-1</i>	Yellow	Yellow	Yellow	Yellow	Yellow	Yellow	Yellow
<i>psal-2</i>	Red	Yellow	Yellow	Yellow	Green	Green	Yellow
<i>psan-2</i>	Green	Yellow	Yellow	Yellow	Yellow	Green	Green
<i>psbs</i>	Yellow	Green	Red	Red	Green	Green	Yellow
<i>pete2</i>	Yellow	Yellow	Yellow	Yellow	Green	Yellow	Green
<i>stn7-1</i>	Yellow	Yellow	Yellow	Yellow	Yellow	Green	Green
<i>stn8-1</i>	Yellow	Yellow	Yellow	Yellow	Yellow	Green	Green
<i>stn7stn8</i>	Yellow	Yellow	Yellow	Yellow	Yellow	Green	Green
<i>oeSTN8</i>	Blank	Red	Yellow	Yellow	Red	Blank	Blank

¹ Days of onset of senescence minus Days of flowering time

² The ratio is between 28 dag and 40 dag.

The natural senescence of *Arabidopsis thaliana* leaves in this study was characterized by their decrease in Chlorophyll content and photosynthetic capacity. The developmental stage of the plants was determined by the arrest of leaf growth and flowering time. Up to the flowering time plants did not appear to induce senescence in leaf. No 6 as without decrease in chlorophyll content for wild-type Col-0 (as a control line here) could be observed. The decline of chlorophyll content only started at 40 dag, suggesting that senescence starts about three to five days after onset of flowering.

In the photosynthesis-related mutants onset of senescence was usually similar to wild-type (Col-0), only for *psal-2* it was 13 days later, and for *psan-2* was 5 days earlier. This shows that in these lines the developmental progress is disturbed. For *psal-2*, a high chlorophyll content during flowering stage can be seen suggesting an efficient photosynthesis and a high concentration of sugar even during flowering. Furthermore, the chlorophyll value was evaluated. Mutant *psal-2* has the strongest decline of chlorophyll content after reaching its maturity. This is also confirmed by the results from chlorophyll fluorescence measurement, at 40 dag where significant reduction of PSII (F_v/F_m) activity could be measured for *psal-2*. This means that *psal-2* exhibited late maturation but a deep decline of chlorophyll, with an early damage of PSII.

On the other hand, *psan-2* exhibits a decline of chlorophyll content directly after initiation of flowering. It represents a strong senescence phenotype. The other mutants have no strong difference compared with Col-0, when compared to the developmental phase.

Interestingly, all the mutants had reduced PSII activity (ϕ_{II} and qP) at the initiation of senescence (40 dag), similar as Col-0. Therefore, the presented data are consistent with the conclusion that there is a parallel loss of chlorophyll and PSII throughout senescence. qN and NPQ on the other hand were not changed in Col-0 (Table 9). This means at the earlier stage of senescence plants have an advantage at maintaining photosynthetic electron flow even at 40 dag. During senescence a higher stability of PSI was observed, which would allow cyclic electron flow (Hilditch et al., 1986). From the results of chlorophyll fluorescence measurement, all the mutants behaved similar to Col-0 except *psbs* (Fig. 12). The difference between Col-0 and *psbs* is that for *psbs*, the F_m' value (the maximum fluorescence, obtained after a saturation flash) remained stable for 3 min, without the decline seen in Col-0. This suggests that the loss of PSII is earlier than PSI in the process of senescence. This perhaps is because of the low non-photochemical quenching of *psbs* (Table 9, Roach and Krieger-Liszkay, 2012).

Analysis of fluorescence quenching parameters at steady state photosynthesis showed that during senescence non-photochemical quenching (qN) increased and photochemical quenching (qP) decreased. It has been concluded that the decrease in qP is the result of an increase in proportion of Q_B non-reducing PSII reaction centers (Zhang et al., 1998). This would increase the risk of photoinhibition since at decreased qP the portion of excitation energy used in the photochemical process is decreased. As shown in Fig. 10 from 28 dag to 40 dag a lower qP and a higher qN can be seen for Col-0 during leaf senescence. This is consistent with the above theory.

But there are two exceptions to this, namely *psbs* and *oeSTN8*. For *psbs*, all the values (ϕ_{II} , qP, qN, NPQ) were nearly half reduced at 40 dag, which means a strong damage in PSII. Li et al. (2000) has shown that mutants lacking PsbS showed a reduced NPQ and was involved in preventing premature cell death. But we found not only decreased NPQ but also decreased ϕ_{II} and qP at 40 dag during earlier senescence of *psbs* mutant. One explanation on the early senescence of *psbs* could be that as the NPQ is very low, the excess energy will difficult to dissipate. This could induce ROS formation. Indeed, it could be shown that the ROS level increased (Fig. 13). ROS has been demonstrated to be an effective response of senescence (Khanna-Chopra, 2012). On the opposite, for *oeSTN8*, the NPQ value at 40 dag was 2-fold increased compared to the value of day 28 (Fig. 10). If we relate its high survival rate at 52 dag to this strong increase of the NPQ value during the early stage of senescence, we infer that the higher non-photochemical quenching during age-dependent senescence can reduce photoinhibitory damage from senescence stress much more efficiently.

The result from real time PCR also revealed that *psan-2*, *pete2*, *stn7-1* already had a little higher expression level of the senescence marker *SAG12* at 33dag, which means senescence is earlier induced than in Col-0, but it is not activated as in Col-0 in the late stages. The result was somewhat contradictory with the above data that *psan-2* and *stn7-1* had early induced senescence. Therefore this experiment should be repeated.

The mutants *psal-2*, *psan-2*, *psbs*, *pete2*, *stn7-1*, *stn8-1* and *stn7stn8* have a shorter life span in comparison to Col-0, whereas *oeSTN8* has a longer lifespan. According to the above information, PSII activity therefore cannot be the only factor to explain the early degradation of chlorophyll in all the mutants.

4.1.2. Dark-induced senescence

To avoid the difference in development stages between mutants and the fluctuation in environmental factors influencing the results senescence in leaves from Col-0 and

photosynthesis mutants was induced by shading under precisely controlled conditions. That senescence can be induced by darkness has been known for many years, and many studies on this dark induced senescence have been published. It has been shown previously by several parameters that senescence is induced in detached *Arabidopsis* leaves in response to darkness (Fujiki et al., 2001; Guo and Crawford, 2005). However, little work has been done in attached adult leaves during dark-induced senescence, in *Arabidopsis* or other species (van der Graaff et al., 2006; Parlitz et al., 2011), and the few related reports have been somewhat contradictory, at least in their conclusions. Therefore this study focuses on studying the senescence of attached leaves.

3 days, 7 days and 10 days of darkness were used for the shading treatments. It could be shown that *Arabidopsis* Col-0 can maintain growth even after seven days shading treatment. Surprisingly, total chlorophyll levels were higher in leaves after darkness after their return to light than in normal conditions. If results of three days and seven days darkness were compared, it was observed that longer darkness resulted in higher chlorophyll content, upon return to normal conditions. However, chlorophyll levels in dark treated leaves declined after the recovery at a faster rate compared to Col-0, with the greatest decline in the leaves that were kept in darkness for the longest time. On the other hand, when whole plants were darkened for ten days, senescence of individual leaves was induced, and this induced senescence could not be reversed after the return to the light.

Many reports revealed that the transfer of whole plants to darkness induces senescence in true leaves, and reversibility of senescence was observed, suggested that chlorophyll and protein losses could be reversed by returning plants to the light, at least within several days of the dark treatment (Blank and McKeon, 1991; Kleber-Janke and Krupinska, 1997). When the expression of various senescence- and photosynthesis-associated genes was examined in response to both whole-plant darkness and natural senescence, however, the results were more varied, with some genes responding similarly to both treatments and some genes responding very differently (Weaver et al., 1998). Three RNases in wheat leaves showed the dark-induced senescence-associated elevation, although the RNase activities were differentially expressed (Blank and McKeon, 1991). During the normal growth phase, a senescence-associated gene (*SENI*) of *Arabidopsis thaliana* was strongly induced in leaves after flowering. Additionally, dark-induced senescence of detached leaves or of leaves in plant also resulted in a high-level induction of the gene *SENI* (Oh et al., 1996). Kleber-Janke and Krupinska (1997) identified five of the cDNA fragments representing transcripts associated with dark-induced senescence, as well as with natural

senescence. Using affymetrix expression data, among the 827 senescence-enhanced genes during developmental senescence, half of the genes were at least threefold up-regulated in the dark-treated leaves, but the others of the genes were either not up-regulated in the dark or up-regulated two- to threefold (Buchanan-Wollaston et al., 2005). Kleber-Janke and Krupinska (working in the primary leaves of barley seedlings) have interpreted this as that when whole plants are darkened, a portion of the senescence program is induced, perhaps one corresponding to an early stage of senescence (a reversible phase). But whether an induced senescence can be reversible depends on both the shading period and the responding genes.

From all the photosynthesis mutants analyzed, only *psan-2*, *pete2*, and the STN mutants showed an early onset of senescence, after whole-plant darkness. Senescence is not induced in *psbs* and *psal-2* during whole-plant darkness although they showed earlier senescence without stress. This means that *psan-2*, *pete2*, and the STN mutants responded strongly to stress. As previously mentioned, age-dependent senescence of STN mutants has no relation with reduced PSII activity. It is well known that STN proteins are essential for thylakoid protein phosphorylation, which control energy allocation to photosystems in response to light quality changes by flowering plants (Tikkanen et al., 2010). We can assume that a defect on protein phosphorylation can lead to abnormal energy allocation during a change from dark to light. This could be the reason why STN mutants showed a strong senescence phenotype in darkness experiment.

From these studies it can be concluded that: (I) Sugar could be an initiation factor of senescence, especially in *psal-2* as the high chlorophyll content suggests strong photosynthesis activity after flowering. But this assumption needs to be proven if there is indeed a high sugar concentration in *psal-2* at flowering time. (II) A correlation between the start of rosette senescence and flowering was found (Levey et al., 2005) when different *Arabidopsis* accessions were analyzed. However, the onset of senescence of the whole rosette and that of individual leaves is not always strongly correlated (Balazadeh et al., 2008). In my result, the early degradation of chlorophyll on *psan-2* can be best explained by its early flowering. (III) The result from the *psbs* mutant confirmed past report that high NPQ can prevent premature cell death during senescence and therefore low NPQ could induce senescence (Roach and Krieger-Liszkay, 2012). (IV) When plants were put into dark conditions, a defect to acclimate to changed light intensities could lead to a stronger senescence situation than age-dependent senescence. That is the case for STN mutants. Among the three mutants (*stn7-1*, *stn8-1* and *stn7stn8*), the survival rate of *stn8-1* was

lower than *stn7-1* and Col-0. Furthermore, the *oeSTN8* shows a higher survival rate. STN7 and STN8 have different functions on protein phosphorylation. The Stt7/STN7 kinase is mainly involved in the phosphorylation of the LHCII antenna proteins and is required for state transitions (Bonardi et al., 2005; Pesaresi et al., 2011). Another kinase, Stt1/STN8, is responsible for the phosphorylation of the PSII core proteins (Pesaresi et al., 2011). The early senescence of *stn8-1* after 10 days darkness was used to perform a suppressor screen, and one *stn8-EMS* line could be identified. This suggests that a second site mutation can suppress this early senescence phenotype.

4.2. RER protein on senescence

4.2.1. Characterisation of RER proteins

Our results confirmed that reticulate-related (RER) gene family is a plastid inner envelope protein that is transcribed mainly in leaves. The results of the *AtRER::GFP* analysis reveals that all the RER proteins were localized in the inner envelope of chloroplast and especially in stromules. Plastids in dark grown cells (onion epidermis cells) were observed that were connected by the long, thin extensions but not connected at any time (Hanson and Sattarzadeh, 2011), as observed in my experiment, stromules can only be seen in young and healthy onion epidermis cells. The data from transient expression in onion epidermis cells displayed high amount of expression, but transient expression in *Arabidopsis thaliana* protoplast showed only weak signals. There are two possibilities to explain this. One hypothesis is that RER localization is much easier to non-green plastid in onion cells. Stromules are reported to be found more frequently on non-green plastids than on chloroplasts (Kohler and Hanson, 2000; Pyke and Howells, 2002; Waters et al., 2004; Natesan et al., 2005). Another hypothesis is that *in vivo* only low protein amounts occur in the inner memberane. This can be confirmed by the overexpression of *AtRER5* and *6* in *Arabidopsis* Col-0, as even in overexpressed lines we did not detect strong expression signals, although RNA levels were strongly increased.

Until now the function of stromules are still not clear. Some reports provided that stromules are important for inter-plastid communication and macromolecule transfer (Kwok and Hanson, 2003, 2004; Radhamony and Theg, 2006), and that they might be involved in signal transduction (Kwok and Hanson, 2004). Additionally, small vesicles were found outside the chloroplasts in leaves (Pyke and Howells, 2002; Chiba et al., 2003; Gunning, 2005). Stromules may be involved in a mechanism to recycle chloroplast proteins under stress. The obvious advantage to recycling only a portion of the chloroplast and retaining the thylakoid membranes is that if conditions improve, photosynthesis could

resume (Hanson and Sattarzadeh, 2011). However, recently news insight of stromules strongly supports plastid independence rather than their interconnectivity. Additional information on stress conditions inducing stromules suggests that stromules are important to increase the envelope surface area of a plastid with the rest of the cytoplasm (Kohler and Hanson, 2000; Waters et al., 2004).

A number of *Arabidopsis thaliana* mutants exhibit leaf reticulation and low cell density in the mesophyll, but normal perivascular bundle sheath cells: *cue* mutants exhibit mesophyll-specific chloroplast and cellular defects, resulting in reticulate leaves (Streatfield et al., 1999) and CUE encodes the plastid inner envelope Phosphoenolpyruvate/Phosphate Translocator (PPT). And also *dov1* has been previously described as a reticulated EMS-mutant (Kinsman and Pyke, 1998; Rosar et al., 2012) and the mutated gene encodes a glutamine phosphoribosyl pyrophosphate aminotransferase 2 (ATase2), an enzyme catalyzing the first step of purine nucleotide biosynthesis. In the *Arabidopsis* RER mutants, two members can cause leaf reticulation, which are the *re* and *rer3* loss-of-function mutants (Barth and Conklin, 2003; Gonzalez-Bayon et al., 2006). They have an aberrant mesophyll structure but an intact layer of bundle sheath cells around the veins. Gonzalez-Bayon (2006) reported that RE and CUE1 act in the same developmental pathway affecting leaf development. But until now the function of RER proteins has not been elucidated.

Taken together, from the data presented here it can be assumed that RER proteins function as transportor in the inner envelope of chloroplasts either for import or for export of molecules from the chloroplasts. Knappe (2003) reported that PPT was involved in the provision of signals for correct mesophyll development, showing the importance of correct allocation of metabolites.

4.2.2. Physiological characteristics of premature senescence mutants in RER

The double mutant *rer5-3/rer6-1* exhibit smaller true leaves, indicating the leaf expansion is affected. But they are different from the previously described *re* mutant, as the leaves of *re* mutant are only slightly smaller than wild type and they do not differ in leaf shape. The reduced parenchyma cell density in *re* results in a lower chlorophyll content and a decreased biomass production per leaf area, but there was no change in the number of chloroplasts per cell or in overall cell size (Barth and Conklin, 2003). Microscope analysis on *rer5-3/rer6-1* showed a reduced palisade cell size compared to WT, but with an increase frequency of stomatal clusters. It suggests that the cell division could be influenced. In addition to their significance for gas exchange, stomata are a

valuable system for studying cell patterning. They are spaced apart from each other by at least one intervening cell (Kagan and Sachs, 1991), as only partially observed in *rer5-3/rer6-1*. Mutations at several Arabidopsis loci result in stomata in direct contact (Yang and Sack, 1995; Geisler et al., 1998; Berger and Altmann, 2000). It has also been shown that stomatal density can be influenced by CO₂ levels (Gray et al., 2000). It could be possible to speculate if *rer5-3/rer6-1* has a higher need for CO₂ leading to this increase of stomatal number. This is supported by the fact that the *rer5-3/rer6-1* can accumulate lower amounts of starch, the ultimate storage of the CO₂. A paler phenotype of *rer5-3/rer6-1* can be explained by the ultrastructural analysis of chloroplast that looked abnormal and contained less abundant thylakoid membranes and smaller starch grains.

If RER5 and RER6 are transporters, the question is which metabolite they transport across membrane. Feeding experiments with myo-inositol showed that myo-inositol can rescue the phenotype of *rer5-3/rer6-1* with 5-folds increase of plant size and production of seeds. Metabolic analysis of *rer5-3/rer6-1* revealed that the double mutant lacked inositol compared to Col-0. This clearly indicates that the mutant has a defect on synthesis or translocation of myo-inositol, or one of the precursors. In conclusion, the function of RER5 and RER6 could be establishing the myo-inositol level between chloroplast and cytoplasm. Perez-Perez (2013) reported that double mutant *rer5 rer6* exhibited functional redundancy. It needs to be clarified if they act in a different pathway with the other *RER* and *RE* mutants. Metabolic profiles of mature leaves revealed that *re* and *rer3* displayed alterations in several biosynthetic pathways downstream of pyruvate, including a reduction of the shikimate pathway and of the downstream products of its pathway such as aromatic amino acids. Also intermediates of the tricarboxylic acid (TCA) cycle were decreased.

The increasing levels of RER5 and RER6 in overexpression lines result in a different morphology: The variegated leaves of overexpression lines of RER5 and RER6, grown either on agar plates with 1% sugar or on soil under long day conditions, were visible. Variegated leaves have been observed also in other mutants such as *atlrGB* grown on agar plates (Myouga et al., 2010). They were described as chlorotic lesion mimic mutants that mis-regulate cell death (Yamaguchi et al., 2011). Some overexpression lines of RER5 and RER6 showed curly leaves and spontaneous production of lesions. Some lines had partially dead leaves. Trypan blue staining revealed that the lesions on curly leaves were due to dead cells. The result showed that more dead cells could be observed than in Col-0 (Fig. 27d). It suggests that protein level of RER5 or RER6 can lead to cell death to some extent according to its expression level.

To elucidate whether a connection between myo-inositol synthesis and cell death exists in the overexpression line, the metabolic analysis on overexpression lines is undergoing. The connection of myo-inositol synthesis and cell death has been recently reported (Meng et al., 2009), as lesion formation in *atips1* (defective in AtIPS1, a myo-inositol synthase) mutants is due to programmed cell death. Myo-inositol and galactinol are the only metabolites whose accumulation is significantly reduced in the mutant, and supplementation of the mutant with these compounds is sufficient to prevent PCD. Signals coming from chloroplasts may involve in the onset of PCD in *atips1*. A defect in Inositol-requiring enzyme 1 (IRE1) showed enhanced cell death as the unfolded protein response is no longer up-regulated (Mishiba et al., 2013). In fact, we have an enhanced cell death phenotype when high amount of RER5 or RER6 are present. Therefore, the levels of myo-inositol in these lines have to be measured by GC-mass spectrometry in order to resolve this conflict of results. The impaired compartmentalization of compounds such as myo-inositol could also lead to a depletion in the cytosol, but enrichment in the chloroplast or vice versa leading to an apparent loss of myo-inositol in one compartment which induces the cell death pathway.

Although myo-inositol was first isolated from muscles, it is a ubiquitous compound found in all living organisms. In plant cells, inositol derivatives play critical and diverse biological roles. These include phosphate storage in the form of phytic acid, control of auxin physiology (Tan et al., 2007), signal transduction as inositol 1,4,5-trisphosphate and phosphatidylinositol(3)phosphate (Irvine and Schell, 2001; Gillaspay, 2011), membrane biogenesis (Tiede et al., 1999; Peskan et al., 2000; Cullen et al., 2001; Borner et al., 2005), stress tolerance (Smart and Fleming, 1993; Ishitani et al., 1996), and regulation of cell death (via sphingolipids) (Meng et al., 2009; Donahue et al., 2010). They also act as protein cofactors (Macbeth et al., 2005). In salt-tolerant or cold-tolerant plant species, myo-inositol biosynthesis seems to play a pivotal role in protection mechanisms (Rammesmayer et al., 1995). The oxidation product of myo-inositol (D-glucuronic acid) is used for cell wall pectic non-cellulosic compounds (Loewus, 1965, 1969; Loewus, 2006). Thus, myo-inositol synthesis and catabolism has an impact on metabolites involved in many different and critical plant biochemical pathways.

Taken together, studies on two RER proteins revealed that the absence of both RER5 and RER6 can lead to changes in morphology of mesophyll cells, especially increased frequency of stomatal clusters. The low amount of myo-inositol could play an important

role in this phenotype. On the other hand, the overexpression of RER5 and RER6 can cause serious cell death on leaves of *Arabidopsis thaliana*.

Thus, studying leaf senescence will not only enhance our understanding of a fundamental biological process, but also may provide means to control leaf senescence to improve agricultural traits of crop plants.

References

- Adamchuk NI, Guikema JA, Jialo S, Hilaire E** (2002) State of Brassica rapa photosynthetic membranes in microgravity. *J Gravit Physiol* **9**: P229-230
- Allen JF, de Paula WB, Puthiyaveetil S, Nield J** (2013) A structural phylogenetic map for chloroplast photosynthesis. *Trends Plant Sci* **16**: 645-655
- Arrom L, Munne-Bosch S** (2012) Hormonal regulation of leaf senescence in Liliun. *J Plant Physiol* **169**: 1542-1550
- Bailey S, Thompson E, Nixon PJ, Horton P, Mullineaux CW, Robinson C, Mann NH** (2002) A critical role for the Var2 FtsH homologue of *Arabidopsis thaliana* in the photosystem II repair cycle in vivo. *J Biol Chem* **277**: 2006-2011
- Balazadeh S, Parlitz S, Mueller-Roeber B, Meyer RC** (2008) Natural developmental variations in leaf and plant senescence in *Arabidopsis thaliana*. *Plant Biol (Stuttg)* **10 Suppl 1**: 136-147
- Barth C, Conklin PL** (2003) The lower cell density of leaf parenchyma in the *Arabidopsis thaliana* mutant lcd1-1 is associated with increased sensitivity to ozone and virulent *Pseudomonas syringae*. *Plant J* **35**: 206-218
- Bassi R, Marquardt J, Lavergne J** (1995) Biochemical and functional properties of photosystem II in agranal membranes from maize mesophyll and bundle sheath chloroplasts. *Eur J Biochem* **233**: 709-719
- Behera SK, Nayak L, Biswal B** (2003) Senescing leaves possess potential for stress adaptation: the developing leaves acclimated to high light exhibit increased tolerance to osmotic stress during senescence. *J Plant Physiol* **160**: 125-131
- Berger D, Altmann T** (2000) A subtilisin-like serine protease involved in the regulation of stomatal density and distribution in *Arabidopsis thaliana*. *Genes Dev* **14**: 1119-1131
- Besseau S, Li J, Palva ET** (2012) WRKY54 and WRKY70 co-operate as negative regulators of leaf senescence in *Arabidopsis thaliana*. *J Exp Bot* **63**: 2667-2679
- Bindschedler LV, Dewdney J, Blee KA, Stone JM, Asai T, Plotnikov J, Denoux C, Hayes T, Gerrish C, Davies DR, Ausubel FM, Bolwell GP** (2006) Peroxidase-dependent apoplastic oxidative burst in *Arabidopsis* required for pathogen resistance. *Plant J* **47**: 851-863
- Bisanz C, Begot L, Carol P, Perez P, Bligny M, Pesey H, Gallois JL, Lerbs-Mache S, Mache R** (2003) The *Arabidopsis* nuclear DAL gene encodes a chloroplast protein which is required for the maturation of the plastid ribosomal RNAs and is essential for chloroplast differentiation. *Plant Mol Biol* **51**: 651-663
- Blank A, McKeon TA** (1991) Expression of Three RNase Activities during Natural and Dark-Induced Senescence of Wheat Leaves. *Plant Physiol* **97**: 1409-1413

- Boardman NK, Wildman SG** (1962) Identification of proplastids by fluorescence microscopy and their isolation and purification. *Biochim Biophys Acta* **59**: 222-224
- Bolle C, Huet G, Kleinbolting N, Haberer G, Mayer K, Leister D, Weisshaar B** (2013) GABI-DUPLO: a collection of double mutants to overcome genetic redundancy in *Arabidopsis thaliana*. *Plant J*
- Bonardi V, Pesaresi P, Becker T, Schleiff E, Wagner R, Pfannschmidt T, Jahns P, Leister D** (2005) Photosystem II core phosphorylation and photosynthetic acclimation require two different protein kinases. *Nature* **437**: 1179-1182
- Boose JA, Kuismanen E, Gerard R, Sambrook J, Gething MJ** (1989) The single-chain form of tissue-type plasminogen activator has catalytic activity: studies with a mutant enzyme that lacks the cleavage site. *Biochemistry* **28**: 635-643
- Borner GH, Sherrier DJ, Weimar T, Michaelson LV, Hawkins ND, Macaskill A, Napier JA, Beale MH, Lilley KS, Dupree P** (2005) Analysis of detergent-resistant membranes in *Arabidopsis*. Evidence for plasma membrane lipid rafts. *Plant Physiol* **137**: 104-116
- Bryant N, Lloyd J, Sweeney C, Myouga F, Meinke D** (2011) Identification of nuclear genes encoding chloroplast-localized proteins required for embryo development in *Arabidopsis*. *Plant Physiol* **155**: 1678-1689
- Buchanan-Wollaston V, Earl S, Harrison E, Mathas E, Navabpour S, Page T, Pink D** (2003) The molecular analysis of leaf senescence--a genomics approach. *Plant Biotechnol J* **1**: 3-22
- Buchanan-Wollaston V, Page T, Harrison E, Breeze E, Lim PO, Nam HG, Lin JF, Wu SH, Swidzinski J, Ishizaki K, Leaver CJ** (2005) Comparative transcriptome analysis reveals significant differences in gene expression and signalling pathways between developmental and dark/starvation-induced senescence in *Arabidopsis*. *Plant J* **42**: 567-585
- Carol P, Stevenson D, Bisanz C, Breitenbach J, Sandmann G, Mache R, Coupland G, Kuntz M** (1999) Mutations in the *Arabidopsis* gene IMMUTANS cause a variegated phenotype by inactivating a chloroplast terminal oxidase associated with phytoene desaturation. *Plant Cell* **11**: 57-68
- Chase CD** (2007) Cytoplasmic male sterility: a window to the world of plant mitochondrial-nuclear interactions. *Trends Genet* **23**: 81-90
- Chen M, Choi Y, Voytas DF, Rodermel S** (2000) Mutations in the *Arabidopsis* VAR2 locus cause leaf variegation due to the loss of a chloroplast FtsH protease. *Plant J* **22**: 303-313
- Chiba A, Ishida H, Nishizawa NK, Makino A, Mae T** (2003) Exclusion of ribulose-1,5-bisphosphate carboxylase/oxygenase from chloroplasts by specific bodies in naturally senescing leaves of wheat. *Plant Cell Physiol* **44**: 914-921

- Chrost B, Kolukisaoglu U, Schulz B, Krupinska K** (2007) An alpha-galactosidase with an essential function during leaf development. *Planta* **225**: 311-320
- Cullen PJ, Cozier GE, Banting G, Mellor H** (2001) Modular phosphoinositide-binding domains--their role in signalling and membrane trafficking. *Curr Biol* **11**: R882-893
- Dai N, Schaffer A, Petreikov M, Shahak Y, Giller Y, Ratner K, Levine A, Granot D** (1999) Overexpression of *Arabidopsis* hexokinase in tomato plants inhibits growth, reduces photosynthesis, and induces rapid senescence. *Plant Cell* **11**: 1253-1266
- Daudi A, Cheng Z, O'Brien JA, Mammarella N, Khan S, Ausubel FM, Bolwell GP** (2012) The apoplastic oxidative burst peroxidase in *Arabidopsis* is a major component of pattern-triggered immunity. *Plant Cell* **24**: 275-287
- Davis PA, Hangarter RP** (2012) Chloroplast movement provides photoprotection to plants by redistributing PSII damage within leaves. *Photosynth Res* **112**: 153-161
- Demmig-Adams B, Gilmore AM, Adams WW, 3rd** (1996) Carotenoids 3: in vivo function of carotenoids in higher plants. *FASEB J* **10**: 403-412
- Donahue JL, Alford SR, Torabinejad J, Kerwin RE, Nourbakhsh A, Ray WK, Hernick M, Huang X, Lyons BM, Hein PP, Gillaspay GE** (2010) The *Arabidopsis thaliana* Myo-inositol 1-phosphate synthase1 gene is required for Myo-inositol synthesis and suppression of cell death. *Plant Cell* **22**: 888-903
- Dovzhenko A, Dal Bosco C, Meurer J, Koop HU** (2003) Efficient regeneration from cotyledon protoplasts in *Arabidopsis thaliana*. *Protoplasma* **222**: 107-111
- Dunkley TP, Hester S, Shadforth IP, Runions J, Weimar T, Hanton SL, Griffin JL, Bessant C, Brandizzi F, Hawes C, Watson RB, Dupree P, Lilley KS** (2006) Mapping the *Arabidopsis* organelle proteome. *Proc Natl Acad Sci U S A* **103**: 6518-6523
- Erbán A, Schauer N, Fernie AR, Kopka J** (2007) Nonsupervised construction and application of mass spectral and retention time index libraries from time-of-flight gas chromatography-mass spectrometry metabolite profiles. *Methods Mol Biol* **358**: 19-38
- Evans IM, Rus AM, Belanger EM, Kimoto M, Brusslan JA** (2010) Dismantling of *Arabidopsis thaliana* mesophyll cell chloroplasts during natural leaf senescence. *Plant Biol (Stuttg)* **12**: 1-12
- Feller U, Anders I, Mae T** (2008) Rubiscolytics: fate of Rubisco after its enzymatic function in a cell is terminated. *Journal of Experimental Botany* **59**: 1615-1624
- Ferro M, Brugiére S, Salvi D, Seigneurin-Berny D, Court M, Moyet L, Ramus C, Miras S, Mellal M, Le Gall S, Kieffer-Jaquinod S, Bruley C, Garin J, Joyard J, Masselon C, Rolland N** (2010) AT_CHLORO, a comprehensive chloroplast proteome database with subplastidial localization and curated information on envelope proteins. *Mol Cell Proteomics* **9**: 1063-1084

- Ferro M, Salvi D, Brugiére S, Miras S, Kowalski S, Louwagie M, Garin J, Joyard J, Rolland N** (2003) Proteomics of the chloroplast envelope membranes from *Arabidopsis thaliana*. *Mol Cell Proteomics* **2**: 325-345
- Froehlich JE, Wilkerson CG, Ray WK, McAndrew RS, Osteryoung KW, Gage DA, Phinney BS** (2003) Proteomic study of the *Arabidopsis thaliana* chloroplastic envelope membrane utilizing alternatives to traditional two-dimensional electrophoresis. *J Proteome Res* **2**: 413-425
- Fujiki Y, Yoshikawa Y, Sato T, Inada N, Ito M, Nishida I, Watanabe A** (2001) Dark-inducible genes from *Arabidopsis thaliana* are associated with leaf senescence and repressed by sugars. *Physiol Plant* **111**: 345-352
- Fukao T, Yeung E, Bailey-Serres J** (2012) The submergence tolerance gene SUB1A delays leaf senescence under prolonged darkness through hormonal regulation in rice. *Plant Physiol* **160**: 1795-1807
- Geisler M, Yang M, Sack FD** (1998) Divergent regulation of stomatal initiation and patterning in organ and suborgan regions of the *Arabidopsis* mutants too many mouths and four lips. *Planta* **205**: 522-530
- Gillaspy GE** (2011) The cellular language of myo-inositol signaling. *New Phytol* **192**: 823-839
- Gonzalez-Bayon R, Kinsman EA, Quesada V, Vera A, Robles P, Ponce MR, Pyke KA, Micol JL** (2006) Mutations in the RETICULATA gene dramatically alter internal architecture but have little effect on overall organ shape in *Arabidopsis* leaves. *J Exp Bot* **57**: 3019-3031
- Gray JE, Holroyd GH, van der Lee FM, Bahrami AR, Sijmons PC, Woodward FI, Schuch W, Hetherington AM** (2000) The HIC signalling pathway links CO₂ perception to stomatal development. *Nature* **408**: 713-716
- Gregersen PL, Holm PB, Krupinska K** (2008) Leaf senescence and nutrient remobilisation in barley and wheat. *Plant Biol (Stuttg)* **10 Suppl 1**: 37-49
- Guiamet JJ, Tyystjarvi E, Tyystjarvi T, John I, Kairavuo M, Pichersky E, Nooden LD** (2002) Photoinhibition and loss of photosystem II reaction centre proteins during senescence of soybean leaves. Enhancement of photoinhibition by the 'stay-green' mutation cytG. *Physiol Plant* **115**: 468-478
- Gunning BE** (2005) Plastid stromules: video microscopy of their outgrowth, retraction, tensioning, anchoring, branching, bridging, and tip-shedding. *Protoplasma* **225**: 33-42
- Guo FQ, Crawford NM** (2005) *Arabidopsis* nitric oxide synthase1 is targeted to mitochondria and protects against oxidative damage and dark-induced senescence. *Plant Cell* **17**: 3436-3450

- Hanson MR, Sattarzadeh A** (2011) Stromules: recent insights into a long neglected feature of plastid morphology and function. *Plant Physiol* **155**: 1486-1492
- Herbstova M, Tietz S, Kinzel C, Turkina MV, Kirchhoff H** (2012) Architectural switch in plant photosynthetic membranes induced by light stress. *Proc Natl Acad Sci U S A* **109**: 20130-20135
- Higuchi R, Krummel B, Saiki RK** (1988) A general method of in vitro preparation and specific mutagenesis of DNA fragments: study of protein and DNA interactions. *Nucleic Acids Res* **16**: 7351-7367
- Hilditch P, Thomas H, Rogers LJ**. 1986. Two processes for the breakdown of the QB protein of chloroplasts. *FEBS Letters* 208, 313-16
- Holloway PJ, Maclean DJ, Scott KJ** (1983) Rate-Limiting Steps of Electron Transport in Chloroplasts during Ontogeny and Senescence of Barley. *Plant Physiol* **72**: 795-801
- Hortensteiner S, Feller U** (2002) Nitrogen metabolism and remobilization during senescence. *J Exp Bot* **53**: 927-937
- Hortensteiner S, Krautler B** (2011) Chlorophyll breakdown in higher plants. *Biochim Biophys Acta* **1807**: 977-988
- Horton P, Ruban AV, Walters RG** (1994) Regulation of Light Harvesting in Green Plants (Indication by Nonphotochemical Quenching of Chlorophyll Fluorescence). *Plant Physiol* **106**: 415-420
- Hsu SC, Belmonte MF, Harada JJ, Inoue K** (2010) Indispensable Roles of Plastids in *Arabidopsis thaliana* Embryogenesis. *Curr Genomics* **11**: 338-349
- Humbeck K, Krupinska K** (2003) The abundance of minor chlorophyll a/b-binding proteins CP29 and LHCI of barley (*Hordeum vulgare* L.) during leaf senescence is controlled by light. *J Exp Bot* **54**: 375-383
- Hummel J, Strehmel N, Selbig J, Walther D, Kopka J** (2010) Decision tree supported substructure prediction of metabolites from GC-MS profiles. *Metabolomics* **6**: 322-333
- Hurkman WJ, Morre DJ, Bracker CE, Mollenhauer HH** (1979) Identification of etioplast membranes in fractions from soybean hypocotyls. *Plant Physiol* **64**: 398-403
- Ihnatowicz A, Pesaresi P, Varotto C, Richly E, Schneider A, Jahns P, Salamini F, Leister D** (2004) Mutants for photosystem I subunit D of *Arabidopsis thaliana*: effects on photosynthesis, photosystem I stability and expression of nuclear genes for chloroplast functions. *Plant J* **37**: 839-852
- Inaba T, Ito-Inaba Y** (2010) Versatile roles of plastids in plant growth and development. *Plant Cell Physiol* **51**: 1847-1853

- Irvine RF, Schell MJ** (2001) Back in the water: the return of the inositol phosphates. *Nat Rev Mol Cell Biol* **2**: 327-338
- Ishitani M, Majumder AL, Bornhouser A, Michalowski CB, Jensen RG, Bohnert HJ** (1996) Coordinate transcriptional induction of myo-inositol metabolism during environmental stress. *Plant J* **9**: 537-548
- Izumi M, Wada S, Makino A, Ishida H** (2010) The autophagic degradation of chloroplasts via rubisco-containing bodies is specifically linked to leaf carbon status but not nitrogen status in *Arabidopsis*. *Plant Physiol* **154**: 1196-1209
- Jang JC, Leon P, Zhou L, Sheen J** (1997) Hexokinase as a sugar sensor in higher plants. *Plant Cell* **9**: 5-19
- Jasinski M, Sudre D, Schansker G, Schellenberg M, Constant S, Martinoia E, Bovet L** (2008) AtOSA1, a member of the Abc1-like family, as a new factor in cadmium and oxidative stress response. *Plant Physiol* **147**: 719-731
- Kagan ML, Sachs T** (1991) Development of immature stomata: evidence for epigenetic selection of a spacing pattern. *Dev Biol* **146**: 100-105
- Kazama T, Nakamura T, Watanabe M, Sugita M, Toriyama K** (2008) Suppression mechanism of mitochondrial ORF79 accumulation by Rf1 protein in BT-type cytoplasmic male sterile rice. *Plant J* **55**: 619-628
- Keech O, Pesquet E, Ahad A, Askne A, Nordvall D, Vodnala SM, Tuominen H, Hurry V, Dizengremel P, Gardestrom P** (2007) The different fates of mitochondria and chloroplasts during dark-induced senescence in *Arabidopsis* leaves. *Plant Cell Environ* **30**: 1523-1534
- Kessler F, Schnell DJ** (2006) The function and diversity of plastid protein import pathways: a multilane GTPase highway into plastids. *Traffic* **7**: 248-257
- Khanna-Chopra R** (2012) Leaf senescence and abiotic stresses share reactive oxygen species-mediated chloroplast degradation. *Protoplasma* **249**: 469-481
- Kim J, Dotson B, Rey C, Lindsey J, Bleecker AB, Binder BM, Patterson SE** (2013) New clothes for the jasmonic acid receptor COI1: delayed abscission, meristem arrest and apical dominance. *PLoS One* **8**: e60505
- Kinsman EA, Pyke KA** (1998) Bundle sheath cells and cell-specific plastid development in *Arabidopsis* leaves. *Development* **125**: 1815-1822
- Kleber-Janke T, Krupinska K** (1997) Isolation of cDNA clones for genes showing enhanced expression in barley leaves during dark-induced senescence as well as during senescence under field conditions. *Planta* **203**: 332-340
- Kleffmann T, Russenberger D, von Zychlinski A, Christopher W, Sjolander K, Gruissem W, Baginsky S** (2004) The *Arabidopsis thaliana* chloroplast proteome reveals pathway abundance and novel protein functions. *Curr Biol* **14**: 354-362

- Knappe S, Lottgert T, Schneider A, Voll L, Flugge UI, Fischer K** (2003) Characterization of two functional phosphoenolpyruvate/phosphate translocator (PPT) genes in *Arabidopsis*--AtPPT1 may be involved in the provision of signals for correct mesophyll development. *Plant J* **36**: 411-420
- Koch E, Slusarenko A** (1990) *Arabidopsis* is susceptible to infection by a downy mildew fungus. *Plant Cell* **2**: 437-445
- Kohler RH, Hanson MR** (2000) Plastid tubules of higher plants are tissue-specific and developmentally regulated. *J Cell Sci* **113** (Pt 1): 81-89
- Kohler RH, Zipfel WR, Webb WW, Hanson MR** (1997) The green fluorescent protein as a marker to visualize plant mitochondria in vivo. *Plant J* **11**: 613-621
- Koop HU, Steinmuller K, Wagner H, Rossler C, Eibl C, Sacher L** (1996) Integration of foreign sequences into the tobacco plastome via polyethylene glycol-mediated protoplast transformation. *Planta* **199**: 193-201
- Krupinska K, Humbeck K**. 2004. Photosynthesis and chloroplast breakdown. In: Noode´ LD, ed. *Plant cell death processes*. San Diego, CA: Academic Press, 169–187
- Kwok EY, Hanson MR** (2003) Microfilaments and microtubules control the morphology and movement of non-green plastids and stromules in *Nicotiana tabacum*. *Plant J* **35**: 16-26
- Kwok EY, Hanson MR** (2004) In vivo analysis of interactions between GFP-labeled microfilaments and plastid stromules. *BMC Plant Biol* **4**: 2
- Kwok EY, Hanson MR** (2004) Plastids and stromules interact with the nucleus and cell membrane in vascular plants. *Plant Cell Rep* **23**: 188-195
- Lee YJ, Kim DH, Kim YW, Hwang I** (2001) Identification of a signal that distinguishes between the chloroplast outer envelope membrane and the endomembrane system in vivo. *Plant Cell* **13**: 2175-2190
- Leister D, Kleine T** (2011) Role of intercompartmental DNA transfer in producing genetic diversity. *Int Rev Cell Mol Biol* **291**: 73-114
- Lichtenthaler HK** (1969) [Formation of excess plastidquinones in the leaves of *Ficus elastica* Roxb]. *Z Naturforsch B* **24**: 1461-1466
- Lichtenthaler HK, Babani F, Navratil M, Buschmann C** (2013) Chlorophyll fluorescence kinetics, photosynthetic activity, and pigment composition of blue-shade and half-shade leaves as compared to sun and shade leaves of different trees. *Photosynth Res*
- Lim PO, Kim HJ, Nam HG** (2007) Leaf senescence. *Annual Review of Plant Biology* **58**: 115-136
- Lim PO, Nam HG** (2005) The molecular and genetic control of leaf senescence and longevity in *Arabidopsis*. *Curr Top Dev Biol* **67**: 49-83

- Lim PO, Nam HG** (2007) Aging and senescence of the leaf organ. *Journal of Plant Biology* **50**: 291-300
- Lim PO, Woo HR, Nam HG** (2003) Molecular genetics of leaf senescence in *Arabidopsis*. *Trends Plant Sci* **8**: 272-278
- Lindahl M, Tabak S, Cseke L, Pichersky E, Andersson B, Adam Z** (1996) Identification, characterization, and molecular cloning of a homologue of the bacterial FtsH protease in chloroplasts of higher plants. *J Biol Chem* **271**: 29329-29334
- Loewus F** (1965) Inositol metabolism and cell wall formation in plants. *Fed Proc* **24**: 855-862
- Loewus F** (1969) Metabolism of inositol in higher plants. *Ann N Y Acad Sci* **165**: 577-598
- Loewus FA** (2006) Inositol and plant cell wall polysaccharide biogenesis. *Subcell Biochem* **39**: 21-45
- Lu Y, Li C, Wang H, Chen H, Berg H, Xia Y** (2011) AtPPR2, an *Arabidopsis* pentatricopeptide repeat protein, binds to plastid 23S rRNA and plays an important role in the first mitotic division during gametogenesis and in cell proliferation during embryogenesis. *Plant J* **67**: 13-25
- Luedemann A, Strassburg K, Erban A, Kopka J** (2008) TagFinder for the quantitative analysis of gas chromatography--mass spectrometry (GC-MS)-based metabolite profiling experiments. *Bioinformatics* **24**: 732-737
- Macbeth MR, Schubert HL, Vandemark AP, Lingam AT, Hill CP, Bass BL** (2005) Inositol hexakisphosphate is bound in the ADAR2 core and required for RNA editing. *Science* **309**: 1534-1539
- Marquard RD, Tipton JL** (1987) Relationship between extractable chlorophyll and an insitu method to estimate leaf greenness. *Hortscience* **22**: 1327-1327
- Martin-Cabrejas MA, Jaime L, Karanja C, Downie AJ, Parker ML, Lopez-Andreu FJ, Maina G, Esteban RM, Smith AC, Waldron KW** (1999) Modifications to physicochemical and nutritional properties of hard-To-cook beans (*Phaseolus vulgaris* L.) by extrusion cooking. *J Agric Food Chem* **47**: 1174-1182
- Martinez-Gutierrez R, Zavaleta-Mancera H, Ruiz-Posadas LDM, Delgado-Alvarado A, Vaca-Paulin R** (2008) Gas exchange and water relations during delay of leaf senescence in wheat (*Triticum aestivum* L.) by cytokinin BAP. *Interciencia* **33**: 140-145
- Martinez DE, Costa ML, Guiamet JJ** (2008) Senescence-associated degradation of chloroplast proteins inside and outside the organelle. *Plant Biol (Stuttg)* **10 Suppl 1**: 15-22

- Masuda S, Mizusawa K, Narisawa T, Tozawa Y, Ohta H, Takamiya K** (2008) The bacterial stringent response, conserved in chloroplasts, controls plant fertilization. *Plant Cell Physiol* **49**: 135-141
- Matile P, Ginsburg S, Schellenberg M, Thomas H** (1988) Catabolites of chlorophyll in senescing barley leaves are localized in the vacuoles of mesophyll cells. *Proc Natl Acad Sci U S A* **85**: 9529-9532
- Matile P** (1992) Chloroplast senescence, Vol 413-440. Elsevier, Amsterdam
- Matile P, Hortensteiner S, Thomas H** (1999) Chlorophyll Degradation. *Annu Rev Plant Physiol Plant Mol Biol* **50**: 67-95
- Maxwell K, Johnson GN** (2000) Chlorophyll fluorescence--a practical guide. *J Exp Bot* **51**: 659-668
- Meng PH, Raynaud C, Tcherkez G, Blanchet S, Massoud K, Domenichini S, Henry Y, Soubigou-Taconnat L, Lelarge-Trouverie C, Saindrenan P, Renou JP, Bergounioux C** (2009) Crosstalks between myo-inositol metabolism, programmed cell death and basal immunity in *Arabidopsis*. *PLoS One* **4**: e7364
- Mereschkowsky, Konstantin** (1910). "Theorie der zwei Plasmaarten als Grundlage der Symbiogenesis, einer neuen Lehre von der Entstehung der Organismen.". *Biol Centralbl* **30**: 353-367.
- Minamikawa T, Toyooka K, Okamoto T, Hara-Nishimura I, Nishimura M** (2001) Degradation of ribulose-bisphosphate carboxylase by vacuolar enzymes of senescing French bean leaves: immunocytochemical and ultrastructural observations. *Protoplasma* **218**: 144-153
- Mishiba K, Nagashima Y, Suzuki E, Hayashi N, Ogata Y, Shimada Y, Koizumi N** (2013) Defects in IRE1 enhance cell death and fail to degrade mRNAs encoding secretory pathway proteins in the *Arabidopsis* unfolded protein response. *Proc Natl Acad Sci U S A* **110**: 5713-5718
- Moore B, Zhou L, Rolland F, Hall Q, Cheng WH, Liu YX, Hwang I, Jones T, Sheen J** (2003) Role of the *Arabidopsis* glucose sensor HXK1 in nutrient, light, and hormonal signaling. *Science* **300**: 332-336
- Motohashi K, Hisabori T** (2006) HCF164 receives reducing equivalents from stromal thioredoxin across the thylakoid membrane and mediates reduction of target proteins in the thylakoid lumen. *J Biol Chem* **281**: 35039-35047
- Myouga F, Akiyama K, Motohashi R, Kuromori T, Ito T, Iizumi H, Ryusui R, Sakurai T, Shinozaki K** (2010) The Chloroplast Function Database: a large-scale collection of *Arabidopsis* Ds/Spm- or T-DNA-tagged homozygous lines for nuclear-encoded chloroplast proteins, and their systematic phenotype analysis. *Plant J* **61**: 529-542
- Nam HG** (1997) The molecular genetic analysis of leaf senescence. *Curr Opin Biotechnol* **8**: 200-207

- Natesan SK, Sullivan JA, Gray JC** (2005) Stromules: a characteristic cell-specific feature of plastid morphology. *J Exp Bot* **56**: 787-797
- Navari-Izzo F, Pinzino C, Quartacci MF, Sgherri CL** (1999) Superoxide and hydroxyl radical generation, and superoxide dismutase in PSII membrane fragments from wheat. *Free Radic Res* **31 Suppl**: S3-9
- Noh YS, Amasino RM** (1999) Identification of a promoter region responsible for the senescence-specific expression of SAG12. *Plant Mol Biol* **41**: 181-194
- Noh YS, Amasino RM** (1999) Regulation of developmental senescence is conserved between *Arabidopsis* and Brassica napus. *Plant Mol Biol* **41**: 195-206
- Oberhuber M, Berghold J, Breuker K, Hortensteiner S, Krautler B** (2003) Breakdown of chlorophyll: a nonenzymatic reaction accounts for the formation of the colorless "nonfluorescent" chlorophyll catabolites. *Proc Natl Acad Sci U S A* **100**: 6910-6915
- Oh SA, Lee SY, Chung IK, Lee CH, Nam HG** (1996) A senescence-associated gene of *Arabidopsis thaliana* is distinctively regulated during natural and artificially induced leaf senescence. *Plant Mol Biol* **30**: 739-754
- Oka M, Shimoda Y, Sato N, Inoue J, Yamazaki T, Shimomura N, Fujiyama H** (2012) Abscisic acid substantially inhibits senescence of cucumber plants (*Cucumis sativus*) grown under low nitrogen conditions. *J Plant Physiol* **169**: 789-796
- Ostersetzer O, Adam Z** (1997) Light-stimulated degradation of an unassembled Rieske FeS protein by a thylakoid-bound protease: the possible role of the FtsH protease. *Plant Cell* **9**: 957-965
- Parlitz S, Kunze R, Mueller-Roeber B, Balazadeh S** Regulation of photosynthesis and transcription factor expression by leaf shading and re-illumination in *Arabidopsis thaliana* leaves. *J Plant Physiol* **168**: 1311-1319
- Parlitz S, Kunze R, Mueller-Roeber B, Balazadeh S** (2011) Regulation of photosynthesis and transcription factor expression by leaf shading and re-illumination in *Arabidopsis thaliana* leaves. *J Plant Physiol* **168**: 1311-1319
- Peltier JB, Emanuelsson O, Kalume DE, Ytterberg J, Friso G, Rudella A, Liberles DA, Soderberg L, Roepstorff P, von Heijne G, van Wijk KJ** (2002) Central functions of the lumenal and peripheral thylakoid proteome of *Arabidopsis* determined by experimentation and genome-wide prediction. *Plant Cell* **14**: 211-236
- Perez-Perez JM, Esteve-Bruna D, Gonzalez-Bayon R, Kangasjarvi S, Caldana C, Hannah MA, Willmitzer L, Ponce MR, Micol JL** (2013) Functional Redundancy and Divergence within the *Arabidopsis* RETICULATA-RELATED Gene Family. *Plant Physiol* **162**: 589-603

- Pesaresi P, Hertle A, Pribil M, Kleine T, Wagner R, Strissel H, Ihnatowicz A, Bonardi V, Scharfenberg M, Schneider A, Pfannschmidt T, Leister D** (2009) *Arabidopsis* STN7 kinase provides a link between short- and long-term photosynthetic acclimation. *Plant Cell* **21**: 2402-2423
- Pesaresi P, Pribil M, Wunder T, Leister D** (2011) Dynamics of reversible protein phosphorylation in thylakoids of flowering plants: The roles of STN7, STN8 and TAP38. *Biochimica Et Biophysica Acta-Bioenergetics* **1807**: 887-896
- Peskan T, Westermann M, Oelmüller R** (2000) Identification of low-density Triton X-100-insoluble plasma membrane microdomains in higher plants. *Eur J Biochem* **267**: 6989-6995
- Porra RJ** (2002) The chequered history of the development and use of simultaneous equations for the accurate determination of chlorophylls a and b. *Photosynth Res* **73**: 149-156
- Prakash JS, Baig MA, Bhagwat AS, Mohanty P** (2003) Characterisation of senescence-induced changes in light harvesting complex II and photosystem I complex of thylakoids of *Cucumis sativus* cotyledons: age induced association of LHCII with photosystem I. *J Plant Physiol* **160**: 175-184
- Pyke KA** (1999) Plastid division and development. *Plant Cell* **11**: 549-556
- Pyke KA, Howells CA** (2002) Plastid and stromule morphogenesis in tomato. *Ann Bot* **90**: 559-566
- Quirino BF, Noh YS, Himelblau E, Amasino RM** (2000) Molecular aspects of leaf senescence. *Trends Plant Sci* **5**: 278-282
- Radhamony RN, Theg SM** (2006) Evidence for an ER to Golgi to chloroplast protein transport pathway. *Trends Cell Biol* **16**: 385-387
- Rammesmayer G, Pichorner H, Adams P, Jensen RG, Bohnert HJ** (1995) Characterization of IMT1, myo-inositol O-methyltransferase, from *Mesembryanthemum crystallinum*. *Arch Biochem Biophys* **322**: 183-188
- Raskin DM, Judson N, Mekalanos JJ** (2007) Regulation of the stringent response is the essential function of the conserved bacterial G protein CgtA in *Vibrio cholerae*. *Proc Natl Acad Sci U S A* **104**: 4636-4641
- Raval MK, Biswal B, Biswal UC** (2005) The mystery of oxygen evolution: Analysis of structure and function of Photosystem II, the water-plastoquinone oxido-reductase. *Photosynthesis Research* **85**: 267-293
- Raval MK, Biswal UC** (1988) A model for changes in the conformation of oxygen evolving complex of chloroplasts during oxidation of water. *Indian J Biochem Biophys* **25**: 341-343

- Roach T, Krieger-Liszkay A** (2012) The role of the PsbS protein in the protection of photosystems I and II against high light in *Arabidopsis thaliana*. *Biochimica Et Biophysica Acta-Bioenergetics* **1817**: 2158-2165
- Rochaix JD, Lemeille S, Shapiguzov A, Samol I, Fucile G, Willig A, Goldschmidt-Clermont M** (2012) Protein kinases and phosphatases involved in the acclimation of the photosynthetic apparatus to a changing light environment. *Philos Trans R Soc Lond B Biol Sci* **367**: 3466-3474
- Rosar C, Kanonenberg K, Nanda AM, Mielewczik M, Brautigam A, Novak O, Strnad M, Walter A, Weber AP** (2012) The leaf reticulate mutant *dov1* is impaired in the first step of purine metabolism. *Mol Plant* **5**: 1227-1241
- Roulin, S. and Feller, U.** (1998) Light-independent degradation of stromal proteins in intact chloroplasts isolated from *Pisum sativum* L. leaves: requirement for divalent cations. *Planta* **205**: 297-304
- Rowan BA, Oldenburg DJ, Bendich AJ** (2004) The demise of chloroplast DNA in *Arabidopsis*. *Curr Genet* **46**: 176-181
- Sakamoto W** (2003) Leaf-variegated mutations and their responsible genes in *Arabidopsis thaliana*. *Genes Genet Syst* **78**: 1-9
- Sakamoto W, Tamura T, Hanba-Tomita Y, Murata M** (2002) The VAR1 locus of *Arabidopsis* encodes a chloroplastic FtsH and is responsible for leaf variegation in the mutant alleles. *Genes Cells* **7**: 769-780
- Sakamoto W, Uno Y, Zhang Q, Miura E, Kato Y, Sodmergen** (2009) Arrested differentiation of proplastids into chloroplasts in variegated leaves characterized by plastid ultrastructure and nucleoid morphology. *Plant Cell Physiol* **50**: 2069-2083
- Sarwat M, Naqvi AR, Ahmad P, Ashraf M, Akram NA** (2013) Phytohormones and microRNAs as sensors and regulators of leaf senescence: Assigning macro roles to small molecules. *Biotechnol Adv*
- Sato S, Nakamura Y, Kaneko T, Asamizu E, Tabata S** (1999) Complete structure of the chloroplast genome of *Arabidopsis thaliana*. *DNA Res* **6**: 283-290
- Sattarzadeh A, Schmelzer E, Hanson MR** (2011) Analysis of Organelle Targeting by DIL Domains of the *Arabidopsis* Myosin XI Family. *Front Plant Sci* **2**: 72
- Schaper H, Chacko EK** (1991) Relation between Extractable Chlorophyll and Portable Chlorophyll Meter Readings in Leaves of 8 Tropical and Subtropical Fruit-Tree Species. *Journal of Plant Physiology* **138**: 674-677
- Schattat M, Barton K, Baudisch B, Klosgen RB, Mathur J** (2011) Plastid stromule branching coincides with contiguous endoplasmic reticulum dynamics. *Plant Physiol* **155**: 1667-1677
- Schattat MH, Klosgen RB, Mathur J** (2012) New insights on stromules: stroma filled tubules extended by independent plastids. *Plant Signal Behav* **7**: 1132-1137

- Schimper A.F. W (1883)** Über die Entwicklung der Chlorophyllkörner und Farbkörper. In Botanische Zeitung. 105–120, 126–131 und 137–160.
- Schmied J, Hedtke B, Grimm B (2011)** Overexpression of HEMA1 encoding glutamyl-tRNA reductase. *J Plant Physiol* **168**: 1372-1379
- Schubert M, Petersson UA, Haas BJ, Funk C, Schroder WP, Kieselbach T (2002)** Proteome map of the chloroplast lumen of *Arabidopsis thaliana*. *J Biol Chem* **277**: 8354-8365
- Singh S, Yadava HL, Yadava PC, Yadava KL (1986)** A new technique in the study of mixed complexes (M-Nitrilotriacetate-Glycylglycinate Systems). *Zeitschrift Fur Physikalische Chemie-Leipzig* **267**: 153-160
- Smart CC, Fleming AJ (1993)** A plant gene with homology to D-myo-inositol-3-phosphate synthase is rapidly and spatially up-regulated during an abscisic-acid-induced morphogenic response in *Spirodela polyrrhiza*. *Plant J* **4**: 279-293
- Soll J, Schleiff E (2004)** Protein import into chloroplasts. *Nat Rev Mol Cell Biol* **5**: 198-208
- Sonoike K (2011)** Photoinhibition of photosystem I. *Physiol Plant* **142**: 56-64
- Sosso D, Canut M, Gendrot G, Dedieu A, Chambrier P, Barkan A, Consonni G, Rogowsky PM (2012)** PPR8522 encodes a chloroplast-targeted pentatricopeptide repeat protein necessary for maize embryogenesis and vegetative development. *J Exp Bot* **63**: 5843-5857
- Staal J, Abramoff MD, Niemeijer M, Viergever MA, van Ginneken B (2004)** Ridge-based vessel segmentation in color images of the retina. *IEEE Trans Med Imaging* **23**: 501-509
- Streatfield SJ, Weber A, Kinsman EA, Hausler RE, Li J, Post-Beittenmiller D, Kaiser WM, Pyke KA, Flugge UI, Chory J (1999)** The phosphoenolpyruvate/phosphate translocator is required for phenolic metabolism, palisade cell development, and plastid-dependent nuclear gene expression. *Plant Cell* **11**: 1609-1622
- Takechi K, Sodmergen, Murata M, Motoyoshi F, Sakamoto W (2000)** The YELLOW VARIEGATED (VAR2) locus encodes a homologue of FtsH, an ATP-dependent protease in *Arabidopsis*. *Plant Cell Physiol* **41**: 1334-1346
- Tan X, Calderon-Villalobos LI, Sharon M, Zheng C, Robinson CV, Estelle M, Zheng N (2007)** Mechanism of auxin perception by the TIR1 ubiquitin ligase. *Nature* **446**: 640-645
- Tang YL, Wen XG, Lu CM (2005)** Differential changes in degradation of chlorophyll-protein complexes of photosystem I and photosystem II during flag leaf senescence of rice. *Plant Physiology and Biochemistry* **43**: 193-201

- Taylor CB, Bariola PA, delCardayre SB, Raines RT, Green PJ** (1993) RNS2: a senescence-associated RNase of *Arabidopsis* that diverged from the S-RNases before speciation. *Proc Natl Acad Sci U S A* **90**: 5118-5122
- Tiede A, Bastisch I, Schubert J, Orlean P, Schmidt RE** (1999) Biosynthesis of glycosylphosphatidylinositols in mammals and unicellular microbes. *Biol Chem* **380**: 503-523
- Tikkanen M, Grieco M, Kangasjarvi S, Aro EM** (2010) Thylakoid protein phosphorylation in higher plant chloroplasts optimizes electron transfer under fluctuating light. *Plant Physiol* **152**: 723-735
- Trosch R, Jarvis P** (2011) The stromal processing peptidase of chloroplasts is essential in *Arabidopsis*, with knockout mutations causing embryo arrest after the 16-cell stage. *PLoS One* **6**: e23039
- van der Graaff E, Schwacke R, Schneider A, Desimone M, Flugge UI, Kunze R** (2006) Transcription analysis of *Arabidopsis* membrane transporters and hormone pathways during developmental and induced leaf senescence. *Plant Physiol* **141**: 776-792
- Van der Graaff E, Schwacke R, Schneider A, Desimone M, Flugge UI, Kunze R** (2006) Transcription analysis of *Arabidopsis* membrane transporters and hormone pathways during developmental and induced leaf senescence. *Plant Physiology* **141**: 776-792
- Vass I** (2012) Molecular mechanisms of photodamage in the Photosystem II complex. *Biochim Biophys Acta* **1817**: 209-217
- Voelker R, Barkan A** (1995) Nuclear genes required for post-translational steps in the biogenesis of the chloroplast cytochrome b6f complex in maize. *Mol Gen Genet* **249**: 507-514
- Voll L, Hausler RE, Hecker R, Weber A, Weissenbock G, Fiene G, Waffenschmidt S, Flugge UI** (2003) The phenotype of the *Arabidopsis cue1* mutant is not simply caused by a general restriction of the shikimate pathway. *Plant J* **36**: 301-317
- von Arnim AG, Deng XW** (1994) Light inactivation of *Arabidopsis* photomorphogenic repressor COP1 involves a cell-specific regulation of its nucleocytoplasmic partitioning. *Cell* **79**: 1035-1045
- Wang L, Ouyang M, Li Q, Zou M, Guo J, Ma J, Lu C, Zhang L** (2010) The *Arabidopsis* chloroplast ribosome recycling factor is essential for embryogenesis and chloroplast biogenesis. *Plant Mol Biol* **74**: 47-59
- Waters MT, Fray RG, Pyke KA** (2004) Stromule formation is dependent upon plastid size, plastid differentiation status and the density of plastids within the cell. *Plant J* **39**: 655-667

- Weaver LM, Amasino RM** (2001) Senescence is induced in individually darkened *Arabidopsis* leaves, but inhibited in whole darkened plants. *Plant Physiol* **127**: 876-886
- Weaver LM, Gan S, Quirino B, Amasino RM** (1998) A comparison of the expression patterns of several senescence-associated genes in response to stress and hormone treatment. *Plant Mol Biol* **37**: 455-469
- Wise RR** (2006) The diversity of plastid form and function. *In* Wise RR, Hooper JK, eds, *The Structure and Function of Plastids*, Vol 23. Springer, The Netherlands pp 3–26
- Wittenbach VA, Lin W, Hebert RR** (1982) Vacuolar localization of proteases and degradation of chloroplasts in mesophyll protoplasts from senescing primary wheat leaves. *Plant Physiol* **69**: 98-102
- Woo HR, Chung KM, Park JH, Oh SA, Ahn T, Hong SH, Jang SK, Nam HG** (2001) ORE9, an F-box protein that regulates leaf senescence in *Arabidopsis*. *Plant Cell* **13**: 1779-1790
- Wu D, Wright DA, Wetzel C, Voytas DF, Rodermel S** (1999) The IMMUTANS variegation locus of *Arabidopsis* defines a mitochondrial alternative oxidase homolog that functions during early chloroplast biogenesis. *Plant Cell* **11**: 43-55
- Wu FH, Shen SC, Lee LY, Lee SH, Chan MT, Lin CS** (2009) Tape-*Arabidopsis* Sandwich - a simpler *Arabidopsis* protoplast isolation method. *Plant Methods* **5**: 16
- Wunder T, Liu Q, Aseeva E, Bonardi V, Leister D, Pribil M** (2013) Control of STN7 transcript abundance and transient STN7 dimerisation are involved in the regulation of STN7 activity. *Planta* **237**: 541-558
- Wunder T, Liu QP, Aseeva E, Bonardi V, Leister D, Pribil M** (2013) Control of STN7 transcript abundance and transient STN7 dimerisation are involved in the regulation of STN7 activity. *Planta* **237**: 541-558
- Yamaguchi M, Takechi K, Myouga F, Imura S, Sato H, Takio S, Shinozaki K, Takano H** (2011) Loss of the plastid envelope protein AtLrgB causes spontaneous chlorotic cell death in *Arabidopsis thaliana*. *Plant Cell Physiol* **53**: 125-134
- Yamazaki JY, Kamimura Y, Nakayama K, Okada M, Sugimura Y** (2000) Effects of light on the photosynthetic apparatus and a novel type of degradation of the photosystem I peripheral antenna complexes under darkness. *J Photochem Photobiol B* **55**: 37-42
- Yang M, Sack FD** (1995) The too many mouths and four lips mutations affect stomatal production in *Arabidopsis*. *Plant Cell* **7**: 2227-2239
- Yang SD, Seo PJ, Yoon HK, Park CM** (2011) The *Arabidopsis* NAC transcription factor VNI2 integrates abscisic acid signals into leaf senescence via the COR/RD genes. *Plant Cell* **23**: 2155-2168

- Yin T, Pan G, Liu H, Wu J, Li Y, Zhao Z, Fu T, Zhou Y** (2012) The chloroplast ribosomal protein L21 gene is essential for plastid development and embryogenesis in *Arabidopsis*. *Planta* **235**: 907-921
- Yoshida S, Ito M, Callis J, Nishida I, Watanabe A** (2002) A delayed leaf senescence mutant is defective in arginyl-tRNA:protein arginyltransferase, a component of the N-end rule pathway in *Arabidopsis*. *Plant J* **32**: 129-137
- Yoshida S, Ito M, Nishida I, Watanabe A** (2001) Isolation and RNA gel blot analysis of genes that could serve as potential molecular markers for leaf senescence in *Arabidopsis thaliana*. *Plant Cell Physiol* **42**: 170-178
- Zentgraf U, Laun T, Miao Y** (2009) The complex regulation of WRKY53 during leaf senescence of *Arabidopsis thaliana*. *Eur J Cell Biol* **89**: 133-137
- Zhang L, Li J, Kong F** (1992) [Sequence and primary structure analysis of specific DNA fragment related to pollen fertility in radish chloroplast genome]. *Yi Chuan Xue Bao* **19**: 156-161
- Zhang MP, Zhang CJ, Yu GH, Jiang YZ, Strasser RJ, Yuan ZY, Yang XS, Chen GX** (2010) Changes in chloroplast ultrastructure, fatty acid components of thylakoid membrane and chlorophyll a fluorescence transient in flag leaves of a super-high-yield hybrid rice and its parents during the reproductive stage. *J Plant Physiol* **167**: 277-285
- Zhang YL, Marepalli HR, Lu HF, Becker JM, Naider F** (1998) Synthesis, biological activity, and conformational analysis of peptidomimetic analogues of the *Saccharomyces cerevisiae* alpha-factor tridecapeptide. *Biochemistry* **37**: 12465-12476
- Zybailov B, Rutschow H, Friso G, Rudella A, Emanuelsson O, Sun Q, van Wijk KJ** (2008) Sorting signals, N-terminal modifications and abundance of the chloroplast proteome. *PLoS One* **3**: e1994

Curriculum vitae

PERSONAL DATA

Date of birth: 06.04.1984

Place of Birth: Tai'an, Shandong, P.R. China

Nationality: Chinese

EDUCATION

September 2009 - now

Ludwig-Maximilians-Universität München

Department Biology I, Botany

CSC program Ph.D., Supervisor Prof. Dr. Dario Leister & Dr. Cordelia Bolle

September 2008 – July 2009

Northwest A&F University, Shaanxi, P.R. China

Department of Horticulture Science

Ph.D., Supervisor Prof. Fengwang Ma

September 2005 - July 2008

Northwest A&F University, Shaanxi, P.R. China

Department of Horticulture Science

Master, Supervisor Dr. Junke Zhang

September 2001 - July 2005

Shandong Agricultural University, Shandong, P.R. China

College of Horticulture Science and Engineering

Bachelor, Supervisor Prof. Xianli Li

RESEARCH EXPERIENCES

September 2009 - now

Ludwig-Maximilians-Universität München

Department Biology I, Botany

Ph.D. Dissertation-Functional Analysis of the Role of Chloroplasts in Senescence

September 2005 - July 2008

Northwest A&F University, Shaanxi, P.R. China

Department of Horticulture Science

Master Thesis-Resistance Genes Screening in *Uncinular Necator* Induced cDNA library
of Chinese Wild Grape

LANGUAGE

Chinese, mother tongue

English, fluent

German, basic

Acknowledgements

First I would like to thank Prof. Dr. Dario Leister for giving me the opportunity to perform my Ph.D. research in his research group.

Additionally, I would like to thank Dr. Cordelia Bolle, for her supervision, and willing to help in the past four years.

I would like to thank GABI-Duplo group for providing seeds of *rer* mutants, Norbert Mehlmer to provide AtOEP7::GFP and AtTic40::GFP construct for performing localization experiment, Prof. Dr. Gerhard Wanner for ultrastructure observation, Dr. Edda von Roepenack-Lahaye for performing GC-mass spectrometry analysis, Dr. Jörg Meurer and Salar Torabi for helping with PAM measurement, Dr Dongjie Gao for helping and discussing my projects, Ingrid Duschaneck for helping with *Agrobacterial* transformation and Angie Dietzmann for her introduction to the Fluorescence Axio Imager microscope, Elli for providing protocols for the isolation of *Arabidopsis* chloroplasts and transient expression, and also for her help with Real-time PCR, Bastian Patzelt for taking care of my plants in the climatic chamber.

I would like to thank other colleagues in this nice research team, who are always willing to discuss experimental problems or novel hypotheses. I would like to thank Angela Dietzmann for helping to solve my computer problems.

I would like to thank my friends in Germany, who give me the best time in a foreign country.

I would like to thank Chinese Scholarship Council for sponsoring my study in Germany.

I would like to thank my parents for supporting and helping me during the stressful Ph.D.time.

Declaration / Eidesstattliche Versicherung

Hiermit versichere ich, dass ich die vorliegende Arbeit selbständig und nur unter Verwendung der angegebenen Hilfsmittel und Quellen angefertigt habe. Die Autorin hat zuvor nicht versucht, anderweitig eine Dissertation einzureichen oder sich einer Doktorprüfung zu unterziehen. Die Dissertation wurde keiner weiteren Prüfungskommission weder in Teilen noch als Ganzes vorgelegt.

München, den.....

.....